RECQ5 promotes recombination and mutagenesis at targeted nicks through disruption of RAD51 filaments

Henry C. Olson

A dissertation

submitted in partial fulfillment of the

requirements for the degree of

Doctor of Philosophy

University of Washington

2016

Reading Committee:

Nancy Maizels, Chair

Lawrence Loeb

Michael Ailion

Program Authorized to Offer Degree:

Biochemistry

University of Washington

Abstract

RECQ5 promotes recombination and mutagenesis at targeted nicks through disruption of RAD51 filaments

Henry C Olson

Chair of the Supervisory Committee:

Nancy Maizels, Professor

Departments of Immunology and Biochemistry

RECQ5 mutation and overexpression have both been associated with human cancer. RECQ5 has been implicated in repair of oxidative DNA damage, a critical pathway in which inherent redundancies may mask a key role for any single factor. Oxidative damage creates DNA nicks. By using CRISPR/Cas9 or CRISPR/Cas9^{D10A} to target double-strand breaks (DSBs) or nicks to specific sites in the human genome our laboratory has shown that nicks can initiate homology directed repair (HDR) by an alternative pathway that is distinct from HDR at DSBs and that efficiently uses single-stranded DNA donors. This alternative pathway is normally inhibited by RAD51, to prevent genomic instability at nicks.

To determine the functions of RECQ5 in HDR, we have assayed the effect of its depletion or overexpression at targeted nicks and DSBs. We found that depletion of RECQ5 inhibited HDR at both nicks and DSBs, by either single-stranded or duplex DNA donors. Conversely,

overexpression of RECQ5 inhibited HDR at DSBs and HDR by dsDNA donors at nicks, but stimulated HDR by ssDNA donors at nicks. While RECQ5 associates with the moving transcription apparatus, we did not find that these activities of RECQ5 depended upon transcription of the target gene for recombination, or were affected by deletion of the domain of RECQ5 that interacts with RNA polymerase 2. Structure-function analysis did show that stimulation of HDR depended on the RECQ5 helicase ATPase activity, and the ability of RECQ5 to interact with RAD51. None of the effects of RECQ5 depletion or overexpression was evident in cells in which RAD51 filament formation had been inhibited by treatment with siRAD51 or siBRCA2.

We conclude that RECQ5 normally supports canonical HDR at both nicks and DSBs, to promote genomic stability. Somewhat paradoxically, RECQ5 overexpression has the unanticipated consequence of promoting genomic instability, apparently overriding the normally suppressive effect of RAD51 to enable nicks to initiate HDR. These results explain the genomic instability associated with both RECQ5 mutations and overexpression.

TABLE OF CONTENTS

LIST OF FIGURES

ACKNOWLEDGEMENTS

I would like to thank Nancy Maizels for her guidance throughout my project and for providing the space and materials to conduct this research. I additionally thank Larry Loeb, Michael Ailion, Conrad Liles, Alex Merz, and Mohomed Oouka for acting as my committee and guiding my research throughout my studies. I would like to thank the Maizels lab members (Luther Davis, Konstantin Kiianitsa, Quy Le, Kevin Khoo, Olivier Humbert, and Lucas Gray) who have aided me either through their helpful discussions or demonstration of techniques. In particular, I would like to thank Luther Davis for the mentorship role he played. I would like to thank Yilun Liu for providing the full length and (1-899) ectopic RECQ5 expression constructs and would like to acknowledge Donna Prunkard for her aid in running the FACS equipment.

CHAPTER 1 INTRODUCTION

The trials and tribulations of the genome

The diploid human genome consists of approximately 3.2 billion base pairs of DNA which encode an estimated 20,000 proteins. The genome is constantly being compacted, expanded, transcribed, and replicated. Faithful replication of the genome allows for the information to be passed along to the next cell or next generation. Errors that arise in the replication or repair of the genome can lead to mutations. These mutations are passed along to the next generation. Mutations are not inherently bad. They are responsible for the diversity of species and drive the continuation of life. However, most non silent mutations decrease the fitness of an individual cell. Ironically, mutations that increase the fitness of an individual cell often are deleterious to the fitness of multicellular organisms as they promote uncontrolled growth in the form of cancer.

Cancer, at a fundamental level, is a disease caused by mutations that allow the cell to grow in a fashion unregulated and out of sync with the surrounding tissue in an organism. Cellular growth is regulated by hundreds of components in a multitude of cell pathways. It is therefore unsurprising that cancer is not defined by a single mutation. One of the most common mutations found in cancer, a homozygous deletion of TP53, is still only observed in approximately half of tumors sampled [1]. Further compounding the tumor's complexity, the severity of a mutation may be dependent upon the location of the tissue in which it is observed. As an example, up to 45% of the familial, early onset breast cancer cases are caused by a mutation in BRCA1 [2-5]. This mutation also confers high risk for ovarian cancers [6]. And yet, this mutation is not observed to be a prominent driver of tumorigenesis in many other tissues.

The heterogeneity observed in tumors is not restricted to types or locations of tumors. Indeed, within an individual tumor, distinct signatures of mutagenesis can be observed. These populations within a tumor can harbor different levels of susceptibility or resistance to various therapies. The cause of this heterogeneity is currently being debated but is likely due to either the presence of cancer stem cells or a pattern of branching mutations within a tumor's growth. Cancer stem cells are thought to be distinct cells within a tumor that have the ability to create and propagate a tumor [7]. These cells will give rise to unique populations in a tumor depending on the initial mutations within the cancer stem cell [8]. Branching mutations refer to the possibility that cells acquire different driver mutations which propel individual populations down different mutation tracks. A driver mutation is a mutation in a key repair or regulatory pathway. The heterogeneity within a tumor may or may not confer fitness to the tumor but it originates from the same cause, genomic instability.

The maintenance of genomic stability is one of the most crucial tasks a cell takes on every moment. The genome can be damaged in numerous ways during normal use (replication, transcription, covalent modifications, etc.) and by external factors. These events can lead to double stranded breaks (DSBs) or nicks in the genome. These instances of damage can lead to improper repair and subsequent mutation. Once a mutation is present in the genome, the cell has no means by which to remove it. It is thus critical for cells to properly address and repair the damage that occurs[9].

This work examines a key member of the DNA damage repair mechanism; a helicase known as RECQ5. Prior to examination of RECQ5 it is important to understand how DNA damage can occur and what mechanisms are currently known to repair it.

Mechanisms of DNA damage

While DNA is a form of long term information storage, portions of it are constantly undergoing activity such as replication, transcription, or repair. This activity exposes the DNA to various forms of damage ranging from that brought in by normal cellular functions to events brought on by external sources. While the factors that lead to DNA damage events may differ, they often create a similarly modified or damaged base or strand. Each DNA nucleotide (nt) is a complex molecule with multiple locations capable of alteration. These modifications include oxidation, alkylation, hydrolysis, pyrimidine dimers, mismatches, or damage such as single stranded breaks, double stranded breaks, and cross linking events between strands of DNA.

Oxidative damage

Reactive oxygen species (ROS) are a common instigator of DNA damage in the cell [10-13]. When they react with a nucleic acid they cause oxidative damage. ROS molecules have highly reactive oxygen components and can arise from a variety of sources. Exogenously, they are primarily induced by smoke inhalation (tobacco and other), pollutants, and ionizing radiation [10, 14-16]. Radiation is particularly dangerous as it can create hydrogen peroxide. Hydrogen peroxide is stable enough that it can transit throughout the cell and into the DNA before inducing oxidative damage. Endogenously, reactive oxygen species are a common and crucial component of cellular metabolism [9, 17, 18]. The electron transport chain functions by passing an electron across multiple protein complexes to generate a proton gradient so that ATP can be produced. Studies on mitochondrial respiration estimate that up to 2% of the electrons are prematurely added to oxygen, resulting in a superoxide anion and subsequent conversion to hydrogen peroxide via the Mn-superoxide dismutase [19, 20]. The superoxide radical is not as reactive as other ROS but can still result in oxidation of proteins, fatty acid chains, and DNA.

Regardless of the origin of ROS, their interactions with nucleic acids have been well documented. When a ROS comes into contact with a nucleic acid it will react with one of the bases, thereby adding itself to the DNA, or can remove a hydrogen from a methyl or CH2 group [19]. Twenty unique oxidations to the bases have been documented but the most common form of oxidative damage is 8-hydroxyguanine. This modification of guanine adds a hydroxyl group onto C8 of the guanine ring. This creates a reactive resonance structure with the nitrogen molecules surrounding the carbon which can lead to further damaging cellular reactions. 8-hydroxyguanine is such a common form of damage that it exists at a steady level in the cell [21]. An estimated 2400 such oxidized bases are present at any given time in the genome even though the cell has repair pathways in place to eliminate these base alterations. Typically, the cell will use the Base Excision Repair (BER) pathway to remove oxidized bases and subsequently replace them with normal copies [22].

An elevated level of ROS is a hallmark of many tumors due, in part, to their increased metabolism [13]. The elevated levels lead to an increase in mutagenesis which can further drive tumor development and differentiation. Increased levels of ROS can also cause persistent inflammation [23]. The recruitment of immune cells to the tumor can lead to angiogenesis which provides the cell with more nutrients and the means to continue growth. However, there is a balance even in tumors. ROS levels that rise too high (either through persistent high levels or exacerbation with chemotherapeutics) will lead to programmed cell death due to excessive damage to the genome and/or the mitochondria.

Methylation

A very common form of physiological modification of DNA is the methylation of CpG sites with an estimated 90% of CpG sequences having the modification[24]. A methyl group is transferred

onto a cysteine by DNA methyltransferase 1 (DNMT1) on the C5 position resulting in 5 – methylcytosine [25]. This modification is an important part of development and gene expression regulation. Many promoter regions have CpG islands which do not have methylation. If these regions become methylated, the genes can become transcriptionally silent. If this occurs at the promoter of a tumor suppressor, the cell may begin to grow in an unregulated fashion and form a tumor [26-28]. Distinctive methylation signatures have been considered as a useful diagnostic of the presence of cancer as methylated DNA can be found in blood though this has not yet translated to a therapy [29].

Deamination/Depurination

In a hydrolysis reaction chemical bonds are cleaved by the addition of water. Deamination results in the loss of a nitrogen, replace by an oxygen. This will often result in a nt binding with an inappropriate base pair. For example, 5-methylcytosine will undergo spontaneous deamination to become thymine. This mismatch mutation can be corrected if found prior to replication. Depurination results in the complete loss of the base from the sugar backbone. In cases of both deamination and depurination, an abasic site can be formed[30]. This is repaired via the BER pathway which progresses through a nick intermediate. The steady state level of abasic sites in a human cell is estimated to be 30,000 [21], and abasic sites represent a major and spontaneous source of DNA damage in the cell.

Pyrimidine dimers

While DNA damage can occur in each cell in the body, the skin faces a unique challenge as it is constantly bombarded with UV light which is a potent source of DNA damage. Exposure of DNA to UV radiation, such as that which is found in sunlight, can cause a photochemical reaction between two adjacent pyrimidines that generates a cyclobutane ring [31]. Both thymine

and cytosine are susceptible to this form of damage. The resulting damage forms a kink in the DNA which prevents transcription and replication. It can lead to mutagenesis if left unresolved either through further disruption and damage of the DNA at the site or by necessitating the use of error prone translesion polymerases [32]. Fortunately, this damage is recognized by DNA repair pathways. In most organisms, it can be repaired through a reverse photochemical reaction [33]. However, in humans, it must be repaired through the nucleotide excision repair (NER) pathway in order to avoid mutagenesis.

Single Stranded Breaks

All of the previously mentioned forms of DNA damage, except some forms of programmed methylation which can be reversed through direct repair, will result in a nick as an intermediate in normal repair. While a majority of these nicks are fully repaired, some will persist. An estimated 10,000 self-inflicted nicks in the genome will form in each cell per day [21]. Nicks can also arise on their own as a result of ionizing radiation, which generates 50-fold more nicks than DSBs [34].

The cell has evolved numerous strategies by which it can repair damage to its bases and nicks in the genome. These include Base Excision Repair (BER) and Nucleotide Excision Repair (NER) as well as the Mismatch Repair (MMR) pathway.

Base Excision Repair

BER is one of the most active DNA repair pathways in the cell. It is chiefly responsible for the processing and repair of DNA damage that does not result in a distortion of the double helix [22, 35-37]. This can occur as a result of oxidative damage of a base, inappropriate alkylation,

incorporated uracil, and abasic sites. While BER is involved with the processing of these forms of DNA damage, the ligation that follows the end processing is broadly applicable to nick repair.

A DNA glycosylase initially recognizes an inappropriate or damaged base in the DNA. Different glycosylases recognize different substrates [38, 39]. For example, the Uracil DNA Glycosylase (UNG) family tracks along DNA without stably binding until it finds an incorporated uracil [40, 41]. Once this base is identified, the base is inverted out of the duplex and the N-glycosidic bond is cleaved by the glycosylase. Another DNA glycosylase with a distinct activity is 8-Oxoguanine glycosylase (OGG1) [36, 42]. This glycosylase will recognize and excise 8-oxoguanines formed by the activity of a ROS at a guanine. For each of these glycosylases, the cleavage results in an abasic site.

There are two classes of glycosylases: mono-functional and bifunctional [40, 42, 43]. The UNG family members are mono-functional glycosylases. Once they have created an abasic site their role in BER is complete. In contrast, OGG1 is a bifunctional glycosylase. Following the creation of an abasic site, it will cleave the phosphodiester backbone. Notably, the activity of bifunctional glycosylases creates a unique signature on the DNA. They leave a 3' aldehyde group next to the 5' phosphate. This can then be processed to create a 3' hydroxyl.

If the abasic site was not cleaved by a glycosylase it may instead by processed by Apurinic/apyrimidinic (AP) endonuclease, which uses its AP lyase activity to cleave to generate a 5'-phosphate and 3'-dRP. Humans possess two AP endonuclease: APE1 and APE2 [44-47]. APE1 accounts for approximately 95% of AP endonuclease activity in humans and requires a magnesium catalyst [48]. APE2 accounts for a small amount of the AP endonuclease activity in the cell but has the unique characteristic of being 5-fold more active when using a manganese

catalyst as opposed to a magnesium catalyst [44]. This suggests it may have some specific activity promoted by ion availability. Both of these endonuclease selectively bind abasic sites and alter local DNA structure [47]. This allows them to cleave the DNA.

Following DNA cleavage, either short or long patch repair may occur [49, 50]. Short and long patch differ in the length of the nt sequences added as well as the specific DNA ligases used to repair the final nick. In short patch repair, DNA polymerase B (POLB) catalyzes the removal of the 5'-terminal deoxyribophosphate (dRP) from the cut site [50]. It then adds a single nt and the 3'-hydroxyl of this nt is ligated to the 5'-phosphate. DNA LIG3 and XRCC1 are believed to be the primary actors in the ligation step in short patch BER. XRCC1 and LIG3 form a complex in the cytoplasm at which point they are recruited to the site of the break [48]. In long patch repair, POLB displaces the nicked strand as it adds at least two new nt at the 3' end. The replicative ligase, Lig1, is primarily responsible for the ligation of the two strands [51]. A great deal of redundancy has been noted among human DNA ligases, suggesting that some loss of activity in one can be rescued by activity of another.

The mechanism that determines whether short or long patch repair occurs is unclear. There are two competing hypotheses [50]. One states that in areas of high ATP concentration, short patch repair is the favored mechanism while in lower concentration areas long path is the preferred mechanism. The other theory is that the 3' and 5' ends at sites cleaved by APE1 are the determining factors. If POLB can remove the dRP, then short patch BER will be preferred. If POLB is unable to easily remove the dRP then long patch will be preferred[50].

Unsurprisingly, mutations in the BER pathway genes cause an increased mutagenic load and have been shown to contribute to tumorigenesis [36, 52]. As an example, heritable mutations

in MUTYH, a glycosylase that removes oxidative damage induced mispaired adenine, have been shown to increase the incidence of colon cancer by 93% [53, 54].

Nucleotide Excision Repair

NER is a vital pathway that prevents DNA damage from proceeding to mutation by recognizing bulky DNA damage events and facilitating their repair [12, 55-58]. Pyrimidine dimers produced by UV radiation are the primary substrate for the NER pathway. These aforementioned bulky DNA damage sites can cause mutations through the necessitated use of translesion polymerases during their repair. The NER pathway can remove them but first it must find them.

The NER pathway has two distinct mechanisms by which it locates DNA damage [56]. Repair of transcribed regions of the genome occurs via the transcription coupled NER (TC-NER) while repair of all regions of the genome can occur through the global genomic NER (GG-NER). In TC-NER RNAPII is unable to bypass the damaged bases and stalls [59, 60]. This causes the recruitment of XPG and CSB which initiate the NER pathway and help to stabilize R loops (regions where a strand of RNA has cotranscriptionally formed an RNA-DNA duplex) [60]. In GG-NER, the damaged bases must be recognized by constantly scanning proteins. XPC-Rad23B and DNA damage binding (DDB) proteins DDB1 and DDB2 recognize the damaged bases and recruit other components of the NER machinery [61-63]. Different pathways exist, in part, due to the random location of damage that occurs from exposure to UV light. If damage exists in un-transcribed or otherwise silent portions of the genome, the damaged bases must still be repaired lest they contribute to mutations during replication. Defects in GG-NER are known to cause Xeroderma pigmentosum and an increased rate of tumorigenesis in all tissue exposed to the sun while defects in TC-NER can lead to many genetic disorders including Cockayne syndrome [56].

Following recognition of the damage site, both TC - and GG - NER proceeds through the recruitment of a number of factors [12, 55, 57, 62]. XPA, RPA, XPD, XPG and TFIIH bind the site (if they were not already present) [62]. XPD and XPG then unwind the DNA which allows the XPF/ERCC1 complex to bind. XPF and XPG then cut the same strand of DNA, upstream and downstream of the damaged base respectively, approximately 30 nt apart resulting in a gap [56]. The ssDNA fragment containing the damage is removed in complex with TFIIH and the resulting gap can then be bound by RPA [57, 64]. DNA polymerase δ is recruited by CDT2 mediated XPG degradation where it fills the gap which is then ligated by either Lig1 or the XRCC1/LIG3 complex [65].

Mismatch Repair Pathway

In the course of DNA replication, repair or mutation, base mismatches can form. The mismatch repair (MMR) pathway can correct the incorrectly paired nt in an efficient manner [66]. Briefly, a mismatch causes a deformation in the double helix which is detected in eukaryotes by the MutS alpha homolog or MutS beta homolog for base-base or short stretch (2-14 bp) mismatches [67, 68]. MutL will nick the DNA away from the mismatch on the newly synthesized strand followed by excision of the DNA between the nick site and the mismatch by Exo1. The gap is then filled by DNA polymerase delta. Failures or mutations in the MMR pathway can result in hyper mutation frequencies and tumorigenesis [69-71].

Double Strand Break Repair

Double strand breaks (DSBs) represent an especially dangerous form of DNA lesion. While they can be repaired efficiently by the cell, they can also result in large insertions, deletions, and genomic rearrangements [72]. These are potent drivers of tumorigenesis as they can disrupt

multiple gene functions from each event. Many tumor suppressors play a role in signaling or repair of this form of damage.

DSBs are created via two main pathways. The DNA can be cleaved outright, resulting in a DSB. This can occur due to numerous exogenous stimuli such as exposure to certain chemical compounds, radiation, and certain viral or bacterial infections [73-76]. These DSBs can be formed at any time. DSBs can also be formed from nicks in the genome during replication. An estimated 3000 nicks form during each S phase of the cell cycle. When the replication machinery encounters a nick, it may generate an endogenous DSB if the replication fork stalls and subsequently collapses. Endogenously derived DSBs are usually formed during S phase while DSBs formed by exogenous factors can occur at any phase in the cell cycle

DSB repair can occur through two classes of pathways. The first class attempts error free repair of the DSB. This is known as homology directed repair (HDR) and is the preferred form of repair during late-S/G2/M phases as the sister chromatid provides a homologous donor [72, 77]. HDR can result in crossover and non-crossover events. While HDR can result in error-free high fidelity repair, it can also promote genomic instability through translocations, inversions, or even disrupt chromosome segregation via improper repair during replication. Alternatively, a DSB can be repaired in an efficient but error-prone mechanism using either the non-homologous end joining (NHEJ) pathway, primarily in G0/G1 phase, or the alternative NHEJ pathway (altNHEJ), which is most active in early S phase [72, 78-80]. These pathways shall be discussed in further detail following discussion of the various HDR pathways.

Homology Directed Repair (HDR)

HDR is repair that uses a homologous donor to provide missing or damaged sequence information. HDR is one of the most tightly regulated forms of repair as aberrant HDR can result in genomic rearrangements which can lead to tumorigenesis. HDR at DSBs has been extensively studied. It can result in either crossover or non-crossover events. In the event of a crossover, information from one chromosome can be transferred to the other. This is a dangerous event for cells as it can result in the loss of heterozygosity (LOH). This would occur when a functional gene on one chromosome was inactivated by sequence transferred from a non-functional copy of the gene on the homologous copy. Mitotic cells possess multiple mechanisms to promote non-crossover events as this limits the chance of LOH. Below follows a brief discussion of the mechanism of crossover recombination and non-crossover recombination.

BRCA2 and RAD51

BRCA2 and RAD51 are key proteins in the HDR process. RAD51 is a 339 aa protein that can form helical filaments on both ssDNA and dsDNA [81-83]. Notably, RAD51 prefers to form filaments on dsDNA; a trait that partially helps explains its role in strand invasion and recombination [83, 84]. When loaded onto ssDNA by BRCA2, it facilitates a homology search by the strand it is bound to in a mechanism not yet understood. In part it may facilitate the homology search by elongating the ssDNA by up to 50% relative to B form DNA, while protecting it from exonucleases [83, 85]. This elongation only occurs when RAD51 is bound to ATP which confers high affinity to ssDNA and dsDNA [86, 87]. In yeast, the affinity of RAD51 binding to ssDNA is 5-fold greater in the presence of ATP than ADP. If RAD51 hydrolyzes its bound ATP, it loses its ability to elongate the B form DNA-bound filament and the filament can begin to slowly dissociate in small bursts from either end[88, 89]. This dissociation is quite slow

and often requires other proteins to facilitate its removal. RAD54 is one protein which can remove RAD51 from dsDNA at D loops , regions of DNA where the dsDNA is separated by a piece of ssDNA [90-99]. This step is crucial as RAD51 on its own will stay bound to the D loop and inhibit further HDR. This process requires an active ATPase domain on both the RAD54 and RAD51 molecules [92]. Proteins that remove RAD51 from ssDNA will be discussed in detail below but include the RECQ family of helicases.

BRCA2 is a key regulator and facilitator of recombination [95, 96]. It possesses eight ~35 aa long identical domains known as BRC domains. These regions are highly conserved between species though, interestingly enough, the spacing regions between them are not. The BRC domains allow BRCA2 to carry out a crucial function; that of binding and sequestering RAD51 [97, 98]. Following the resection of a DSB, BRCA2 can form a complex with BRCA1 and PALB2 and localize to the site of damage while bound to four molecules of RAD51. BRCA2 inhibits RAD51 hydrolysis of ATP and facilitates the displacement of RPA from the DNA [99, 100]. Once BRCA2 has loaded four units of RAD51, it uses its other four BRC domains to facilitate the addition of four more RAD51 molecules [101, 102]. BRCA2 has then been reported in vitro to stay on the RAD51 filament as this stabilizes it and prevents RAD51 from dissociating. BRCA2 has also been implicated in the protection of replication forks from degradation by MRE11 though this activity is believed to be a function of its RAD51 loading at the stalled fork and thus protecting it from MRE11 degradation [103-105]. This theme of different applications of the same core function is a theme that shall be revisited in this manuscript.

Crossover Recombination

An explanation of crossover events at DSBs is useful to begin our discussion as many of the non-crossover mechanisms are simply early exits from crossover HDR (Fig. 1.1). Following identification of the DSB, the MRN (MRE11, RAD50, NBS1) complex, in conjunction with the other factors, uses its 5'-3' exonuclease activity to create a 3’ overhang. RPA, a ssDNA binding protein, then self-loads onto the single-stranded overhangs. RPA is unable to promote reannealing and can even inhibit the strand it is bound to from binding to complementary sequence. RPA is replaced by RAD51 in a BRCA2-dependent fashion. The RAD51 bound 3’ overhang is called the presynaptic filament. RAD51 then promotes homology search by the 3’ overhang and subsequent strand invasion of a homologous donor. This creates a D loop with the point of strand invasion called a Holliday Junction (HJ). At this point RAD51 is removed from the DNA by RAD54 in a process that requires the ATPase activities of both RAD51 and RAD54. In addition, RAD52 is required to facilitate the annealing of the DNA strand in the D loop. DNA polymerase can then extend the break site using as template the homologous donor. For a crossover to occur, the second strand must also invade. This substrate is known as a double Holliday junction (dHJ). If non-specific endonucleases cleave this substrate the chromosomes can undergo a crossover event. While this pathway is common during meiosis, certain regulator proteins act to limit this non-specific cleavage of double HJs in mitotic cells. BLM, a member of the RECQ family of helicases specifically promotes cleavage of this substrate such that there is a non-crossover event.

Synthesis Dependent Strand Annealing (SDSA)

SDSA is mechanistically similar to crossover HDR up until the initial strand invasion (Fig. 1.1) [109-111]. In SDSA RAD51 will coat the 3’ overhang and cause strand invasion and DNA

synthesis by DNA polymerase. However, unlike crossover HDR, the second strand is inhibited from invading the donor [110]. This prevents the formation of a double HJ and preempts the possibility of a crossover. Following synthesis of new DNA, the D loop is disrupted and the strand can bridge the gap of the DSB and reanneal to the target. RECQ5 promotes SDSA at DSBs by disrupting RAD51 filaments and thus preventing the formation of a double HJ [112]. Any remaining gaps are filled in by the polymerase and the DNA is religated. This mechanism is error free and is a common mechanism of HDR in mitotic cells.

Single Strand Annealing (SSA)

SSA is a form of repair similar to altNHEJ. In SSA, the cell finds two regions with stretches of homology away from the initial break site (Fig. 1.1) [72]. These regions of homology anneal to each other resulting in the loss of any and all genetic information between them. This happens in a RAD52 and RAD59 dependent manner [113-116]. Interestingly, RAD51 is not required for this process and may actually inhibit it [117]. In Drosophila, RECQ5 has been shown to be required for this pathway and inhibit LOH [118].Mismatch repair proteins MSH2 and MSH3 in addition to RAD1 and RAD10 also appear to be required for SSA and are thought to function by removing the resulting 3' flaps formed by the annealing of the regions of homology [119, 120]. This form of repair may be particularly useful in regions of repeat sequence such as ribosomal DNA or could represent a pathway of last resort to repair a DSB before it induces apoptosis [72].

Alternative Homology Directed Repair

Nicks have long been thought to undergo repair by simple religation, but they have recently been described as the starting substrate for a form of homology directed repair (HDR) [121-124]. This form of repair is distinct from HDR at DSBs as it is inhibited by the crucial DSB HDR proteins RAD51 and BRCA2 [121]. When the nick recombines with a ssDNA oligo donor (SSO) it

follows and alternative form of HDR but shares similarities with DSB HDR when recombining with a dsDNA donor (Fig. 1.2) [123]. In addition, it shows a bias towards nicks on the transcribed strand of DNA and can recombine with SSO's complementary to the intact (cI) or nicked (cN) strand of DNA. In the case of a cI donor, it is hypothesized that the donor binds an opened nick and promotes gene conversion if the donor possesses new sequence information or simple repair if the donor is completely homologous [121]. A cN donor is thought to bind the 3' flap of the unwound nick and promote DNA synthesis along the SSO [121]. These SSO donors could come from many endogenous DNA processes including Okazaki fragment formation, long overhangs, a loose strand of a D loop, or even mRNA transcribed by RNAPII. Yeast has recently been shown to undergo recombination at nicks using RNA as a donor though this has yet to be shown in humans [125, 126].

Non Homologous End Joining (NHEJ)

NHEJ is the most commonly used form of repair at DSBs [72, 79, 80]. It is the primary form of DSB repair in G0 and G1 phases of the cell cycle and still occurs at high frequencies in S/G2/M. This form of repair can occur rapidly as there is no need for a homology search, however inappropriate NHEJ can join two DSB ends from different parts of the chromosome and cause translocations and chromosome segregation errors. As mentioned previously, the choice between HDR and NHEJ pathways is decided by processing at the ends of the DSBs [127]. NHEJ preferentially acts on ends that have undergone limited resection.

In NHEJ, the DSB undergoes end binding and tethering, processing, and ligation to induce repair. The ends are first bound by KU70/80, which form a complex with DNA Protein Kinases (DNAPK's) which acts, in part, to hold the ends of the break in close proximity [127]. The ends are then processed by the MRN complex such that a 3' hydroxyl and 5' phosphate

remain. The X family DNA polymerases Pol λ and Pol μ then fills in any gaps on the DNA and the ends are ligated back together by Lig4/XRCC4 [128-130]. This form of repair can be error free if there is no need for end processing but if there is any need for limited resection or addition of nt then the lack of a homologous template inherently makes this form of repair mutagenic.

Alternative NHEJ

AltNHEJ, also known as microhomology- mediated end joining (MMEJ), is a form of repair with similarities to SSA HDR [131, 132]. It acts in early S phase when NHEJ begins to be less prevalent and HR has yet to be fully upregulated [133]. AltNHEJ acts at DSBs by resecting the DNA to expose 5' ends 5 to 25 nt in length, containing very short homologies that anneal to each other. In human cells, this form of repair uses the same mechanism of end resection as does HR [134]. In yeast, altNHEJ is independent of KU70/80 and DNAPK and usually results in a deletion of the sequence between the microhomologies [135]. In humans, a similar KU70/80 and DNAPK independent pathway has been observed though the reaction kinetics are much slower (hours rather than minutes) and often does not result in a deletion of the intervening sequence [131, 132].

Helicases

DNA helicases allow the duplex to be unwound. This unwinding is necessary for nearly all functions involving DNA from replication and transcription to many of the repair pathways. The first DNA helicase was discovered in E.coli in 1976 [136, 137]. Since then many helicases have been discovered. They are one of the most common classes of genes, with approximately 1% of all described eukaryotic genes encoding a helicase or protein with helicase motifs. In humans, 95 nonredundant helicases have been described by sequence analysis. Of those, 31 encode DNA helicases while 64 encode RNA helicases. Helicases are molecular machines that can progress

along the DNA or RNA and catalyze its transformation from duplex to single-stranded, or structured to unstructured. Typically, a helicase has preferred directionality and will unwind in the 5' to 3' direction or the 3' to 5' direction [136, 138].

Helicase unwinding of DNA or RNA requires three common functions: helicase binding of the DNA or RNA, hydrolysis of NTP (typically ATP), and NTP hydrolysis dependent unwinding of the substrate [136, 137]. Helicase unwinding can be passive or active. This is a fundamental property of the helicase and is based on the helicases ability to catalyze the disruption of the base pair hydrogen bonds. Active helicases will power their unwinding of the DNA by ATP hydrolysis and will unwind at a rate equal to their translocase rate. Passive helicases function similarly to active helicases but will unwind at a rate less than their translocase rate and dependent upon the identity of the base pairs and the presence of additional factors which are influencing the DNA binding stability.

An example of helicase activation can be seen in the study of HELQ [139, 140]. This DNA helicase has poor helicase activity unless it is in the presence of RPA, a ubiquitous ssDNA binding protein. Another example which will be described in more detail later is the interaction between PARP and RECQ5[141]. PARP activation significantly reduces RECQ5 helicase and increases RECQ5 annealing activities.

RECQ family of helicases

The RECQ family of helicases is comprised of five different helicases in human cells: BLM, WRN, RECQ1, RECQ4 and RECQ5. The RECQ family was first identified in E.coli, and these helicases represent a subset of the Super Family 2 (SF2) subset of helicases (Fig. 1.3) [136]. They have been called guardians of the genome as they function in preserving genomic integrity

in transcription, replication, and repair [142]. RECQ helicases share conserved helicase motifs and the presence, or partial presence, of the RQC (RecQ C terminal) domain. This domain is only found in RECQ family helicases and is made up of a zinc binding domain crucial for helicase activity and a winged helix domain (WH) which allows for DNA binding where the helicase can bind the ends of DNA DSBs. The RECQ helicase family is notable for its prevalence across all organisms, from single-celled prokaryotes (RecQ) to yeast (Sgs1), and through multicellular organisms. While RECQ1 through 5 have the helicase domain, RECQ4 does not have the RecQ Core domain while RECQ5 has only the zinc binding motif but not the WH domain. Helicases in this family also carry flanking regions which grant unique functional specificity.

RecQ (E. coli)

RecQ is the sole RECQ family helicase found in E.coli (Fig. 1.3) [143, 144]. It plays numerous roles in nucleic acid metabolism and possesses the capability to unwind a wide range of DNA substrates including G quadreplex DNA, three or four way junctions of DNA, D loops, Holliday Junctions, and duplex DNA with either blunt ends or a 3' or 5' overhang. This wide range of substrate activity allows RECQ to play numerous roles in the cell. It has been implicated in recombination, cell damage signaling pathways, and interacting with Topo isomerase III in order to allow resolution of replication forks.

Sgs1 (S. Cerevisiae)

Like E coli, S. Cerevisiae has a single RecQ helicase called Sgs1, or slow growth suppressor 1[145, 146]. Sgs1 is homologous to RecQ in E. coli and BLM and WRN in humans (Fig. 1.3). Similar to BLM and WRN, it possesses a complete RecQ core domain consisting of the helicase and RQC region as well as the HRDC domain but also has a large N terminal domain which

gives it further functionality. Sgs1 is highly cell cycle regulated, with upregulation occurring in S phase and low levels seen in M and G1 phase. Sgs1 plays critical roles in recombination, replication, and cell cycle progression.

RECQ1

RECQ1 (or RECQL) is the most abundant RECQ helicase in human cells. At DSB's RECQ1 plays a role in both recombination and non-homologous end joining. In end joining, RECQ1 can bind and facilitate the loading of Ku70/80 and subsequent unwinding of DNA[147]. In addition, RECQ1 has also been implicated in promoting replication by restart of stalled replication forks.

BLM (RECQ2)

BLM aids in the maintenance of genomic stability. Individuals who lack BLM have Bloom's syndrome, a disorder associated with higher rates of sister chromatid exchange and tumorigenesis [142, 148]. The BLM protein is 1417 aa long and possesses a core domain (642-1290) which contains its RecQ helicase domain. This domain is sufficient to grant BLM its helicase and DNA binding domains and behaves very similarly to RECQ1 in in vitro biochemical assays[149]. Like most of the RECQ helicases, BLM can act on many DNA substrates including G quadraplexes, D loop disruption, and can facilitate the migration of HJ branches. BLM plays a crucial role in DSB repair by preventing crossovers following dHJ formation [150].

WRN (RECQ3)

Like BLM, WRN helicase has a conserved RECQ domain and a large N terminal flanking region which confers additional interactions and function specificity (Fig. 1.3) [142, 149]. Lack of WRN results in Werner Syndrome, a disorder typified by premature aging, progeroid

phenotypes, and increased tumorigenesis [142, 151]. WRN helicase is 1432 aa long and shares similar helicase properties with both RECQ1 and BLM [142, 149]. WRN may act to help resolve stalled replication forks possibly by clearing a blocking DNA structure such as a G quadreplex out of the way or by reversing the stalled fork. In addition to its role in replication, WRN is known to play a role in telomere maintenance [151, 152]. WRN has been shown to disrupt the T loop structure of DNA at the ends of chromosomes in telomeres to allow for replication of much more of the telomere in each cycle of replication.

RECQ4

RECQ4 loss in the germline is associated with three different diseases: Rothmund-Thomson, Baller-Gerold, and RAPADILINO syndromes [142, 153]. These disorders are all due to genomic instability and manifest with high sensitivity to UV light, alopecia, osteopenia, cataracts, and an increased incidence of cancer with developmental skeletal abnormalities specific to each syndrome. The role of RECQ4 in replication has been extensively studied. It acts in the replication of both genomic and mitochondrial DNA [142, 154]. In the genome, RECQ4 associates with MCM10 to promote firing of replication origins. This interaction is required for normal cell cycle progression but not for the localization of RECQ4 to the chromatin [155].

RECQ5

RECQ5 beta (RECQ5) was first described in a genetic screen in 1998 [156]. Since then, it has been studied less extensively than its human relatives, BLM and WRN, in part because no genetic disease has been linked to mutations in RECQ5. There are three isoforms of RECQ5: alpha, beta, and gamma (Fig. 1.3). RECQ5 alpha and gamma are truncated versions of the full length protein and lack nuclear localization signals. Little is known regarding their function.[142, 157, 158]. Mice lacking RECQ5 are more susceptible to cancer and show an increased sensitivity

to oxidative damage due to lipopolysaccharide/D-galactosamine-induced liver injury [159, 160]. In humans, the loss of RECQ5 leads to genomic instability and low levels have been implicated in a poor prognosis in osteosarcomas while high levels have been associated with progression of breast cancer [161-164]. Perhaps the most interesting aspect of RECQ5 in human disease is not its down regulation in tumors but rather the reverse. When examining alterations (mutations, deletions, and copy number amplifications) in RECQ5 we noted that this helicase is highly amplified across a wide range of tumors and that this amplification is present in a significant number of those tumors (Fig. 1.4) [165, 166]. This is particularly notable in comparison with the related helicase WRN, which carries predominantly deletions or mutations in cancer.

Is the copy number increase in RECQ5 causing high rates of tumorigenesis by promoting genomic instability? Is the increase in RECQ5 a desirable trait in tumors already suffering from a high rate of genomic instability, and do amplifications confer a selective advantage in rapidly dividing cells? These questions defined a driving theme in my studies: is RECQ5 maintained in a necessary state of balance in the cell where either an increase or decrease in activity can lead to genomic instability?

RECQ5 is 991 aa long and contains a 3' to 5' helicase domain, but lacks the winged helix (WH) binding domain that is unique to members of the RECQ helicase family [142]. The lack of the WH domain limits the type of DNA substrates RECQ5 can use. RECQ5 can facilitate the unwinding of forked substrates and nicks or breaks with a 3' overhang [149, 167], but it cannot act on D loops nor unwind G quadraplexes in vitro. Like other RECQ helicases, its processivity is enhanced by RPA. Unlike BLM, WRN, and RECQ4, it is expressed in all phases of the cell cycle [142]. RECQ5 localizes to the nucleus and has been observed in PML bodies, matrix associated bodies that can recruit and store proteins within the nucleus [158].

RECQ5 plays a role in replication by processing stalled replication forks to facilitate proper replication and chromosome segregation [142]. In Drosophila and humans, anaphase bridges have been observed in cells lacking RECQ5 [168, 169]. RECQ5 interacts with Mus81 – EME1 endonucleases to promote cleavage of forked DNA intermediates at common fragile sites [168]. Based on the frequency of observed DNA damage, these are sites in the genome which are more likely to suffer DNA damage than others. This activity is likely due to the ability of RECQ5 to disrupt RAD51 filaments at stalled forks, thereby promoting processing and halting unwanted recombination which can lead to anaphase bridges and mis-segregation of chromosomes. Thymidine slows replication by depleting dCTP levels in the cell.RECQ5 confers resistance to thymidine slowing of replication and can interact both in vivo and in vitro with proliferating cell nuclear antigen (PCNA), a processivity factor that associates with Polymerase delta in replication [170].

RECQ5 plays multiple roles in promoting genomic stability during transcription [171, 172]. RECQ5 has two domains which allow it to interact with RNAPII [173-176]. One of these domains contains a KIX motif and is called the IRI domain. This domain allows RECQ5 to bind to RPB1, the largest subunit of RNAPII. The IRI domain competes for the same binding site as TFIIS, a protein that promotes reinitiation of stalled RNAPII [174, 177]. Thus, the IRI domain can maintain RNAPII in a stalled configuration, potentially allowing for completion of DNA repair which may block or disrupt transcription, though how this activity is controlled is unknown. RECQ5 also has an RNAPII interaction domain at its C terminus called the SRI domain. This domain allows RECQ5 to interact with the 3',5' phosphorylated C terminal domain of elongating RNAPII [175]. This interaction has led RECQ5 to be called a general elongation factor. In tissue culture experiments, the depletion of RECQ5 enhanced genomic instability

which was counteracted by inactivation of RNAPII [176]. In addition, an increase in levels of RAD51on DNA in transcribed regions occurred following inhibition of RECQ5, though it was not known whether this was due to a lack of removal or increased recruitment of RAD51. Recently, RECQ5 has been shown to act as a scaffold to promote the sumoylation of TopoI in transcribed regions of DNA [178]. TopoI alpha is thought to cleave at R loops while sumoylation is believed to block this activity [179]. Excess TopoI alpha cleavage can induce genomic instability and thus must be regulated. Treatment of cells with camptothecin (CPT)inhibits Topo1 activity and traps the protein in a covalent intermediate state, bound to the DNA. This activity of RECQ5, linked to transcription, explains why RECQ5 deficiency increases sensitivity to CPT, as more Topo1 would be acting on the DNA and thus susceptible to CPT, and why CPT-sensitivity is mitigated by the chemical inhibition of transcription [180].

RECQ5 is an important factor in the repair of DSBs [142]. It localizes to DSBs through its interaction with the MRN complex [181] which consists of MRE11, RAD51, and NBS1. MRN is activated by the ATM kinase and plays a key role in DNA damage signaling [181]. RECQ5 interacts directly with MRE11 and NBS1. This interaction inhibits the 3' to 5' exonuclease activity of MRE11, though has no effect on RECQ5's 3' to 5' helicase activity.

RECQ5 acts to regulate levels of recombination in the cell through its interaction with RAD51 [182]. As discussed above, RAD51 is required for strand invasion in homology directed repair. RECQ5 has been shown to promote noncrossover events by disrupting RAD51 presynaptic filaments at DSBs[112]. RECQ5 can remove RAD51 filaments from ssDNA in a 3' to 5' direction in an ATP dependent manner [112, 182]. Notably, it cannot remove RAD51 from dsDNA precluding it from acting to disrupt RAD51 filaments following D loop formation [182]. RECQ5 is thus relegated to disrupting presynaptic filaments solely and thus regulating

recombination. If RECQ5 activity is very high, RAD51 presynaptic filaments can be disrupted completely and the DSB will likely undergo SSA repair due to an inability to form filaments. More moderate activity of RECQ5 can disrupt RAD51 filaments that would form a double HJ. This activity then promotes SDSA by allowing only the initial strand invasion [112]. Too little RECQ5 activity and the cell will form more double HJ's at DSBs due to the decreased disruption of RAD51 filaments. These can lead to crossover events and increased genomic instability. The activities of RECQ5 in repair that have been described thus far are limited to recombination. RECQ5 is not known to cause changes in the NHEJ pathway or altNHEJ pathway [183].

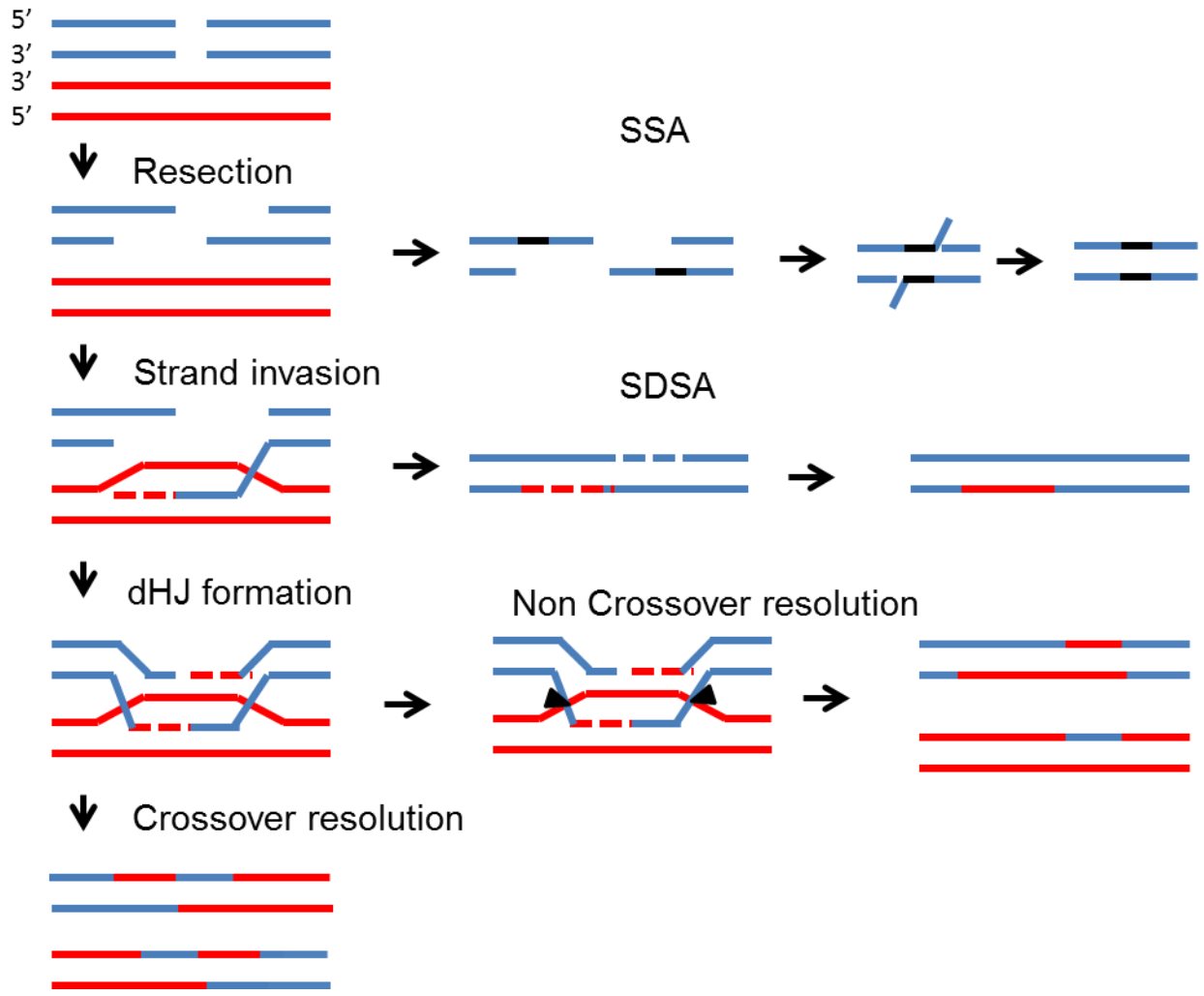

Figure 1. 1 Pathways of Homology Directed Repair at DSBs.

Following the creation of a DSB the DNA can undergo HDR or NHEJ. The first step in HDR at a DSB is resection resulting in 3' overhangs. If there is no homologous donor, the cell can undergo single strand annealing (SSA) where resection continues until a region of homology is found. SSA is typically mutagenic as the region between the sections of homology is lost. If there is a homologous duplex DNA donor, a 3' overhang can invade the donor and form a D loop. Synthesis can then proceed and bridge the initial gap created by the DSB. If the D loop is subsequently disrupted, the DSB can be repaired via the synthesis dependent strand annealing (SDSA). If the second 3' overhang of the cleaved strand of DNA invades the donor then a double Holliday junction (dHJ) is formed. This can be resolved into a non-crossover event or crossover event.

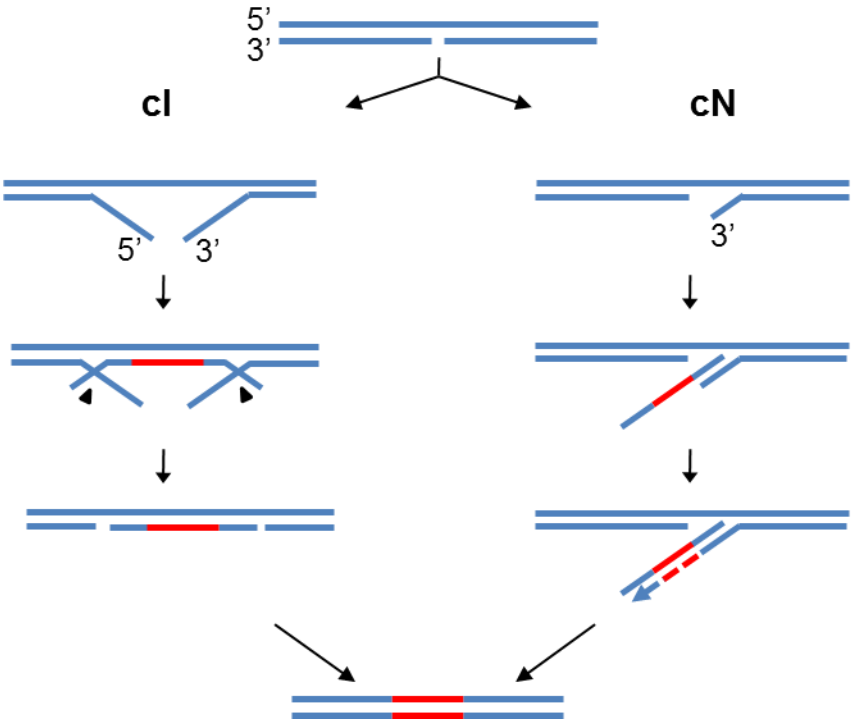

Figure 1.2 HDR at nicks with SSO donors.

Nicks can undergo HDR with SSO donors complementary to either the intact (cI) or nicked (cN) strand. For recombination using the cI donor, the nick is unwound and the donor can anneal to the complementary region of the target. Recombination using a cN donor occurs when the 3’ end of the nick is unwound and anneals to the cN donor. The 3' end of the nick then primes DNA synthesis using the donor as a template.

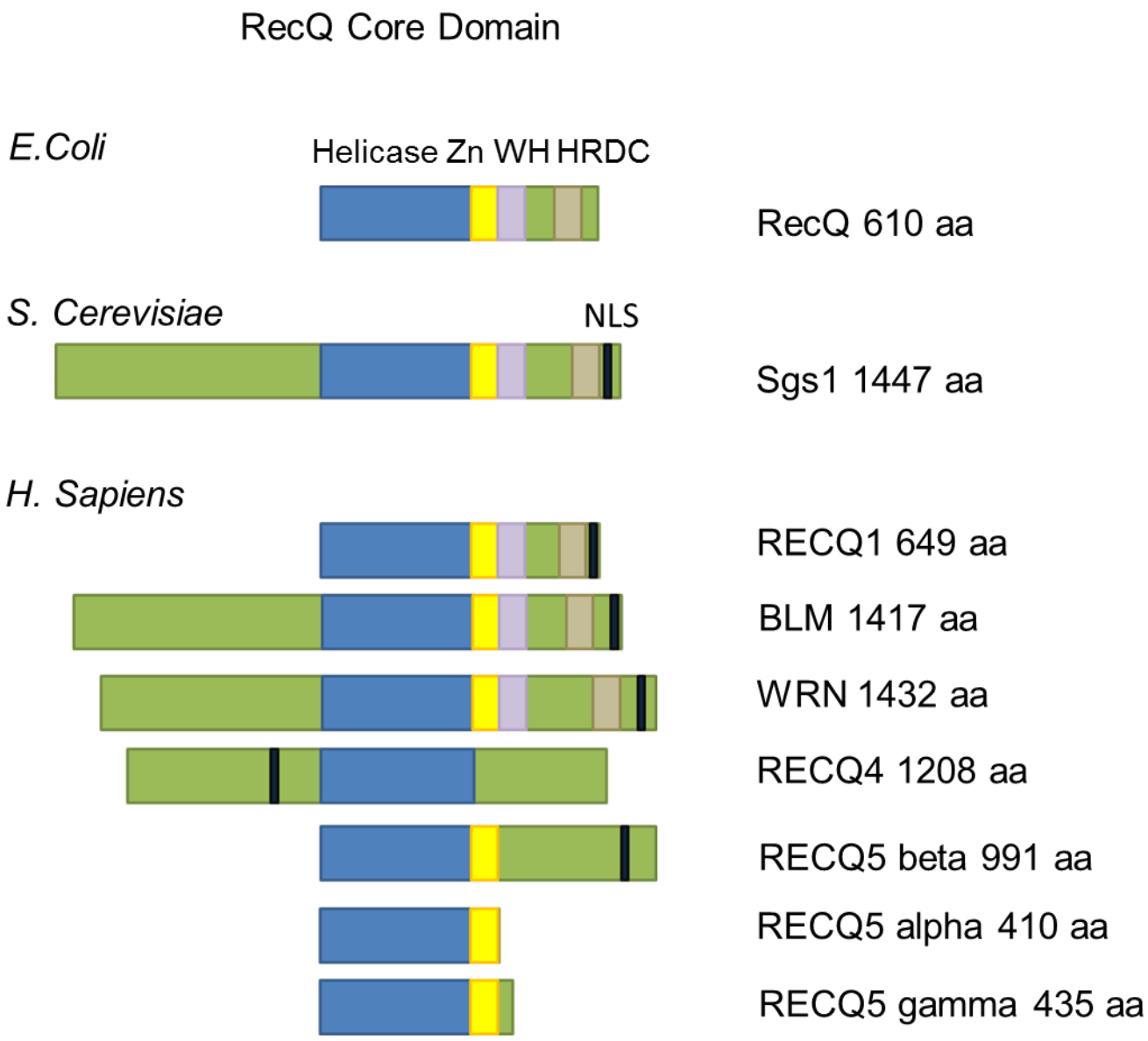

Figure 1.3 The RECQ Family of helicases.

RECQ helicases are shown from E. coli, S. cerevisiae, and, H. sapiens along with their shared helicase, Zn, and WH domains and their length in amino acids (aa). Each RECQ helicase shares a similar helicase domain. All but RECQ4 have a zinc binding (Zn) domain which is thought to link ATPase activity to DNA unwinding. All but RECQ4 and RECQ5 have the winged helix (WH) domain which allows for the recognition of unique DNA structures such as G quadraplexes. The HRDC regulatory domain is likewise shared by all members of the family but RECQ4 and RECQ5. Nuclear localization signal locations are shown in black.

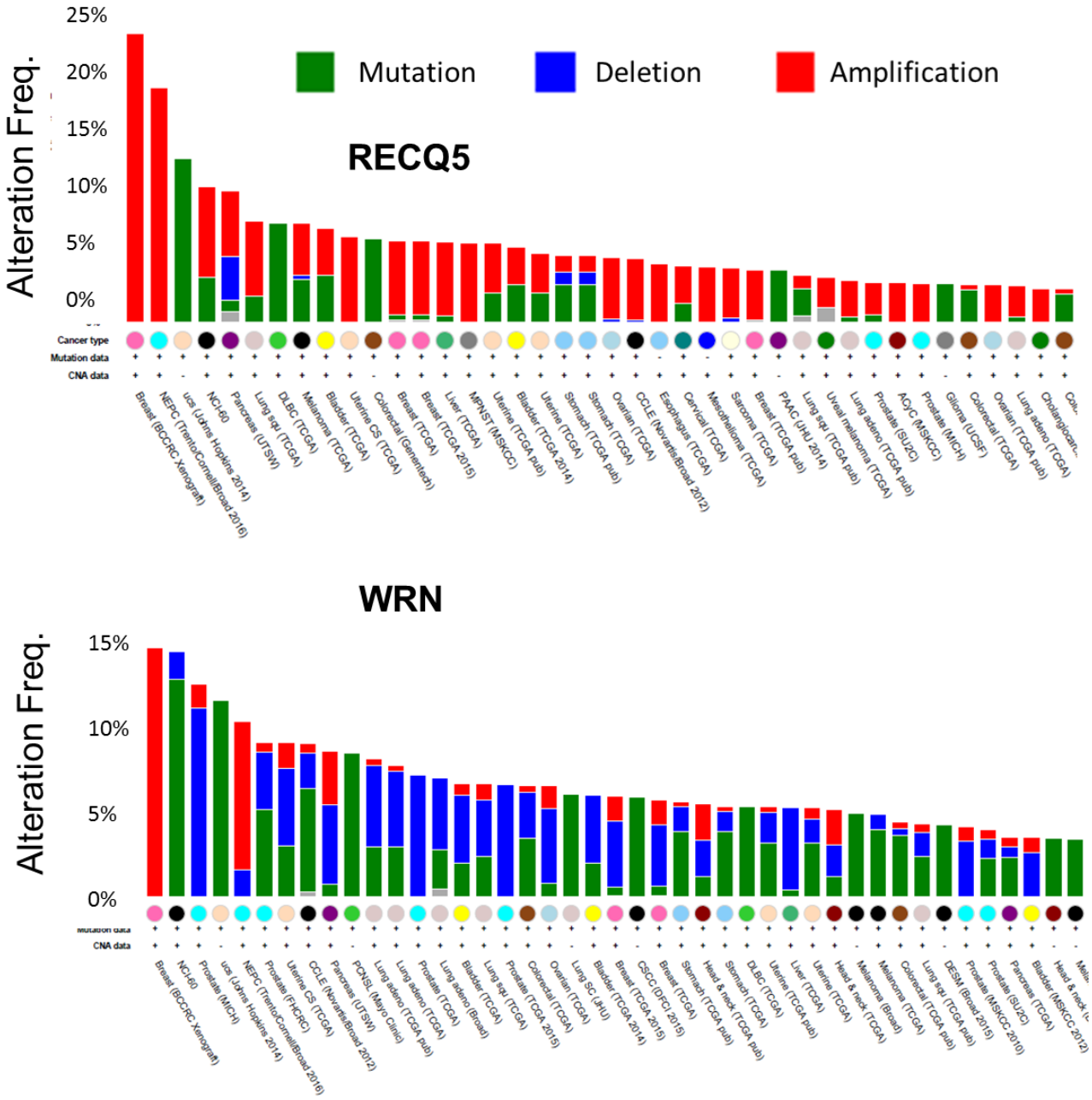

Figure 1.4 Alterations of RECQ5 and WRN observed in tumors.

The frequency of alterations (y axis) observed in RECQ5 and WRN among various tumor sample collections (x axis). Green bars are indicative of mutations (of all types) while blue and red bars represent copy number variations (deletions and amplifications respectively.

Chapter 2 KEY METHODOLOGY

This thesis focuses on the study of DNA repair at the site of nicks and DSBs in mammalian cells. We examined the repair of damaged DNA in two different human cell lines: HEK 293T and HT1080. Cells for analysis carried the Traffic Light (TL) Reporter integrated into the chromosome, which we used to quantify the efficiency of Homology Directed Repair (HDR) and mutagenic end-joining (mutEJ). We targeted DNA nicks or DSBs using the I–AniI homing endonuclease or the CRISPR/Cas9 system.

Human cell lines

Cells were grown in DMEM supplemented with 10% FBS, L-glutamine, and penicillin at 37°C in 5% CO_2 and normal O_2 (~21%) levels. The levels of O_2 are much higher than typically experienced in the body, where levels are 1-10% O_2. These hyperoxic conditions may promote elevated oxidative damage, which may lead to the creation of single stranded breaks. However, these effects should not influence the results discussed in this thesis as they are non-specific damage events while we are studying targeted DNA damage events. Both of the cell lines used are adherent cell lines which grow in a mono-layer. While this system will lack the cellular architecture that typifies the complexity of organs, this should not overly influence DNA damage pathway mechanisms which make up the focus of this study.

HEK 293T and HT1080

Human Embryonic Kidney (HEK) cells were developed as a scientific tool by Alex van der Eb in 1973 in his 293rd experiment [184]. They are a robust adherent cell line which are easy to grow and transfect. HEK cells immortalized with the SV40 T virus are often used in mammalian tissue culture. HEK cells are believed to be more closely related to adrenal cells which come from a neuronal linage [185] than to kidney cells. Adrenal means ‘next to kidney’ so it is possible that

this cell type was present in the original transformation of HEK cells by adenovirus. Their transcriptome also most closely resembles that of adrenal cells and naïve neurons. These observations preclude this cell line from being used as a model of kidney tissue despite its name. HEK cells are also hyplotriploid meaning that they have more than two but less than three times the usual number of chromosomes [186]. They have a modal chromosome number of 64 and are presumed to be female in origin as they do not have a Y chromosome. Most lines of HEK cells carry four copies of chromosome 17. This is notable as the gene that encodes RECQ5 lies on Chromosome 17.

For the research described in this thesis, HT1080 cells were used to check the initial findings of the importance of RECQ5 in HDR at nicks in the TL reporter. HT1080 cells derive from fibrosarcoma tissue[187]. They have a relatively normal karyotype with a modal number of 46, the same as normal diploid cells. They originated in a 35 year old male and, while more difficult to transfect than HEK cells, they can be used for mammalian tissue culture experiments.

Traffic Light reporter

The Traffic Light (TL) reporter (Fig. 2.1A) [188] is stably integrated into the chromosome in the HEK 293T and HT1080 reporter cells. The TL reporter lines used in this experiment are clonal lines with a single integration of the TL reporter at an unknown site in the genome, however, the cell lines produce GFP and mCherry at rates equivalent to mixed populations, with varied insertion sites, of TL reporter cells. The TL reporter consists of a promoter region followed by a non-functional GFP linked via a T2A tag to an out of frame mCherry gene (+2 reading frame) [188]. The T2A tag causes both the GFP and mCherry to be expressed on the same transcript but for translation to yield two separate protein products. This ensures that differences in levels of

GFP and mCherry are not due to differences in the rate of transcription. The GFP gene contains a 38 bp insert that contains 2 premature stop codons rendering the cell GFP negative.

We target DNA nicks or DSBs to the insert in GFP using either I-AniI homing endonuclease or CRISPR/Cas9 (Fig 2.1C) [121-123]. If a donor DNA (either ssDNA or dsDNA) carrying a region that can convert the 38bp insert in the donor to 17bp of correct GFP sequence, the GFP gene will encode functional protein causing GFP+ cells. The dsDNA donors are truncated such that they cannot express functional GFP. Single-stranded oligonucleotide (SSO) donors are only 99 nt long and thus cannot express functional GFP. By targeting nicks or DSBs to the 38 bp insert region, we can avoid targeting damage to the donor piece of DNA.

As discussed in Chapter 1, DSBs undergo either crossover or non-crossover HDR with dsDNA donors. In the TL reporter, only SDSA events will result in GFP+ cells following HDR with dsDNA donors. Crossover events will result in GFP- cells as the target will acquire the truncation at the end of GFP of the donor. If the targeted DNA nick or DSB results in a frameshift mutation which puts the mCherry in frame with the promoter, the cell will become mCherry+. It is worth noting that the mCherry+ cells make up only a fraction of those that have undergone mutagenesis, as only frameshifts to the +2 reading frame will score in this assay.

To score HDR and mutagenic end joining (mutEJ), cells can be collected and sorted via flow assisted cell sorting (FACS) using a LSRII flow cytometer (Fig. 2.1B). Cells are initially screened for live cells (at the time of collection) and subsequently screened for single cells. Single cells are then sorted for BFP+ population (transfection control) and subsequently analyzed for GFP+ (HDR) or mCherry+ (mutEJ) cells.

Targeted DNA nicks and DSBs

Over the past 10 years there has been a great advance in the technology enabling DNA nicks or DSBs to be targeted to specific sites in DNA. We initially used the I-AniI homing endonuclease to study the repair of nicks and DSBs. It is a member of the LAGLIDADG family of homing endonucleases, so named for the distinctive amino acid sequence found in its members [189]. Members of this family function as monomers or homo-dimers. I-AniI (Fig. 2.1C) is a member of this family and binds to a specific target sequence, CCGTGAGGAGGTTTCTCTGTAAAGCTAAG. The LAGLIDADG homing endonucleases carry two active sites, and cleave DNA by bending the DNA backbone and using these two active sites to nick opposite strands.

Zinc-finger nucleases and TAL effector nucleases both have the ability to target almost any sequence of DNA[122]. These are engineered fusion proteins that rely upon the zinc finger DNA binding domains and the Transcription Activator Like (TAL) DNA binding domains to target a FokI endonuclease domain to a specific sequence. These proteins are relatively large, complicating transfections, and their specificity can be imperfect.

CRISPR/Cas9 relies upon a guide RNA that anneals to the target to direct the cleavage activity of the endonuclease activity of the Cas9 protein [190]. This system was discovered in bacteria and confers resistance to bacteriophage by using a sequence captured from the viral genome in one round of infection to identify the target in future infections [191, 192]. The captured sequence is called the spacer, and is integrated just upstream of the proto-spacer adjacent motif, or PAM sequence. For the commonly used CRISPR/Cas9 system, the PAM sequence is NGG. A guide RNA carrying the spacer and PAM sequence binds to the Cas9 protein to form the CRISPR/Cas9 ribonucleoprotein complex. Initially, CRISPR/Cas9 scans the

DNA searching for PAM sites, the gRNA anneals to a specific target, Cas9 stabilizes the target DNA and rotates the first few bases towards the guide RNA (gRNA) sequence, whereupon the Cas9 endonucleases cleave the phosphodiester backbone of the target DNA at the position just between the third and fourth nt from the PAM site.

Cas9 has two endonuclease sites (HNH and RuvC) which allow it to generate DSBs (Fig. 2.1C) [193]. If either of these sites is inactivated (by the D10A or H840A mutations, respectively), the target will be nicked either on the strand bound to the gRNA or on the opposite strand. The obvious use of CRISPR/Cas9 in therapeutics has been hampered by the initial off target and non-specific activities of the CRISPR/Cas9 system. Many of these concerns have been addressed by the redesign of Cas9 to produce higher specificity, by careful selection of gRNA sequences to have limited homology to non-target regions of the genome, and by other strategies such as using paired nickases to generate a DSB [194-196]. Fortunately, CRISPR/Cas9 provides an excellent tool to study DNA repair at specific sites in the genome.

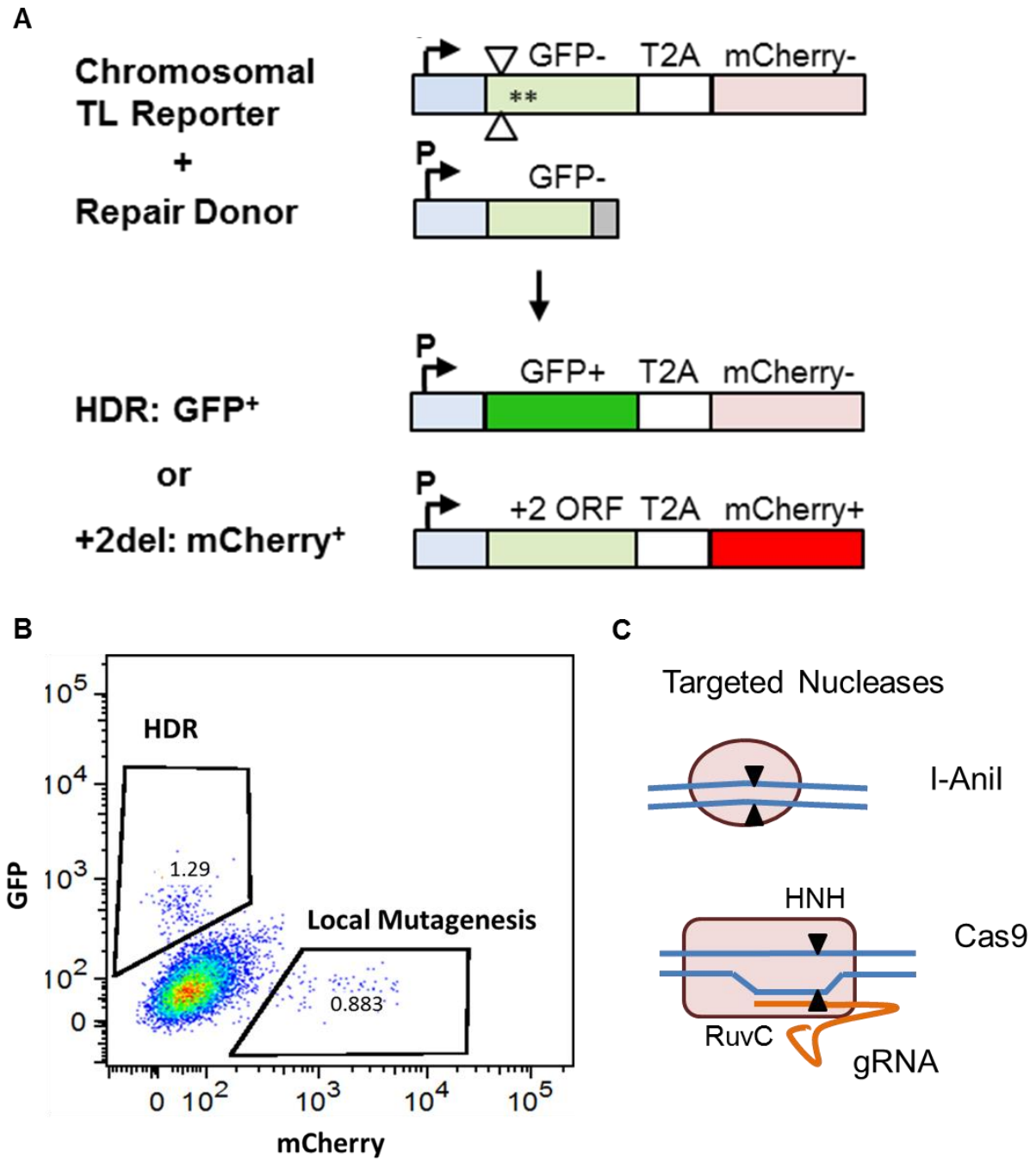

Figure 2.1 Traffic Light (TL) Reporter

(A) The TL reporter is stably integrated into HEK 293T or HT 1080 cells. In this reporter, a CMV promoter (+1 reading frame) controls the transcription of a GFP rendered non-functional by insertion of a 38 bp region containing an I-AniI target sequence and two premature stop codons; and an out-of-frame mCherry gene (in the +2 reading frame) linked by a T2A sequence. Nicks and DSBs are introduced by the transient transfection of I-AniI or CRISPR/Cas9. The targeted nick or DSB will initiate undergo HDR using either a dsDNA donor or a SSO, which

results in GFP+ cells. Alternatively, if the nick or DSB causes a deletion or insertion that moves mCherry into the correct reading frame, cells become mCherry+.

(B) The frequencies of HDR and mutEJ are thus readily scored in a single experiment by quantifying GFP+ and mCherry+ cells by flow cytometry, as shown in this example.

(C) Targeting of DNA nicks or DSBs can be achieved by transient transfection of I-AniI or CRISPR/Cas9, which create DSBs; or derivatives of these enzymes in which one active site has been inactivated to cause the nuclease to nick DNA rather than generate DSBs.

Chapter 3 THE ROLE OF RECQ5 IN RECOMBINATION AT DSBS AND NICKS

Nicks are the most common form of DNA damage in the cell with more than 10,000 occurring per day [197, 198]. Recently, nicks have been shown to be capable of homology directed repair (HDR) with a variety of DNA donors, but the mechanism of repair remains unclear (Fig 3.1) [121-124]. In this study we analyzed what role RECQ5 plays in HDR and mutagenesis at nicks on the transcribed and non-transcribed strands (Fig. 3.1). Cellular levels of RECQ5 were altered by siRNA depletion, or by ectopic expression of recombinant protein. We found that depletion of RECQ5 reduced frequencies of HDR at nicks 4-fold, and diminished mutEJ comparably (Fig. 3.1). Conversely, ectopic expression of RECQ5 increased HDR frequencies at nicks by an SSO donor, but decreased HDR frequencies at nicks with a dsDNA plasmid donor (Fig. 3.3). Frequencies of mutEJ were increased upon ectopic expression of RECQ5 independent of the identity of the donor. These effects were found to be dependent upon functional RECQ5 helicase and RAD51 interaction domains (Fig. 3.4). Furthermore, concurrent depletion of RAD51 or BRCA2 overrode the effects of RECQ5 ectopic expression or depletion, suggesting that RECQ5 acts on RAD51 bound to DNA (Fig. 3.5). In contrast, expression of $RAD51^{K133R}$, a dominant negative ATPase deficient mutant of RAD51 which can form filaments on DNA but resists removal following D loop formation, increased HDR frequencies at nicks but, unlike siRAD51 treatment, showed a subsequent decrease in HDR frequencies upon concurrent depletion of RECQ5. These results strongly suggest that RECQ5 functions to remove RAD51 filaments from DNA, and that this enhances HDR frequencies with ssDNA donors. This suggests that RAD51 filaments may promote religation at nicks, following RAD51 removal from the dsDNA, and thus prevent inappropriate HDR and mutEJ.

Materials and Methods

Materials

Plasmids and Cell Lines

The Traffic Light Reporter plasmid, Cas9, Cas9^{D10A}, guide RNA (gRNA), I AniI, dsDNA donor, RAD51^{K133R}, and ssOligo donor are as previously described[121, 123]. Cas9, Cas9^{D10A} and I AniI each coexpress a BFP protein in addition to the nuclease. This was used as a transfection control. The siRNA resistant RECQ5 full length and 1-899 were kindly provided by the Liu Lab[176]. Point mutations in FLAG-RECQ5 render it immune to siRECQL5-2, target site 976) but not siRECQL5-1 (target site 435). Point mutations (D157A, K598E, F666A) and the truncation mutant (1-899) were created using QuikChange II XL Site-Directed Mutagenesis Kit (Agilent Technologies) as per manufacturer's directions.

Quikchange primers (with reverse complement)

D157A - CTTACTTGGTGGTGGCTGAAGCTCATTGTG

K598E - GTGGCCAACCTCTACGAGGCCAGCGTGCTG

F666A – CAAAGGCTCCTGCCCGGCCCAGACGGCCAC

gRNA sequences

gTL1 gtgtccggcctcgaccgtgAGG (PAM in caps)

gTL2 CCGtgaggaggtttctctgtaa

gTL9 aaagctaagagctcacctaCGG

siRNA

siRNAs assayed included siNT2, siBRCA2, siRAD51, siRECQ5-1 (ID# 4390847, s2085, s11734, and s17988 respectively; ThermoFisher Scientific) and siRECQ5-2 (GCCCAUUGGAAUAUUGCCAAGUCUA)

Antibodies

Anti FLAG – Mouse monoclonal, Origene – TA50011

Anti Actin – Goat polyclonal. Santa Cruz Biotechnology sc-1616

Cell lines

Cell lines (HEK 293T and HT1080) were cultured at 37°C in Dulbecco-modified Eagle's medium (Hyclone) supplemented with 10% fetal bovine serum (Atlanta Biological, Lawrenceville, GA) and 200 units/ml penicillin, 200 µg/ml streptomycin (Hyclone) and 2 mM L-glutamine (Hyclone) at 37°C and 5% CO_2.

Methods

Traffic Light Reporter assay

Reporter cell lines were seeded into a poly lysine coated 24 well plate at $1x10^5$ (HEK 293T), $1.2x10^5$ (293), or $0.6x10^5$ (HT1080) cells per well in 500 µl of media or in 96 well plates (HEK 293T only) at $4x10^3$ cells per well in 100 µl of medium. siRNA transfections were carried out with the ThermoFischer RNAiMax kit (final concentration 10 nM) 4 hours after seeding. At 24 hours after seeding, cells were transfected with plasmids expressing CRISPR/Cas9 or CRISPR/$CAS9^{D10A}$ or Ani-I or Ani-I nickase, and donor SSOs using lipofectamine LTX kit (ThermoFIscher) as per manufacturers guidelines. For each 24 well plate well, 100 µl or 20 µl of

transfection mixture was prepared using the Standard transfection recipe I listed below. At 24 hours post LTX transfection, treated cells in 24 well plates were transferred to lysine coated 6 well plates in 2.5 ml media. 48 hours post transfer, cells were collected by treatment with 300 µl 0.05% trypsin in PBS and 100 µl 4% formaldehyde (final concentration 1%). Cells were then stored at 4°C in the dark until they could be counted using an LSR II flow cytometer (Becton Dickinson, Franklin Lakes, NJ) and analyzed using the FlowJo software (version 9.6).

Standard transfection recipe I

For each 100 µl of transfection mixture required:

100 µl FBS free media (Optimem)

150 ng Cas or $Cas9^{D10A}$ or I-AniI or I-AniI nickase expression plasmid

75 ng gRNA (Cas9 or $Cas9^{D10A}$ only)

50 ng overexpression construct

1.2 µl LTX transfection reagent

Flow cytometry

Live cells were identified by forward scatter area and linear side scatter area and sorted for single cells by subsequent side scatter height by width. Approximately 100,000 cells were collected and sorted for each replicate. For TL Reporter experiments BFP+ (405 nm laser) cells were then selected in Cas9/Ani-I transfected cells and subsequently analyzed for GFP (488 nm laser) or mCherry+ expression. The analysis of FACS data was performed in the FlowJo version 9.6 software and the frequencies of live cells, singlets, BFP+, GFP+ and mCherry+ cells were copied to excel files for further analysis.

Data Analysis

Each experiment was repeated at least twice in triplicate. Data was analyzed by averaging the replicates and taking the standard deviation and standard error of the mean using Excel. Significance was determined by a two tailed T test with unequal sample variance. P values < 0.05 were deemed to represent statistical significance.

Western blot

HEK 293T cells were seeded in 24 well plates at $1x10^5$ cells/well and transfected with RECQ5 variants (6 replicates per variant) and Cas9-BFP (but no gRNA) at levels listed in the standard transfection recipe. After 24 hours the cells were transferred to 6 well plates and allowed to grow for 48 hours, at which time 2 of the 6 replicates were collected and analyzed via flow cytometry to record transfection efficiency based upon BFP levels. Populations in which transfection efficiency was below 20% were not further analyzed, nor were experiments where transfection efficiency deviated by more than 10% between samples.

Whole cell extracts were prepared from four replicates. Briefly, cells were extracted using RIPA buffer [20 mM Tris-HCl (pH 7.5), 150 mM NaCl, 1 mM Na_2EDTA, 1 mM EGTA, 1% NP-40, 1% sodium deoxycholate, 2.5 mM sodium pyrophosphate] supplemented with protease inhibitor cocktail (complete, EDTA-free; Roche). Samples were incubated on ice for 10 min followed by sonication (3X10sec) and centrifugation (5 min at 8000 RPM). Then 1% of cell lysate was loaded and run on NuPAGE 4-12% Bis-Tris Gels (Invitrogen) according to the manufacturer's instructions. Proteins were transferred to PVDF membrane and subsequently probed with indicated antibodies (mouse anti-DDK or mouse anti-beta-actin). Primary antibody concentration was used at manufacturers recommendation (1:1000). HRP tagged secondary antibody was used to bind primary antibody at manufacturer's recommended concentration

(1:10,000). Immune complexes were visualized using ECL reagent (Pierce) on a BioRad ChemiDox XRS+ imagine system.

siRNA transfection

siRNA transfections were carried out 24 hours post cell plating in 96 well plates. RNAiMax transfection reagents were used and manufacturer's instructions were followed (Thermo-Fischer Scientific). Briefly, to each well was added 20 µl of transfection reagent containing siRNA at a final concentration in the well of 10 µM. Transfection master-mixes were prepared using the following recipe. Knockdowns were carried out using previously validated siNT2 (mock), siRAD51, siBRCA2, siRECQ5-1, siRECQ5 -2.

Standard transfection recipe

For each 100 µl of transfection mixture required:

100 µl FBS free media (Optimem)

20 pmol siRNA

1.2 µl RNAiMax transfection reagent

Results

Depletion of RECQ5 Diminishes HDR at DNA Nicks and DSBs

We assayed HDR using HEK 293T cells bearing the Traffic Light (TL) reporter stably integrated into the chromosome (Fig. 2.1A) [121, 123, 188]. DSBs and nicks were generated by CRISPR/Cas9 or CRISPR/Cas9^{D10A}, respectively, using guide RNAs gTL1, gTL2, or gTL9 targeted to sites within or immediately adjacent to the 38 bp region of heterology in the TL defective GFP gene (Fig. 3.1A). Cells were provided with either a duplex plasmid or single-stranded deoxyoligonucleotide (SSO) donor for repair. SSO donors complementary either to the nicked (cN) or intact (cI) strand support HDR at nicks via distinct pathways (Davis and Maizels, submitted; Fig. 3.1B), and both pathways were tested using target/donor pairs previously shown to promote efficient HDR (cN: gTL9/SSO-2; cI: gTL1/SSO-1).

We first asked if depletion of RECQ5 affects repair of nicks, as suggested by the reported role of RECQ5 in repair of oxidative damage [152, 160]. Treatment with an siRNA targeted to RECQ5 reduced the frequency of HDR at both DSBs and nicks, with DSB HDR reduced 3-fold and nick HDR reduced 4-fold with a dsDNA donor, 4-fold with a cI SSO donor and 2- fold with a cN SSO donor Fig. 3.1C). We were able to rescue this reduction by ectopic expression of siRNA resistant RECQ5, demonstrating that the effect was due specifically to a loss of RECQ5 (Fig. 3.2C). Treatment with siRECQ5 strongly reduced HDR at the TL reporter in HT1080 cells, a human fibrosarcoma line (Fig 3.2A), thus the observed dependence of HDR on RECQ5 was not cell type-specific. A similar effect of siRECQ5 was also evident at nicks generated by the I-AniI homing endonuclease when recombining with a SSO donor (cI) (Fig. 3.2B).

Ectopic Expression of RECQ5 Stimulates HDR at Nicks by SSO donors

RECQ5 is amplified in many tumors. We therefore asked whether ectopic expression of RECQ5 affects HDR at nicks and DSBs. Cells bearing the TL reporter, and targeted for nicks by gTL1 and gTL9 or DSBs by gTL1 were transiently transfected with a RECQ5 expression vector and a SSO or dsDNA repair donor (Fig. 3.3). Ectopic RECQ5 expression supplemented endogenous levels, to cause a 3-fold decrease in HDR supported by dsDNA donors at DSBs, a 2-fold decrease at nicks with a dsDNA donor and a 3-fold increase in HDR supported by SSO donors at nicks repaired by either the cN or cI pathway (Fig. 3.3B). Thus, increased RECQ5 expression promotes HDR at nicks with SSO donors but prevents recombination at nicks or DSBs with dsDNA donors. This activity at nicks and DSBs may thereby contribute to genomic instability when excess RECQ5 is present due to gene amplification, as is the case in many tumors [165, 166].

RECQ5 Interactions with RNAPII are not Responsible for its Promotion of HDR at Nicks

We asked if the effects of ectopic expression of RECQ5 on HDR depended upon interactions of RECQ5 with RNAPII by asking how HDR frequencies were affected if those interactions were abolished. Two distinct regions of RECQ5 mediate its interactions with RNAPII (Fig. 3.3A). The internal RNAPII interaction (IRI) region competes with TFIIS for binding to RNAPII, and interactions by this region are abolished by the RECQ5^{K598E} mutation [174, 176, 177]. The 91 amino acid SRI domain at the C-terminus of the protein binds the 3,5-phosphorylated CTD of elongating RNAPII, an interaction abolished in the RECQ5$^{1-899}$ deletion mutant [174, 177, 199]. Cells were treated with siRECQ5-1, which targets endogenous RECQ5 but not the ectopically expressed gene[176], and HDR assayed following transient ectopic expression. Expression was confirmed via western blot (Fig 3.3A). DSBs were targeted with gTL1; and nicks were targeted

either to the transcribed or non-transcribed strand, using gTL1 and gTL2, respectively; and HDR was supported by the SSO cI donor for both nicks.

HDR at DSBs with a duplex plasmid donor was reduced by 3-fold upon ectopic expression of RECQ5, and 7-fold upon expression of RECQ5^{K598E} or RECQ5$^{1-899}$ (Fig. 3.3C). Thus, the deleterious effect of excess RECQ5 upon HDR at DSBs is exacerbated by mutation of either of RECQ5's two RNAPII interaction domains.

HDR at nicks by the cI donor was stimulated upon ectopic expression of RECQ5^{K598E} or RECQ5$^{1-899}$ mutants to reach frequencies comparable to or greater than those achieved upon ectopic expression of RECQ5 (Fig. 3.3D). Notably, at nicks on the non-transcribed strand, the frequency of HDR was quite low in cells in which endogenous RECQ5 was depleted following siRNA knockdown, but rebounded upon expression of REC5, and especially RECQ5$^{1-899}$. Ectopic expression of this deletion mutant, which is unable to interact with the RNAPII CTD, also had the greatest stimulatory effect on HDR at transcribed strand nicks. Thus, interaction of RECQ5 with elongating RNAPII is modestly inhibitory to its ability to stimulate HDR at nicks on the non-transcribed strand.

RECQ5 Helicase Activity Promotes RAD51 Eviction

To determine whether the effects of ectopic expression of RECQ5 on HDR frequencies depend upon its helicase activity or on its interaction with RAD51, we assayed the effect of transient expression of derivatives bearing point mutations in the corresponding domains in cells (Fig. 3.4A) [112, 167, 182, 200, 201]. Protein expression was confirmed by western blot (Fig. 3.4A). Frequencies of HDR at DSBs were decreased relative to mock transfectants in cells expressing RECQ5 or RECQ5^{F666A}, which is deficient in RAD51 interaction (Fig. 3.4B). This decrease was dependent upon the RECQ5 helicase ATPase activity, as it was not evident in cells expressing

the RECQ5^{D157A} derivative, in which this activity is disrupted. Frequencies of HDR at nicks were 4-fold higher (cI) and 3-fold higher (cN) in cells expressing RECQ5 than in cells with mock transfection (Fig. 3.4C). Ectopic expression of RECQ5^{F666A} had no effect on HDR at nicks in either cI or cN HDR. Intriguingly at nicks, RECQ5^{D157A} ectopic expression had no effect on cN HDR as repair levels were equal to the mock treated cells but it did promote a 2-fold increase in cI HDR levels (Fig. 3.4C). This suggests that the helicase ATPase activity is absolutely required for RECQ5 promotion of HDR at cN nicks but not as important in the cI mechanism.

The results presented in Fig. 3.4B,C are consistent with the hypothesis that RECQ5 evicts RAD51 from DNA filaments. At DSBs, eviction would be predicted to inhibit canonical HDR and thus diminish HDR frequencies. At nicks, treatments that diminish RAD51 levels or activity stimulate frequencies of HDR by SSOs while at DSBs, eviction of RAD51 from DNA filaments would be predicted to decrease frequencies of HDR. The results in Fig. 3.4B,C further show that eviction of RAD51 by RECQ5 depends upon the RECQ5 helicase ATPase, as expression of RECQ5^{D157A} does not reduce HDR frequencies at DSBs and is important for enhancing HDR at nicks.

The HDR frequencies at nicks in cells expressing RECQ5^{F666A} were equal to mock transfectants (Fig. 3.4C). This suggests that the RAD51 interaction disrupted by the RECQ5^{F666A} mutation is crucial for promoting HDR at nicks in both the cI and cN pathways. At DSBs, ectopic expression of RECQ5^{F666A} was capable of inhibiting HDR nearly as efficiently as ectopic expression of full length RECQ5. This finding is curious as RECQ5 functions by removing RAD51 from DSB's and promoting SDSA. However, in these experiments, endogenous RECQ5 is still present. This may explain the stimulation of HDR by ectopic expression of the mutant that

lacks the RAD51 interaction domain. It may suggest a mechanism of cooperative eviction of RAD51 from DNA by RECQ5 helicase.

RECQ5 Regulates HDR in a RAD51 Dependent Manner

If the contrasting effects of RECQ ectopic expression on HDR at DSBs and nicks evident in Fig. 3.4B,C do indeed reflect the ability of RECQ5 to remove RAD51 from DNA filaments, then those effects should depend upon RAD51 DNA loading, and they should be abolished in cells treated with siBRCA2 or siRAD51. We tested this using HEK 293T cells bearing the TL reporter and treated with siRAD51 or siBRCA2 for 24 hours prior to transient expression of RECQ5. We then compared the fold change in HDR between cells with a mock transfection and cells transfected with ectopic RECQ5 (Fig 3.4D). Similar to our previous observations, RECQ5 expression increased HDR at nicks by 4.5- and 2.5-fold, respectively, when cI or cN donors were used. However, in cells pre-treated with siBRCA2 or siRAD51, ectopic expression of RECQ5 had no effect on HDR. This supports the hypothesis that RECQ5 interacts with RAD51 at nicks as when RAD51 is either depleted (siRAD51) or not loaded onto ssDNA (siBRCA2) ectopic expression of RECQ5 has no effect.

RECQ5 disrupts pre-synaptic RAD51 filaments

The results above suggested that exogenous RECQ5 regulates HDR by acting on RAD51 bound to DNA at nicks. We therefore asked how depletion of RECQ5 affected HDR frequencies at nicks in cells treated either to prevent formation of RAD51 filaments, or to inhibit activity of those filaments (Fig 3.5B). HEK 293T cells bearing the traffic light reporter were cultured in the presence of siRECQ5 or a nonspecific siRNA. Concurrently, they were treated with siBRCA2 or siRAD51; or transfected with a construct of the $RAD51^{K133R}$ mutant, which can bind but not hydrolyze ATP [202-205]. $RAD51^{K133R}$ forms filaments on ssDNA with compromised activity.

They can carry out strand invasion but do not readily dissociate from dsDNA rapidly and thus inhibit HDR with duplex DNA donors [202, 204-207]. In cells transiently expressing ectopic RAD51^{K133R}, DNA filaments will include endogenous RAD51 and RAD51^{K133R} mutant enzyme. Nicks were targeted with gTL1 or gTL9 and provided cI and cN donors respectively. The fold change in HDR was then compared in cells that received siRECQ5 with those that received control siRNA in addition to their other treatments.

Inhibition of RAD51 DNA loading, by treatment with siBRCA2 or siRAD51, or expression of RAD51^{K133R}, stimulated HDR at nicks by SSO donors, as predicted if RAD51 inhibits HDR by SSO donors (Fig. 3.5A). Depletion of RECQ5 reduced HDR frequencies at nicks 4-fold (cI) and 2-fold (cN) in cells in which RAD51 had not been depleted or inhibited (Fig. 3.5C,D). Depletion of RECQ5 did not affect HDR frequencies at nicks in cells treated with siBRCA2 or siRAD51, two conditions that would prevent RAD51 filament formation. In contrast, in cells expressing RAD51^{K133R}, which will create mixed filaments of RAD51 and RAD51^{K133R} that resist dissociation from dsDNA, depletion of RECQ5 caused a 4-fold (cI) or 6-fold (cN) reduction in frequencies of HDR at nicks by SSO donors, to a level similar to that observed in untreated cells. These results therefore establish that RECQ5 functions to evict RAD51 from presynaptic DNA filaments that have formed following creation of a nick. We have established that the helicase domain is crucial for the function of RECQ5 through ectopic expression experiments. The results above suggest endogenous RECQ5 is sufficient to remove RAD51^{K133R} filaments from ssDNA in vivo; RECQ5 has previously been shown to be capable of RAD51^{K133R} removal in vitro [182]. This suggests that the RECQ5 ATPase is the only ATPase required for the disruption of RAD51 filaments.

Conclusions

We have shown that RECQ5 activity helps determine what DNA repair pathway occurs at nicks and DSBs. Depletion of RECQ5 led to decreases in frequencies of HDR at both nicks and DSBs suggesting that at least some activity of RECQ5 is required for repair of these lesions. However, RECQ5 overexpression decreased HDR at DSBs and at nicks provided with a dsDNA donor. This indicates that while some RECQ5 activity is required for these pathways, too much can be just as inhibitory as too little. A depletion of RECQ5 may stimulate DSBs to undergo a crossover HDR event while overexpression may result in enhanced single strand annealing (SSA). Neither pathway will result in GFP+ cells in the TL reporter. Increased levels of RECQ5 specifically increased HDR at nicks with ssDNA donors. These findings are of increasing importance in light of recent observations that mutations or variations in expression level of RECQ5 are observed in many tumor types. Overexpression has recently been linked to poor prognosis in breast cancer while low expression is common in high proliferation rates in osteosarcoma. Our results show that excess RECQ5 can mimic RAD51 and BRCA2 knockout mutations, a hallmark of breast cancer, while low levels of RECQ5 can result in low HDR levels at both DSBs and nicks.

Our results provide detail on the mechanism of RECQ5 activity. We have demonstrated that RECQ5 acts in a BRCA2- and RAD51-dependent manner, likely removing RAD51 filaments from ssDNA. Using these results, we have created a model of known repair factor activity at the site of a nick (Fig. 3.5B). If a nick becomes unwound, rather than religated, RPA will coat the ssDNA, protecting the DNA from resection and decreasing the chance of spontaneous reannealing [100, 208]. The open conformation of the nick allows for alternative HDR. If BRCA2 displaces RPA and loads RAD51 onto the ssDNA, RAD51 will promote homology

search that results in reannealing of the nicked strand and its chromosomal complement. RAD51 prefers to bind dsDNA and thus helps keep the nick closed. Following RAD51 removal from the dsDNA, the nick can be religated. If RECQ5 removes RAD51 from ssDNA the nick will remain in an open configuration longer, thus promoting alternative HDR. The comparable effect of RECQ5 on alternative HDR frequencies with both cI and cN ssDNA donors suggest its activity may be upstream of donor interaction with the nicked target. The lack of an effect of RECQ5 overexpression upon RAD51 depletion suggests that the effect of RECQ5 is dependent upon RAD51, and in particular that RECQ5 is not the helicase responsible for opening up the nick in the first place. This mechanistic step remains an active area of study.

We had hypothesized that RECQ5 would require RNAPII for its function; however, it appears to act independently of RNAPII. Nicks on the transcribed strand resulted in higher alternative HDR frequencies than nicks on the non-transcribed strand, but RECQ5 overexpression gave an equal fold increase in HDR frequencies in both contexts. Disruption of the RECQ5 IRI domain had little to no impact while disrupting the SRI domain (which enables RECQ5 interaction with elongating RNAPII) increased its ability to promote alternative HDR. These results suggest that RNAPII may actually be acting to inhibit the ability of RECQ5 to promote alternative HDR by sequestering it away from nicks. The TL reporter only reports on HDR (GFP+ cells) and +2 frameshift mutations (mCherry+ cells), thus it is possible the RNAPII interaction of RECQ5 is required for repair of nicks that does not result in HDR or mutEJ.

Several functions of RECQ5 are analogous to functions of the prokaryotic helicases UvrD (in E.coli) and PcrA (in B. subtilis) [209-214]. Both prokaryotic helicases function in resolution of the conflict between replication and the transcription machinery; both have a 3’ to 5’ polarity, as

does RECQ5; and both can remove RecA, the prokaryotic homolog of RAD51, from DNA [209-211, 214-216]. Additionally, all three helicases have the ability to interact with RNA polymerases [214]. As previously mentioned, RECQ5 can stall RNAPII by inhibiting reinitiation. UvrD can stop and facilitate backtracking of RNAP which allows for repair of the damaged site while PcrA has a conserved C terminal domain which allows for interaction with RNAP and also prevents transcription associated genomic instability. We suggest that RECQ5 may play a role in resolution of the conflict between transcription and recombination in mammalian cells.

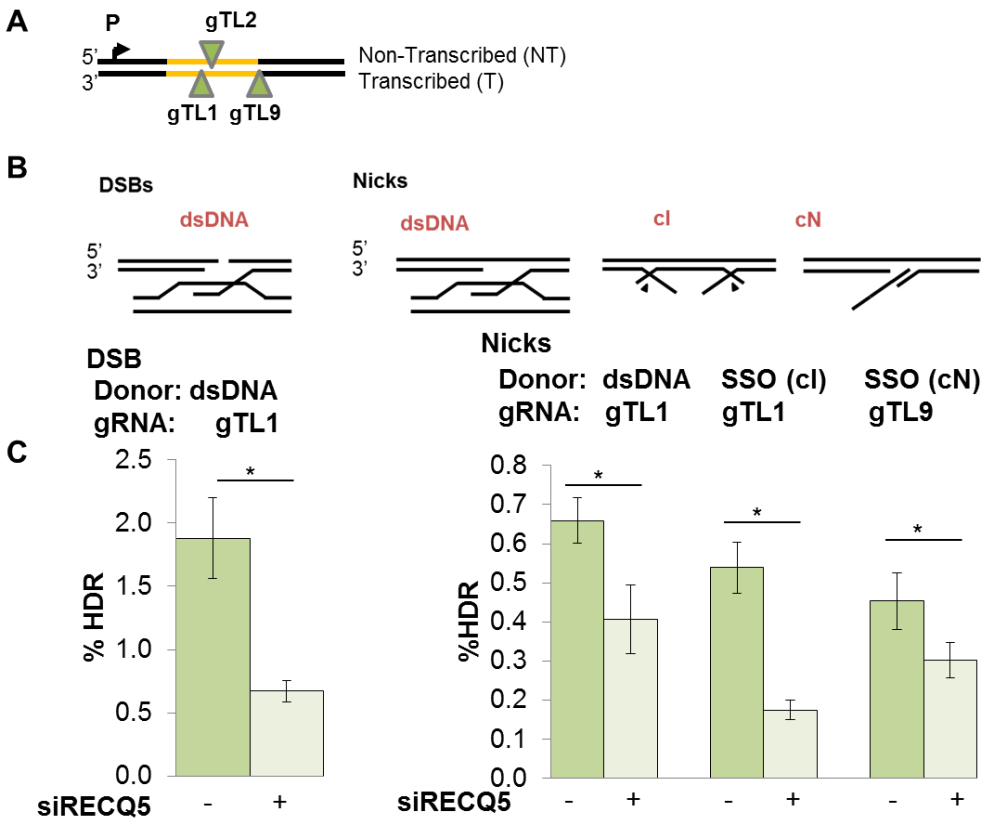

Figure 3.1 RECQ5 is required for Canonical and Alternative Homology Directed Repair (HDR)

Experiments were performed in HEK293T TL reporter cells. P values (*) of less than 0.05 are indicated.

(A) Diagram of gRNAs used to initiate nicks and DSBs in the TL reporter. All cut sites are targeted to the region of heterology (yellow) within the GFP region except for gTL9 which lies immediately adjacent to the site of heterology.
(B) Diagram of HDR at DSBs with a dsDNA donor and nicks with dsDNA and SSO (cI and cN) donors.
(C) HDR frequencies (GFP+ cells) at DSBs (targeted by Cas9 and gTL1) with a dsDNA donor and at nicks (Cas9 ^{D10A} with gTL1 or gTL9) with the SSO preferred donor were calculated from FACS measurements of GFP following siRNA treatment with siNT2(mock – green)) or RECQ5-2 (white).

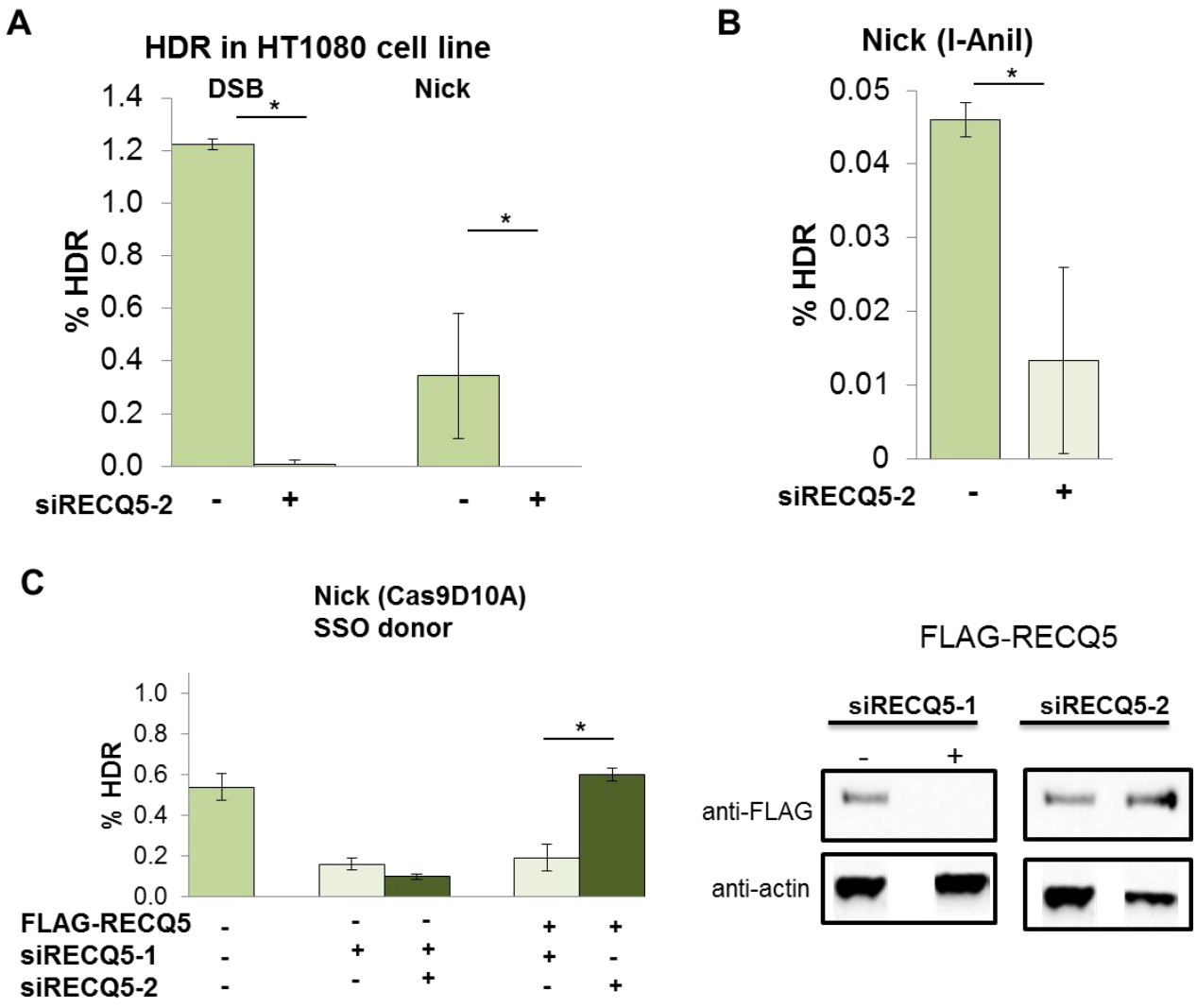

Figure 3.2 RECQ5 effects are consistent and can be rescued by ectopic expression

Experiments were performed in HEK293T, or HT1080 cells where indicated, TL reporter cells. P values (*) of less than 0.05 are indicated.

(A) Frequencies of HDR at DSBs (dsDNA donor) and nicks (SSO cI donor) targeted by Cas9 or $Cas9^{D10A}$ in HT1080 TL reporter cells pre-treated with either siNT2 (mock - green) or siRECQ5-2(white)
(B) Frequencies of HDR initiated by the I-AniI nickase (SSO cI donor) in HEK 293T TL reporter cells pretreated with either siNT2 or siRECQ5.
(C) Frequencies of HDR at nicks ($Cas9^{D10A}$ with gTL1 and SSO donor (cI)) in HEK 293T TL reporter cells following treatment with siRECQ5 -1 (white) or siRECQ5-2 (white) and subsequent expression of FLAG-RECQ5 (dark green) which is resistant to siRECQ5-2.
(D) Western blot showing levels of FLAG-RECQ5 in transient transfectants treated with siRECQ5-1 and siRECQ5-2

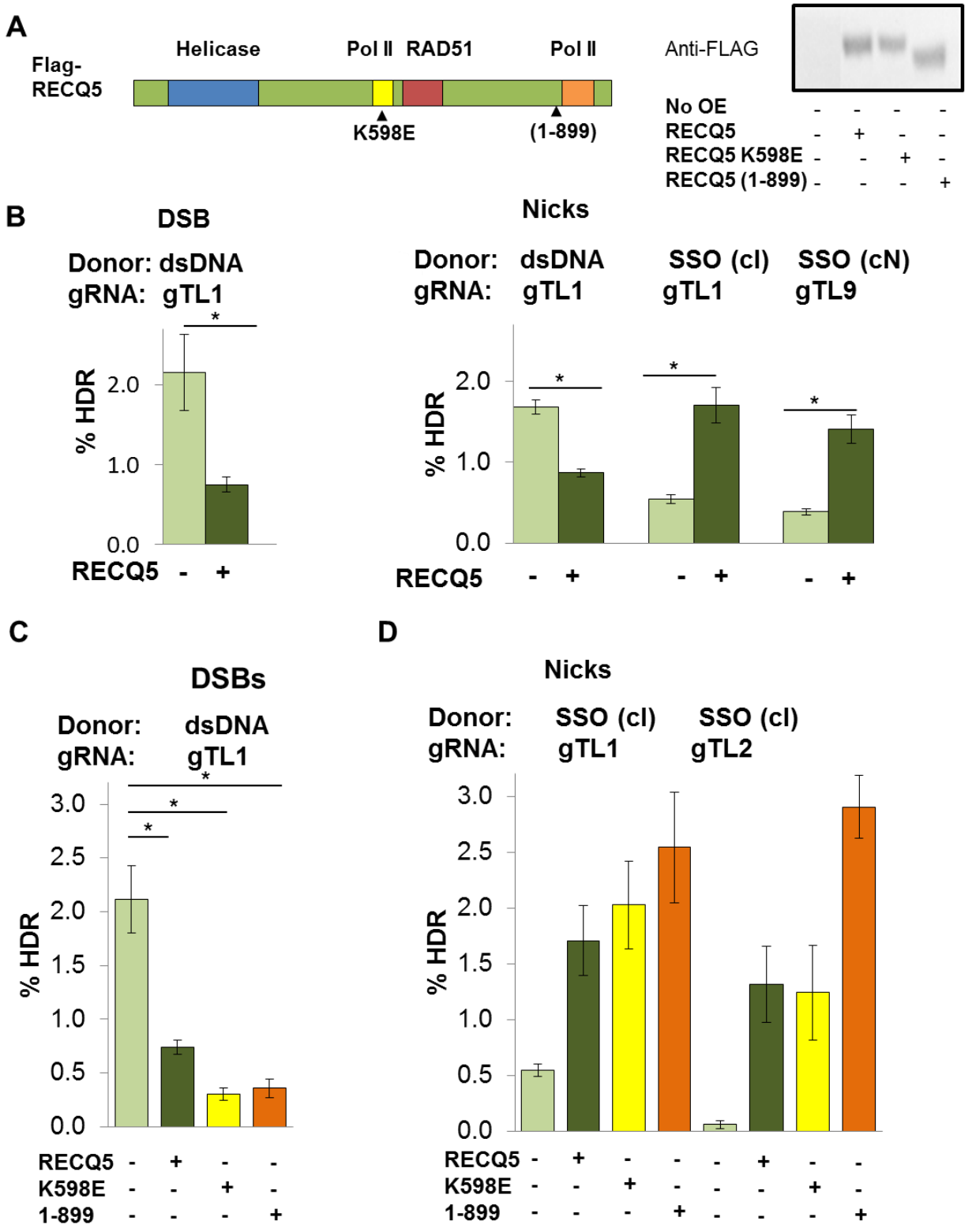

Figure 3.3 RECQ5 ectopic expression stimulates HDR at nicks by SSOs

Experiments were performed in HEK293T TL reporter cells. P values (*) of less than 0.05 are indicated.

(A) Diagram of RECQ5 and the point mutation that disrupts the IRI (K598E) and truncation mutation (1-899) that disrupts the SRI RNAPII interaction domains.
(B) Frequencies of HDR at DSBs (left) and nicks (right) targeted by Cas9 or $Cas9^{D10A}$ in HEK 293T TL reporter cells provided with indicated donor. Cells were transfected with empty vector (light green) or the FLAG-RECQ5 expression vector (dark green).
(C) Frequencies of HDR at DSBs in HEK 293T TL reporter cells treated with Cas9, gTL1, and provided a dsDNA plasmid donor with either a mock plasmid or RECQ5, $RECQ5^{K598E}$(yellow), or RECQ5 (1-899) (orange) expression plasmids.
(D) Frequencies of HDR at nicks in HEK 293T TL reporter cells treated with $Cas9^{D10A}$, gTL1 (transcribed strand nick) or gTL2 (non-transcribed strand nick), and provided the preferred SSO donor with either a mock plasmid or RECQ5, $RECQ5^{K598E}$, or RECQ5 (1-899) expression plasmids.

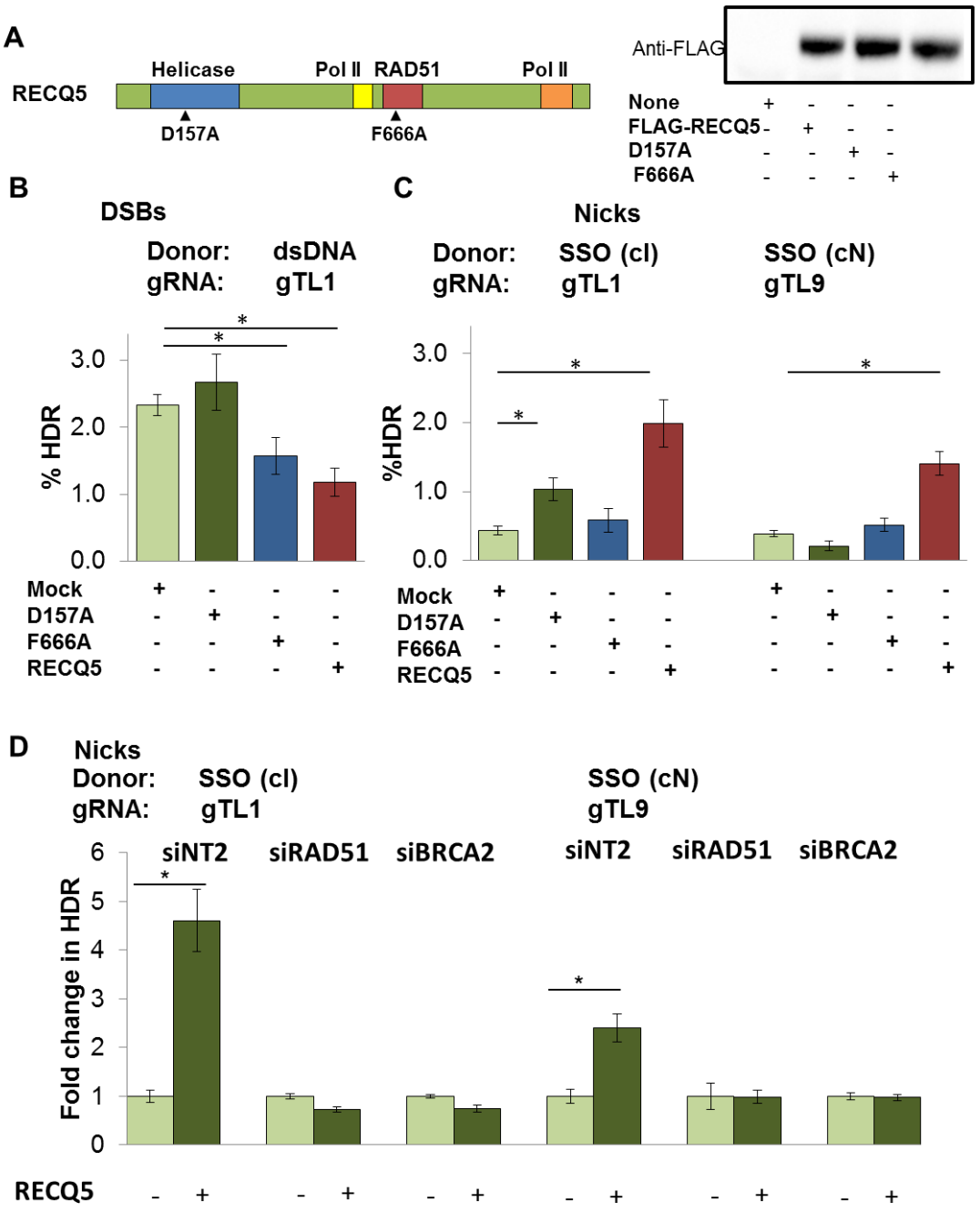

Figure 3.4 Ectopic expression of RECQ5 depends upon its RAD51 interaction domain and helicase ATPase activity to promote HDR at nicks

Experiments were performed in HEK293T TL reporter cells. P values (*) of less than 0.05 are indicated.

(A) Diagram of RECQ5 and the point mutations that disrupt the helicase ATPase (D157A) and RAD51 interaction domains (F666A).
(B) Frequencies of HDR at DSBs targeted by Cas9 and gTL1 in HEK 293T TL reporter cells, with indicated donors and RECQ5 (dark green), RECQ5^{D157A} (blue), RECQ5^{F666A} (red), or empty expression vectors (light green).
(C) Frequencies of HDR at nicks in HEK 293T TL reporter cells treated with Cas9^{D10A} and indicated gRNA, donor, and RECQ5 expression vector.
(D) Fold change in HDR at nicks in cells treated with indicated siRNA with and without ectopic RECQ5 expression (- and +, respectively). siNT2, non-specific control siRNA. HDR fold change was calculated by dividing HDR frequencies of samples expressing ectopic RECQ5 relative to those transfected with empty vector.

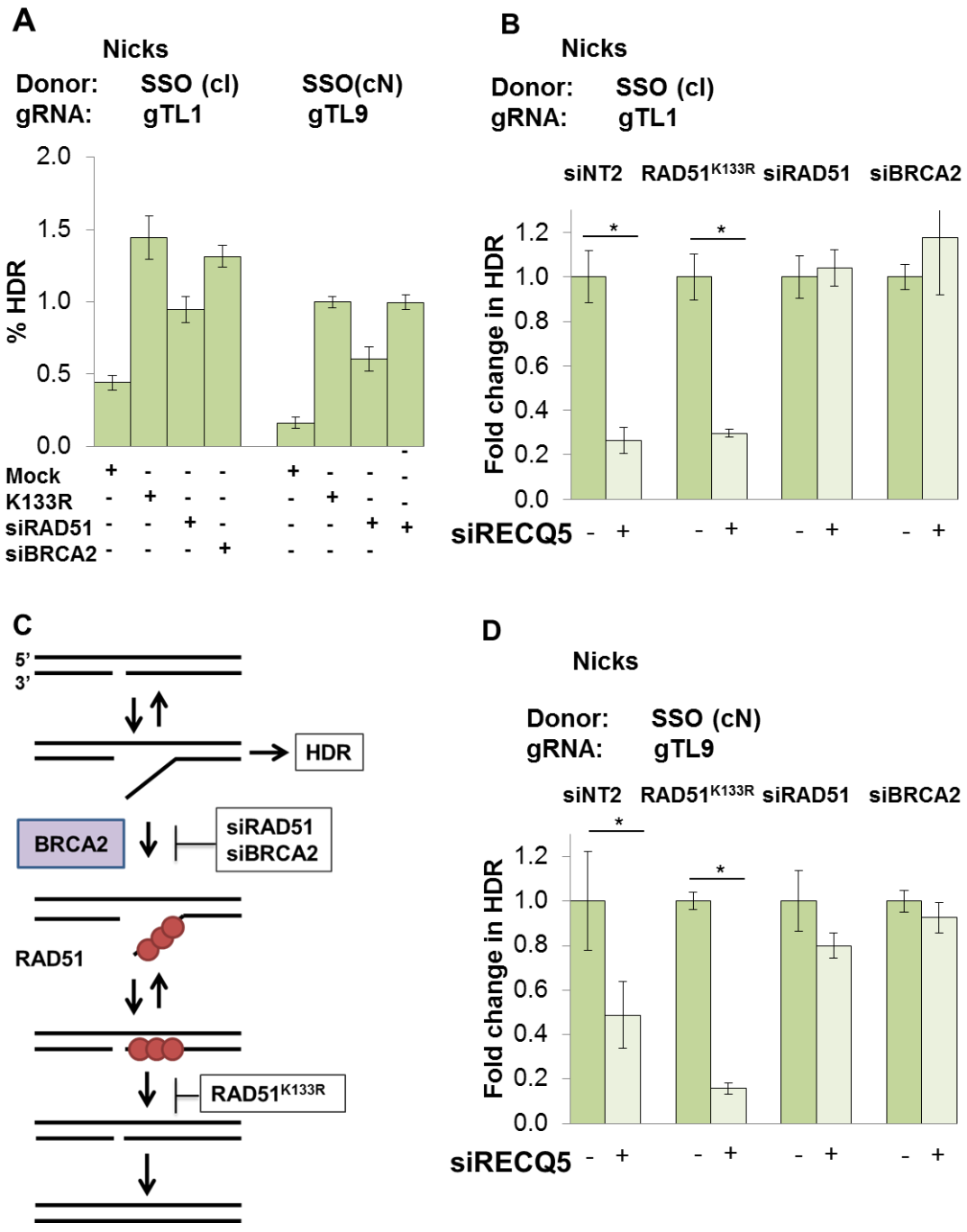

Figure 3.5 RECQ5 disrupts RAD51 pre-synaptic filaments

Experiments were performed in HEK293T TL reporter cells. P values (*) of less than 0.05 are indicated.

(A) Frequencies of HDR at nicks in HEK 293T TL reporter cells treated with Cas9^{D10A} and indicated gRNA, donor, and expression vector.

(C) Model for HDR at a nick. BRCA2 can load RAD51 onto open nicks which promotes reannealing and subsequent religation. RAD51 filament formation can be inhibited by depletion of BRCA2 or RAD51 with siRNA. Filament resolution can be inhibited by expression of the $RAD51^{K133R}$ dominant negative mutant.
(B,D) Fold change in HDR at nicks with and without siRECQ5 treatment. HEK 293T TL reporter cells were treated with siNT2, $RAD51^{K133R}$, siRAD51, or siBRCA2 and nicks were targeted with $Cas9^{D10A}$ and either gTL1 or gTL9. The preferred SSO donor was provided (cI for gTL1, cN for gTL9). Samples were treated with either siNT2 or siRECQ5. HDR fold change was calculated by dividing HDR frequencies of samples treated with siRECQ5 relative to samples treated with siNT2.

Chapter 4 RECQ5 PROMOTES MUTAGENESIS AT NICKS

In Chapter 3 we provided evidence that RECQ5 regulates HDR at nicks by disrupting RAD51 presynaptic filaments. Here we address the ability of RECQ5 to regulate mutagenic end-joining (mutEJ), scored as the frequency of mCherry+ cells in the TL reporter assay. RECQ5 levels were modulated by depletion or ectopic expression of RECQ5. DSBs or nicks were targeted by transient transfection of constructs that expressed Cas9 or Cas9^{D10A} nickase along with a guide RNA. Use of gTL1 and gTL2 allows us to target nicks to specific sites on the transcribed or non-transcribed strand. Cells were provided with either a SSO or dsDNA donor or no donor to determine if the presence of a donor had an effect on mutEJ. Briefly, we discovered that RECQ5 promotes mutEJ at nicks while having minimal effects at DSBs The depletion of RECQ5 results in a decrease in mutEJ at nicks while overexpression results in an increase in mutEJ proportional to the increase observed in HDR. We sequenced populations of cells that had undergone mutEJ to find the mutagenic signature associated with increased RECQ5 expression and identified a unique mutEJ signature at nicks (Fig. 4.3,4). This is of special interest when coupled with the observation that RECQ5 levels are dramatically increased in many tumors, implicating RECQ5 as a potential driver of mutagenesis at nicks.

Materials and Methods

Materials

Plasmids, siRNA, and Cell Lines

Plasmids and cell lines used are identical to those described in the Materials section for Chapter 3.

Sequencing Primers

TGGTGCCCATCCTGGTCGAG (Forward)

CAGCTTGCCGGTGGTGCAGA (Reverse)

Methods

Traffic Light Reporter assay and transfections

The TL reporter assay and subsequent data analysis as well as transfection with siRNA and plasmids were carried out as described in the Methods section of Chapter 3**.**

Sequencing library preparation

Genomic DNA was prepared from a confluent 10 cm plate of cells 72 hours post transfection. A DNeasy genomic DNA prep kit (Qiagen) was used to prepare the DNA by following the manufacturer's instructions. A 150 bp region surrounding the TL reporter in the genomic DNA was amplified by PCR. This product was then purified and concentrated using the Zymo Researcher Clean and Concentrate kit. This sample was then delivered to our collaborators at the UW Precision Diagnostics Center for 100 bp paired end Illumina sequencing.

Sequencing data analysis

We received two FASTQ files of sequencing data. The files were merged such that each read was joined with its paired read so that we had one FASTQ file of 150 nt long sequences. Only

sequences with an average quality score above 30 and less than 5% N's were merged. This was accomplished using the PRINSEQ program (http://prinseq.sourceforge.net/). The merged FASTQ file was then uploaded to the CRISPRESSO sequence alignment tool (crispress.rocks) which allows sequence comparison with a reference sequence (the PCR amplicon). The 30 nt to either side of the cut site were used as a window for calling NHEJ, insertions, or deletions to limit the impact of N's found at the end of the reads. As point mutations (green lines) were not expected and were of low and equal quantity in all samples, they were used as a measure of background.

Results

RECQ5 increased mutagenesis at nicks but not at DSBs

We initially asked whether alterations of RECQ5 cellular levels would impact mutEJ at nicks and DSBs (Fig. 4.1B). We targeted $Cas9^{D10A}$ and Cas9 to the transcribed strand of the TL reporter using gTL1 in cells that had been treated with a mock siRNA or siRECQ5, or were transiently transfected to permit ectopic expression of RECQ5. We observed a significant 10-fold decrease in mutEJ at nicks upon depletion of RECQ5, indicating that RECQ5 can stimulate mutEJ. The transient transfection of ectopic RECQ5 resulted in a similarly significant 4-fold increase in mutEJ frequencies at nicks. While the magnitudes differ, the trends in mutEJ and HDR frequencies are very similar upon RECQ5 depletion or overexpression. Interestingly, depletion or overexpression of RECQ5 did not have any significant impact on mutEJ at DSBs (Fig 4.1B). This is in agreement with previous reports which show no impact of RECQ5 on NHEJ [183], it suggests there may be a difference in the process of mutEJ at nicks and DSBs.

We next asked if the presence of a donor affected the levels of mutEJ or the ability of RECQ5 to impact those levels (Fig 4.1C). To test this we targeted nicks to the transcribed strand of the TL reporter using $Cas9^{D10A}$ and gTL1. We then provided cells with either dsDNA plasmid or SSO donor or no donor and subsequently transiently transected with an empty vector (mock) or a RECQ5 expression vector. While the levels of mutEJ were relatively low at nicks (05-.1% of cells), in physiological contexts cells experience approximately 10000 nicks per day. Thus even low frequencies of mutagenesis may be potent drivers of tumorigenesis. The overexpression of RECQ5 increased the levels of mutEJ to approximately 0.14% independent of donor indicating that RECQ5 is likely acting independent of donor interaction with the nick.

Having compared the effect of donors on mutEJ, we next compared the effect of the location of the nick (Fig 4.1D). We transiently transfected HEK 293T TL reporter cells with $Cas9^{D10A}$ to nick the target. $Cas9^{D10A}$ was targeted to either the non-transcribed strand (gTL2) or to the transcribed strand (gTL1) and mutEJ frequencies scored. Ectopic expression of RECQ5 caused a significant increase in mutEJ at all sites (2-2.5-fold). We found no difference in the frequencies of mutEJ among cells that was dependent upon the location of the targeted nick.

The increase of mutEJ at nicks depends upon the helicase and RAD51 interaction domains of RECQ5

We next asked what domains of RECQ5 were important for promoting mutEJ at nicks (Fig. 4.1F). Cas9 and $Cas9^{D10A}$ were transiently transfected in HEK 293T TL reporter cells. Cas9 DSBs were targeted with gTL1 while $Cas9^{D10A}$ nicks were targeted to both the transcribed strand (gTL1) and non-transcribed strand (gTL2). Cells were then transfected with constructs expressing RECQ5, RECQ5 D157A (helicase ATPase mutant), RECQ5 F666A (nonfunctional RAD51 interaction domain), RECQ5 K598E (disrupted IRI RNAPII interaction domain), or RECQ5 (1-899) which lacks the CTD RNAPII interaction domain.

Nicks targeted to the transcribed strand by gTL1 showed increased levels of mutEJ upon RECQ5 ectopic expression (Fig 4.1F). Ectopic expression of full length RECQ5 resulted in a 10-fold increase in mutEJ levels. Interestingly, no effect on mutEJ was observed when RECQ5 was ectopically expressed in cells that were treated with siRAD51; and a small decrease in mutEJ was observed in BRCA2-depleted cells ectopically expressing RECQ5. Thus, similar to HDR, the effect of ectopic expression of RECQ5 is dependent upon RAD51 and BRCA2. mutEJ levels did not increase upon ectopic expression of RECQ5 D157A or RECQ5 F666A. This indicates

that the RECQ5 helicase ATPase and RAD51 interaction domains are vital for the ability of RECQ5 to enhance mutEJ at transcribed strand nicks. Interestingly, these functional domains were also required to enhance HDR at transcribed strand nicks (Fig. 3.4). Disruption of the IRI domain had no impact on the ability of RECQ5 to enhance mutEJ at nicks as expression of that mutant increased mutEJ frequencies to an equal degree as expression of full length RECQ5. Expression of RECQ5 which could not interact with elongating RNAPII due to a truncation that removes its C terminal RNAPII interaction domain increased mutEJ at a nick by 16-fold relative to mock transfectants, 1.5-fold above the effect of expression of full length RECQ5. This pattern is again consistent with what we observed in analysis of HDR (Fig 3.3). Disruption of the RECQ5 interaction with elongating RNAPII enhanced its ability to promote both mutEJ and HDR.

Similar but not identical effects were observed at nicks on the non-transcribed strand (Fig. 4.1F). RECQ5 ectopic expression increased mutEJ relative to mock by 3-fold. This increase was not observed when either RECQ5 D157A or RECQ5 F666A were ectopically expressed indicating the helicase and RAD51 interaction domains are just as crucial in promoting mutEJ at nicks on both strands. Disruption of the RNAPII interacting domains of RECQ5 differed somewhat at nicks targeted to either strand, where disruption of the IRI RNAPII interaction domain (K598E) significantly decreased mutEJ frequencies. RECQ5 (1-899) ectopic expression had comparable effects to ectopic expression of full length RECQ5. It is difficult to interpret these changes as they are small. The RNAPII interaction domains could be playing a crucial role in the rate of gene correction or mutation; a role which would not be scored by the TL reporter.

Having shown that RECQ5 requires similar domains to enhance mutEJ at both transcribed and non-transcribed strand nicks, we asked if any of the RECQ5 constructs affected

DSB mutEJ frequency (Fig. 4.1G). We ectopically expressed RECQ5 and its derivatives (WT, D157A, F666A, K598E, 1-899) in cells which were co-transfected with Cas9 and gTL1. Consistent with previous observations, full length RECQ5 had no effect on the levels of mutEJ at DSBs. Likewise, disruption of the helicase ATPase (D157A) and RAD51 interaction domains (F666A) had no impact nor did disruption of the IRI RNAPII interaction domain (K598E).

Sequencing confirms mutEJ at nicks and DSBs

The TL reporter only reports mutEJ events that result in a particular frameshift (+1 to +2). Thus any repair pathway which promotes an alternative mutagenic form of repair (large insertions/deletions, +1 to +3 or +1 shifts, etc.) could result in mutagenesis that was hidden from the TL reporter. In order to identify all insertions and deletions at the site of the nick, we prepared genomic DNA for deep sequencing from TL reporter HEK 293T cells targeted for nicks by gTL2, and otherwise treated as described below. We did not sort for mCherry+ cells as this will predetermine what mutations we can observe as they will all, by necessity, result in a +2 frameshift. Six replicates of each sample were created. At 72 hours post transfection, three of the samples were collected to quantify frequencies of mCherry+ cells by flow cytometry. The other three samples were pooled and prepared for sequencing analysis. Briefly, I prepared genomic DNA from the unsorted samples and PCR amplified the TL reporter sequence to create DNA of the proper length for sequencing. This PCR product was then given to our collaborators in the Michael Dorschner lab (5^{th} floor H wing, HSB, UW, Seattle). There, the PCR fragments had adaptor and barcode sequence ligated onto the ends so that they could be sequenced in parallel using 100 base paired-end Illumina sequencing. The sequence files were obtained with approximately 1 million reads per sample. These were filtered for accuracy and quality of the reads and then used in the CRISPRESSO alignment program [217]. This program allows for the

comparison of a large number of sequences with a reference sequence. While there are many outputs available, we initially chose to compare the mutEJ frequency observed through sequencing with that observed by scoring mCherry+ cells.

We compared the frequencies of mutagenesis obtained via FACS TL reporter analysis and the CRISPRESSO program (Fig. 4.2). Both FACS and sequencing analysis showed low background levels of mutagenesis at the nick site in non-treated cells. DSBs at the gTL2 target site resulted in mutEJ frequencies of 31.5% as quantified by FACS. This is much higher than frequencies observed at gTL1 (2.5%) as gTL2 insertions and deletions are less likely to move a stop codon present in the TL reporter (upstream from gTL2 but downstream of gTL1) into frame. The high frequencies provide an excellent positive control for sequencing analysis. Analysis of sequences surrounding the cut site showed the highest levels of mutation in the Cas9 gTL2 treated sample at 25.7% after background levels are subtracted. The sample in which nicks were targeted by gTL2 yielded frequencies of 0.14% mutEJ as assayed by scoring mCherry+ cells vs. 1.4% by sequencing analysis; upon ectopic RECQ5 expression frequencies of 1.1% vs 3.3%; upon siBRCA2 treatment, 3.8% vs 10.3%; and in response to the combination of siBRCA2 treatment and RECQ5 ectopic expression, 2.3% vs 4.4%. At nicks, the frequency of mutagenesis reported by sequencing was always higher than that reported by the TL reporter. In most samples, it was 2- to 3-fold higher. This is expected as the TL reporter reports only +2 frameshift mutations, thus total levels of mutagenesis might be expected to be roughly 3-fold higher when scored by sequencing. However, at DSBs, these relative frequencies were 31.5% vs, 25.7%. This is interesting for two reasons. There is likely a bias in our sequencing protocol against reporting DSB initiated mutagenesis. This could be due to extensive resection resulting in +2 frameshift mutations which effectively delete the region recognized by PCR primers used for amplification;

or could be the result of a bias in gTL2 targeted DSBs to induce almost solely +2 frameshift mutations. This bias may be due to local micro-homologies in the sequence at the TL reporter that guide mutEJ pathways. The distinct patterns observed in consistency of reported frequencies between nicks and DSBs suggest that specific mechanisms of mutEJ operate at nicks and DSBs and that these may result in unique mutagenic signatures. It should be noted that the patterns of frequencies of mutEJ determined by sequencing matched those determined by scoring mCherry+ cells, with DSBs exhibiting by far the highest mutEJ frequencies, followed by Cas9 ^{D10A} nicks with siBRCA2, then Cas9^{D10A} nicks with siBRCA2 and RECQ5 ectopic expression, followed by Cas9^{D10A} nicks with RECQ5 ectopic expression, and finally Cas9^{D10A} nicks (Fig. 4.2).

Analysis of mutation signatures at nicks and DSBs

We next examined the signature of mutation in the aforementioned conditions. Using CRISPRESSO we were able to examine the likelihood of finding a mutation (deletion, insertion, or point mutation) along with the average length of deletion or insertion at any given site. We can thus report on the probability of finding any base deleted, inserted or mutated in a given population, which defines a mutational signature. While this is not the only way to analyze this data, it has produced some interesting contrasts.

We first established a background mutational signature by sequencing non-transfected cells (Fig 4.3A), where no mutEJ was evident by either assay. The mutations noted in this sample are due to PCR and sequencing errors. This sequencing footprint shows very low levels of point mutation (green), deletion (purple), and insertions (red). The frequency of point mutations is of particular use for analysis of other samples going forward as the levels observed are consistent across all samples and provides a marker for the background cut-off.

Analysis of DSBs targeted by gTL2 revealed a clear and striking mutational signature (Fig 4.3B). DSBs show a strong peak of deletions (purple) centered on the site of the DSB. The height of this peak reached a maximum just upstream of the cut site with a value of 12%, indicating that this base was deleted in 12% of the sequences. These breaks averaged 15 nt in length. Notably, there did not seem to be a single type of deletion which would have resulted in a sharp box as seen in the example rather than the sloping peak observed. While the deletions were not all the same, they were found only within 20 nt to either side of the cut site. This pattern is expected based on the typical sequence loss at a DSB in NHEJ [218]. Insertions (red) were also evident at above background (green point mutation frequency line) levels. The insertions averaged 1-3 nt in the region directly surrounding the target site. While deletions could be observed up to 15 nt distant from the cut site, the insertions were only found within 5 nt upstream of the cut site.

Analysis of cells treated with $Cas9^{D10A}$ and gTL2 to nick the non-transcribed strand showed mutation signatures at background levels (Fig. 4.4A). RECQ5 does not play a role in NHEJ but its ectopic expression has been shown to stimulate mutEJ from 2- to 10-fold as measured by scoring mCherry+ cells. Analysis of the sequences at nicks targeted by gTL2 in cells transfected with a RECQ5 expression construct revealed a pattern of repair at nicks distinct from that at DSBs and at nicks in cells depleted for BRCA2 (Fig. 4.4B). There was no increase in insertions above background levels, but deletions were considerably enhanced. The region most commonly deleted was not centered on the nick site, but 15 nt downstream. These deletions averaged approximately 15 nt in length.

Treatment of HEK 293T cells with siBRCA2 prior to nicking the non-transcribed strand caused a 15-fold increase in mutEJ frequencies as scored as mCherry+ cells (Fig. 4.4C). Analysis

of the mutagenic signature revealed an interesting pattern. Deletions were most frequent at the site of the nick and at a region 15 nt downstream in what appears to be a bimodal distribution. The deletions averaged 20 nt in length. This indicates a wide range of similar length deletions as opposed to deletions that begin in the same area but extend different lengths. Interestingly, deletions 15 nt downstream from the nick site were not observed as products of DSBs. The presence of a unique mutagenic signature at nicks in cells depleted of BRCA2 suggests that there may be a unique mechanism of mutagenesis active at nicks.

We next examined the effect of combined BRCA2 depletion and RECQ5 ectopic expression at nicks targeted by gTL2 (Fig. 4.4D). The mutagenic signature obtained from sequence analysis suggests that there may be a slight decrease in downstream deletions which contrasts with the increase in deletions observed in response to either treatment alone. This observation will require further testing in order to validate. We also observed a single peak of deletions centered at the nick site which contrasts with other patterns of mutation. The deletions averaged 12 nt in length, slightly smaller than the 20 nt deletions observed in siBRCA2 treated cells or the 15 nt deletions of the cells ectopically expressing RECQ5. This may be useful in understanding the resection dynamics once more of the mechanisms of mutEJ at nicks is understood.

Conclusions

Mutagenic outcomes at nicks are crucial to understand. Nicks are the most common form of DNA damage with 10,000 occurring in each cell per day. While HDR at nicks does occur, it is limited to occasions when a donor is present. Mutagenesis does not share this limitation and is thus a potential driver of tumorigenesis. In order to understand how nicks can result in mutations we looked at both the frequency and mutagenic signature of Cas9 targeted DSBs and Cas9^{D10A}

targeted nicks while depleting key DNA repair factors (RAD51, BRCA2, RECQ5) or ectopically expressing RECQ5. Consistent with previous publications, DSBs initiated far higher levels of mutEJ than nicks in the TL reporter as measured by scoring the frequency of mCherry+ cells resulting from frameshift mutations. Similar levels of mutEJ were observed at nicks generated by $Cas9^{D10A}$ nicks at gTL1 (0.078%), gTL2 (0.056%), and gTL9(0.054%) , suggesting that the mechanism of nick induction and the distinction between nicks on the transcribed and non-transcribed strands do not affect mutEJ frequency. Ectopic expression of RECQ5 in these samples initiated higher levels of mutEJ, typically increasing mutEJ 2- to 5-fold, while ectopic expression of RECQ5 at DSBs had no effect.

Similar to its role in promoting HDR with SSO donors at nicks, RECQ5 required an active ATPase and RAD51 interaction domain to increase mutEJ frequencies. Neither of the two RNAPII interaction domains were required for the observed increase in mutEJ. Removal of the SRI domain of RECQ5 actually increased the ability of RECQ5 to promote mutEJ at nicks. Depletion of RAD51 or BRCA2 increased mutEJ frequencies although, intriguingly, RAD51 depletion did so less than BRCA2 depletion. This suggests that BRCA2 may be impacting mutEJ frequencies in mechanisms distinct from RAD51 loading on DNA. When either BRCA2 or RAD51 were depleted in conjunction with ectopic expression of RECQ5, the frequencies of mutEJ as measured by scoring mCherry+ cells either decreased slightly or were the same as the levels observed upon RAD51 or BRCA2 depletion alone. This suggests that RECQ5 ectopic expression may be promoting mutEJ in a similar mechanism to BRCA2 or RAD51 depletion.

Our results suggest that the frequency of mutEJ, as scored by mCherry+ cells in the TL reporter, at nicks is linked to the ability of the cell to rapidly religate a nick. Disrupting this through depletion of RAD51 or BRCA2 or ectopic expression of RECQ5 promotes higher levels

of mutEJ. This suggests that the longer a nick remains 'open' or unrepaired, the more likely it is for the nick to undergo mutEJ.

Analysis of the sequence surrounding the Cas9 and Cas9^{D10A} target site revealed interesting differences between the mutagenic signatures of DSBs and nicks. DSBs primarily resulted in deletions averaging 15 nt centered on the cut site. These deletions fell within 10 nt to either side of the break. This pattern is consistent with both NHEJ and altNHEJ. Insertions were also observed and averaged 2 nt in length though these took place at a far lesser frequency than deletions. Nicks, on their own, did not initiate mutEJ enough to be above background noise. However, when nicks were targeted with Cas9^{D10A} concurrent with depletion of BRCA2 or ectopic expression of RECQ5, the levels of mutEJ rose above background and displayed striking differences from the mutagenic signature created at DSBs. When BRCA2 was depleted, nicks showed deletions centered at both the site of the nick and 15 bases downstream. Similar to BRCA2 depletion, ectopic RECQ5 expression promoted deletions 15 bases downstream but did not cause deletions at the cut site. The deletions were both of similar size (15-20 nt) suggesting a similar mechanism of mutEJ may be taking place but that the location may be differentially specified or restricted. RECQ5 travels in the 3' to 5' direction which would carry it upstream from the site of a gTL2 targeted nick, suggesting that the helicase activity alone of RECQ5 is not the reason for the deletions. Curiously when BRCA2 was depleted concurrent with RECQ5 ectopic expression nicks initiated deletions only at the site of the nick but not downstream. While these deletions (~12nt) were slightly smaller than those observed at nicks with depleted BRCA2 (~20nt) or ectopic RECQ5 expression (~15 nt) alone, they are close enough in size to suggest a similar mechanism may be acting in all examples. Why these treatments lead to different locations of deletions remains unknown and is an active area of research in the lab.

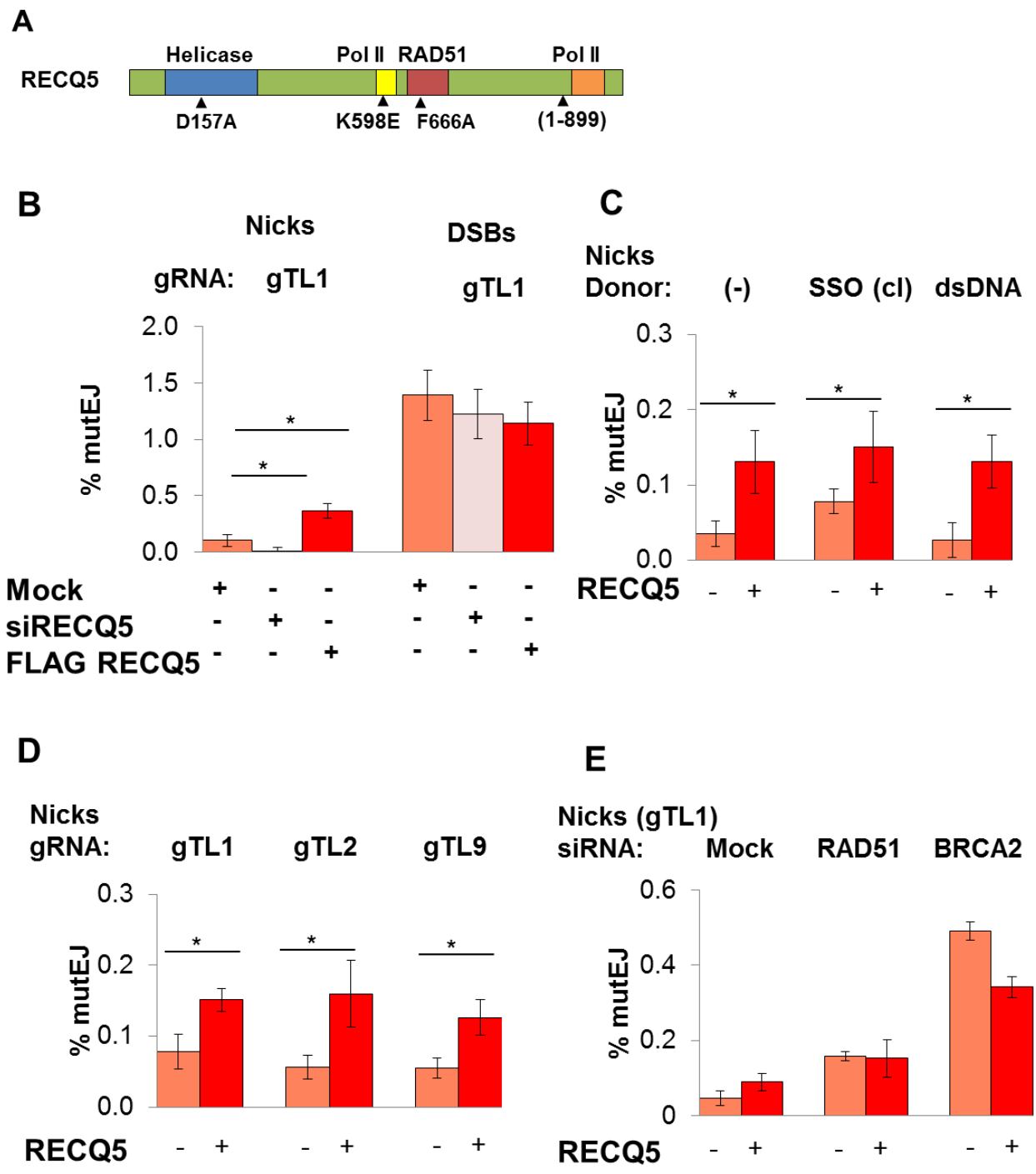
A
RECQ5
Helicase
Pol II
RAD51
Pol II
D157A
K598E
F666A
(1-899)
B
Nicks
DSBs
gRNA: gTL1
gTL1
% mutEJ
2.0
1.5
1.0
0.5
0.0
*
*
Mock + - - + - -
siRECQ5 - + - - + -
FLAG RECQ5 - - + - - +
C
Nicks
Donor: (-) SSO (cl) dsDNA
% mutEJ
0.3
0.2
0.1
0.0
*
*
*
RECQ5 - + - + - +
D
Nicks
gRNA: gTL1 gTL2 gTL9
% mutEJ
0.3
0.2
0.1
0.0
*
*
*
RECQ5 - + - + - +
E
Nicks (gTL1)
siRNA: Mock RAD51 BRCA2
% mutEJ
0.6
0.4
0.2
0
RECQ5 - + - + - +

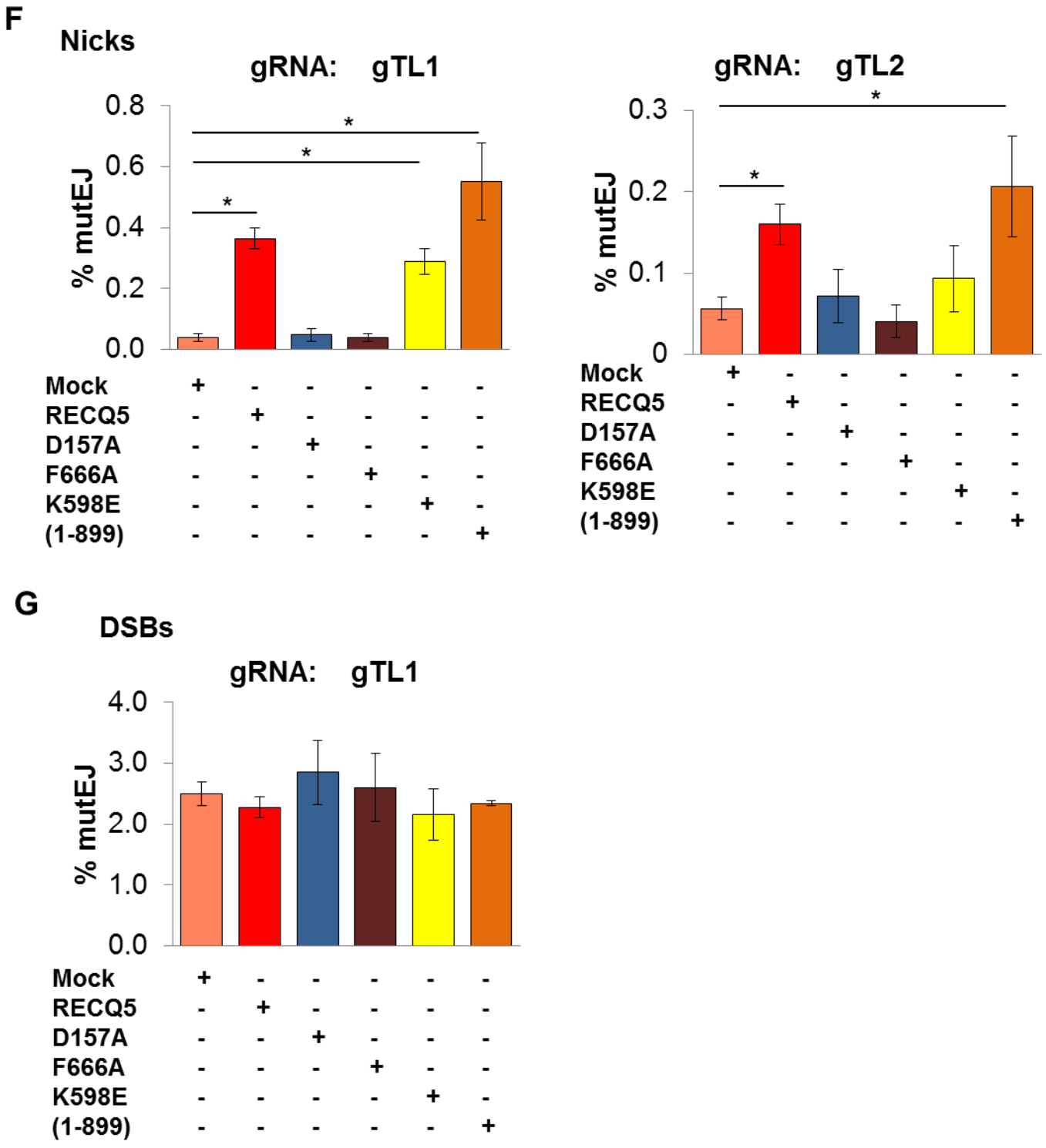

Figure 4.1 RECQ5 promotes mutEJ at nicks but not at DSBs

Experiments were performed in HEK293T TL reporter cells. P values (*) of less than 0.05 are indicated.

(A) Diagram of RECQ5 with indicated point mutations which disrupt the labeled domains.

(B) Frequencies of mutEJ at nicks and DSBs in HEK 293T TL reporter cells provided with $Cas9^{D10A}$ or Cas9 expression constructs, indicated gRNA and donor, and siNT2 (pink), siRECQ5 (white) or ectopic RECQ5 expression vectors (red).

(C)Frequencies of mutEJ at nicks in HEK 293T TL reporter cells provided with $Cas9^{D10A}$ expression construct and gTL1; no donor, SSO (cI) donor, or a dsDNA donor; and indicated expression constructs.

(D) Frequencies of mutEJ at nicks in HEK 293T TL reporter cells provided with $Cas9^{D10A}$ expression construct, indicated gRNA, and indicated donor and expression constructs.

(E) Frequencies of mutEJ at nicks in HEK 293T TL reporter cells treated with siNT2, siRAD51 or siBRCA2 and provided with Cas9D10A and indicated donor and expression construct.

(F) Frequencies of mutEJ at DSBs in HEK 293T TL reporter cells provided with $Cas9^{D10A}$ expression construct, gRNA, and indicated RECQ5 expression constructs (RECQ5 – red, $RECQ5^{D157A}$ – blue, $RECQ5^{F666A}$ – brown, $RECQ5^{K598E}$ – yellow, RECQ5(1-899) – orange).

(G) Frequencies of mutEJ at DSBs in HEK 293T TL reporter cells provided with Cas9 expression construct, gTL2, and indicated RECQ5 expression constructs.

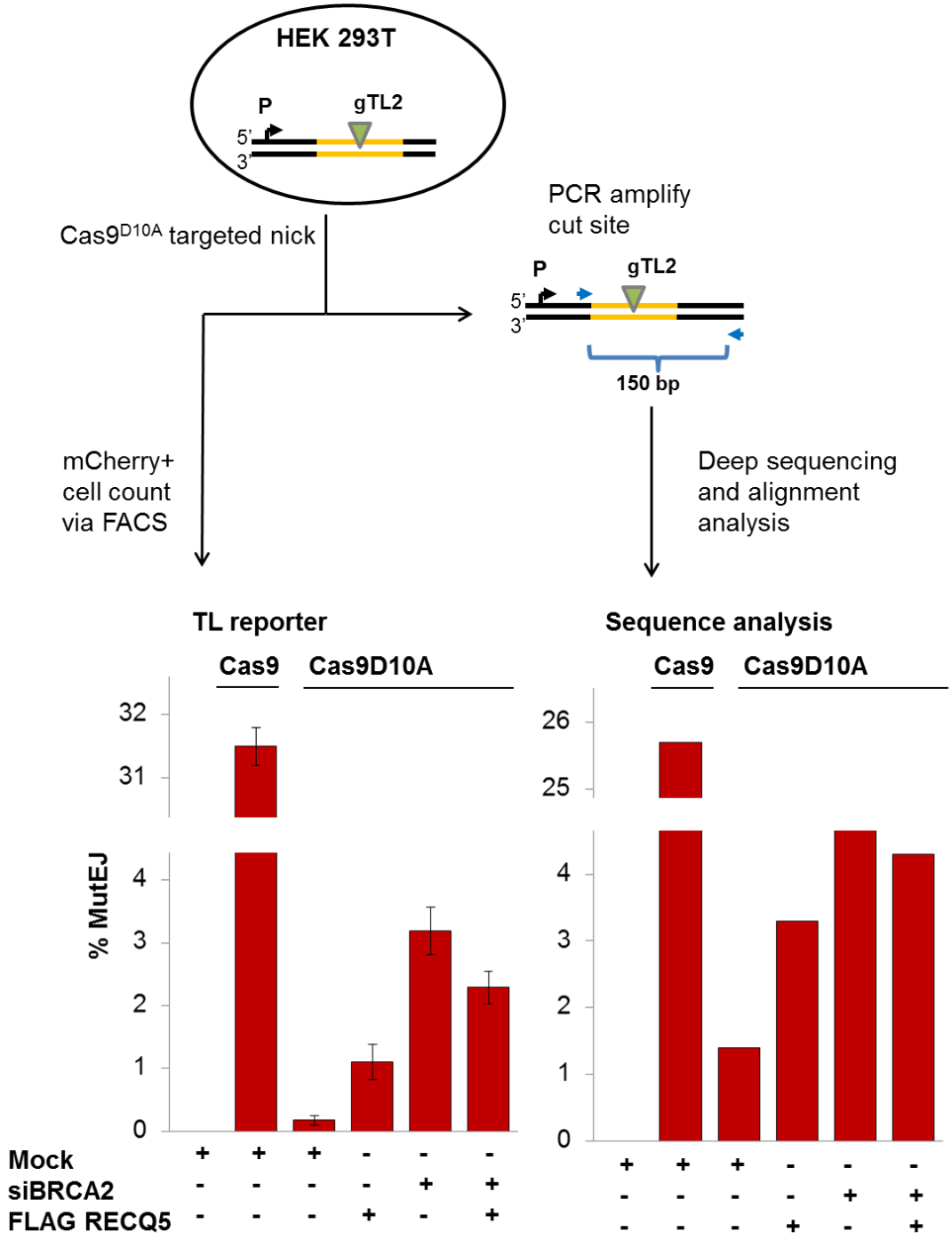

Figure 4.2 Comparison of mutEJ frequencies as assayed by flow cytometry and by deep sequencing

Frequencies of mutEJ in the TL reporter in cells treated with Cas9 or Cas9^{D10A} to gTL2 with indicated siRNA or ectopic expression were determined by scoring mCherry+ cells by flow cytometry; and sequencing analysis.

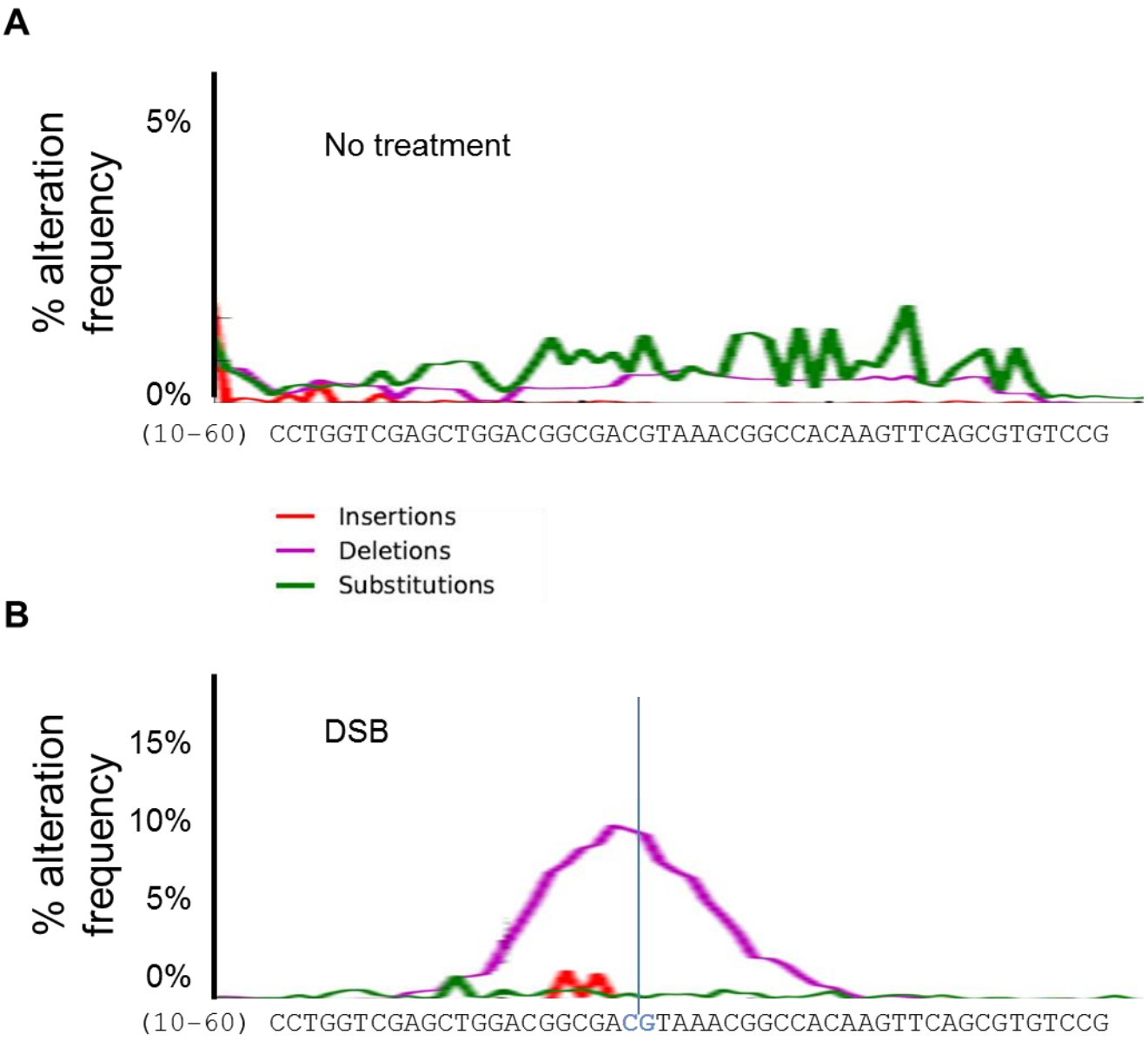

Figure 4.3 DSBs induce deletions and insertions at the targeted cut site

Mutagenic signature of cells treated with mock (A) transfection or Cas9 (B) targeted with gTL2 (blue). Alteration frequency at each nucleotide is indicated for deletions (purple), insertions (red), and point mutations (green).

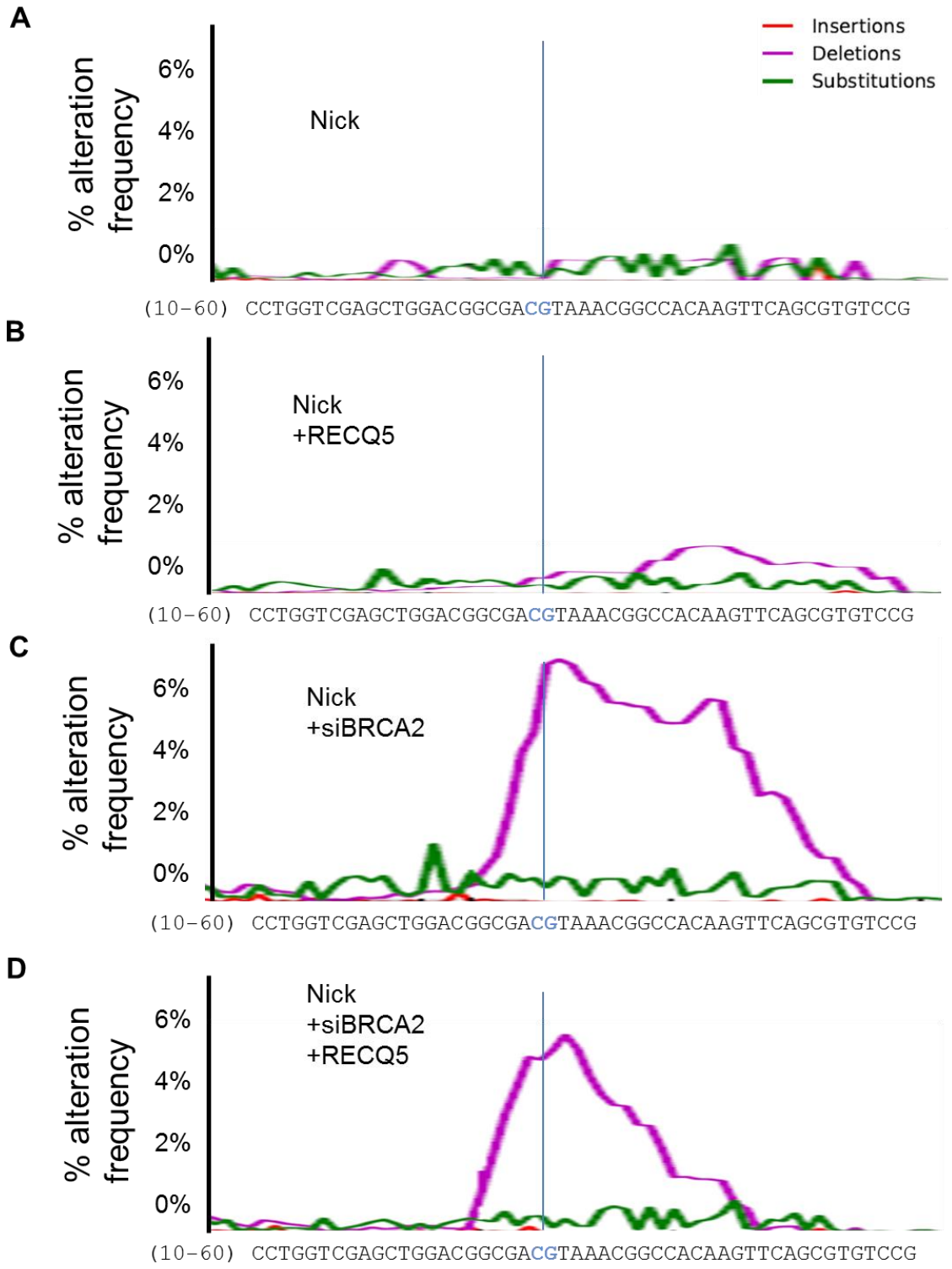

Figure 4.4 Nicks induce varied and unique mutagenic signatures

Mutagenic signature of cells treated with mock Cas9^{D10A} (A) targeted to gTL2 (blue) with either RECQ5 ectopic expression (B), siBRCA2 (C), or both RECQ5 ectopic expression and siBRCA2

(D). Alteration frequency at each nucleotide is indicated for deletions (purple), insertions (red), and point mutations (green).

Chapter 5 SPATIOTEMPORAL CONTROL OF CAS9 AND UNIQUE ACTIVITIES OF THE CAS9/CRISPR SYSTEM

While the majority of work discussed focuses on the mechanism of nick repair, the nickase itself may be playing a role in directing repair. We observed the effects of fusing Cas9 and Cas9^{D10aA} to the estrogen receptor ligand binding domain (ERLBD), a fusion which induces controllable nuclear entry of Cas9, and noted the differences between the two nickase derivatives, Cas9^{D10A} and Cas9^{H840A}. Briefly, the modification of Cas9 by addition of the ERLBD at its C-terminus allows for Cas9 to be localized to the nucleus only upon addition of Tamoxifen. My studies on the two different nickases of Cas9 (D10A and H840A) and their comparison with I-AniI reveal a set of unique characteristics of Cas9. Cas9 appears to alter the repair pathway choices the cell makes by affecting the importance of the XRCC1/LIG3 activity at the site of nicks.

Materials and Methods

Materials

Plasmids, siRNA, and Cell Lines

Plasmids and cell lines used are identical to those described in the Materials section for Chapter 3 with the exception of those listed below

siRNA

siXRCC1 (Ambion – Cat# AM16708)

Plasmids

Cas9 H840A **–** Cas9 H840A was created by Quikchange (Agilent Technologies) from the WT Cas9.

Quikchange primers

CTCTCCGACTACGACGTGGAT Reverse

TATCGTGCCCCAGTCTTTTCTC Forward

Cas9/Cas9^{D10A} ERLBD – The ERLBD DNA sequence was attached to the C terminal end of Cas9 and Cas9^{D10A} directly prior to the stop codon of the Cas9. Gibson cloning manufacturer's protocol was followed (NEB). Briefly, 8 µl reactions were used with 4 µl of 2 x Gibson master mix, 0.01 pmols of DNA (2 fragment assembly), and dH2O to 8 µl. Reaction was then placed at 50°C for 15 minutes and subsequently transformed into XL1 competent cells.

Gibson cloning primers

Cas9 linearization primers

TCACACCTTCCTCTTCTT Reverse

AAGGGTTCGATCCCTAC Forward

ERLBD linearization (lowercase) with Cas9 annealing sequences (uppercase)

tagggatcgaaccttGTGGCAGGGAAACCCTCT Reverse

gaagaggaaggtgtgaATGAAAGGTGGGATACGAAAA Forward

Methods

Traffic Light Reporter assay and transfections

The TL reporter assay and subsequent data analysis as well as the transfections of both siRNA and plasmids were carried out as described in the Methods section of Chapter 3 with the following exceptions.

Cas9/Cas9^{D10A} ERLBD

Cas9 – ERLBD or Cas9^{D10A} – ERLBD was transiently transfected at the same concentrations as WT Cas9 and Cas9^{D10A}. 4-OHT (induces nuclear entry of ERLBD constructs) was added to a final concentration of 1 μM the day of the transfection to designated wells. Cells were collected as described in the TL reporter methods.

Results

Spatiotemporal control of Cas9 and Cas9^{D10A}

It would be useful to be able to synchronize targeting of DSBs or nicks by CRISPR/Cas9 and their derivatives. Temporal control of proteins through fusion of regulatory domains has been described previously by insertion of an estrogen receptor ligand binding domain (ERLBD) at the C terminus of the human O^6-methylguanine-DNA methyltransferase (MGMT) [219]. This fusion construct allowed for nuclear entry of MGMT-ERLBD only upon addition of 4-OHT (Tamoxifen). We asked if we could create Cas9-ERLBD and Cas9^{D10A}-ERLBD fusion proteins in order to impart this spatiotemporal control to targeted DSBs and nicks. Using Gibson cloning, we linearized the Cas9 and Cas9^{D10A} expression plasmids and the ERLBD with overlap to allow the addition of the ERLBD immediately preceding the stop codon of Cas9 or Cas9^{D10A}. Following successful creation of the new constructs, we tested by transient transfection with gTL1 and either a dsDNA or SSO donor for DSBs and nicks respectively (Fig. 5.1). At nicks we saw a 45-fold induction of HDR upon addition of 4-OHT (0.004% to 0.18%) and a 7-fold induction of mutEJ (0.007% to 0.049%). At DSBs we observed an 8-fold induction of HDR (0.019% to 0.144%) and a 13-fold induction of mutEJ (0.37% to 4.8%). Thus, fusion with the ERLBD has made Cas9 and Cas9^{D10A} cleavage responsive to 4-OHT.

Comparison of the Cas9 ^{D10A}, Cas9 H840A, and I-AniI nickases

We examined the effect of the source of the targeted nicks by comparing outcomes of targeted cleavage by I-AniI, Cas9^{D10A} and Cas9^{H840A}. I-AniI binds to and distorts the DNA, and dissociates following cleavage [189]. Cas9^{D10A} and Cas9^{H840A} use a CRISPR gRNA to target cleavage by DNA annealing, and the protein binds the PAM sequence (Fig 2.1C). The D10A

point mutation causes nicks to be targeted to the strand bound by the gRNA while the H840A point mutation causes nicks to be targeted to the unbound strand.

Cas9 remains bound to the DNA after cleavage, and this may slow certain repair pathways. Supporting that possibility, DSBs caused by ionizing radiation were found to be repaired 60 times faster than DSBs targeted by CRISPR/Cas9 in human cells [220]. Additionally, the DNA end opposite that which is bound by the gRNA is released by the Cas9- complex much more quickly than the other three ends of DNA at a DSB [220]. This suggested that nicks generated by the $Cas9^{D10A}$ and $Cas9^{H840A}$ nickases may undergo repair differently from nicks generated by the I-AniI nickase. We tested that possibility in several ways.

XRCC1 is the scaffold protein that recruits LIG3 to nicks [50]). We asked how depletion of XRCC1 affected frequencies of HDR by these different nickases (Fig 5.2A), and found that siXRCC1 treatment increased HDR 10-fold at TL reporters targeted by the I-AniI nickase, but reduced HDR 4- and 10-fold at the same reporter targeted by the $Cas9^{D10A}$ and $Cas9^{H840A}$ nickases respectively. This suggests that XRCC1/LIG3 strongly inhibits HDR at nicks generated by I-AniI nickase, but promotes HDR at nicks created by $Cas9^{D10A}$ and $Cas9^{H840A}$. Depletion of XRCC1 had no effect for cells treated with I-AniI and Cas9 cleavases indicating the effect is specific to the nickases (Fig. 5.2B). We next compared the effects of siRAD51 and siRECQ5 treatments on I-AniI, $Cas9^{D10A}$ and $Cas9^{H840A}$ (Fig. 5.2C). For all three nickases, depletion of RECQ5 resulted in a strong decrease in HDR while depletion of RAD51 resulted in an increase in HDR.

We next examined differences in HDR specific to $Cas9^{D10A}$ and $Cas9^{H840A}$ (Fig. 5.3). We compared donor preference (cI or cN) at various cut sites. At gTL1 $Cas9^{D10A}$ creates a

transcribed strand nick while Cas9^{H840A} creates a non-transcribed strand nick (Fig. 5.3A). Intriguingly, both nickases prefer the same donor even though it imparts different mechanisms (cI for D10A and cN for H840A). At gTL2 Cas9^{D10A} creates a non-transcribed strand nick while Cas9^{H840A} creates a transcribed strand nick. Cas9^{D10A} prefers a cI donor while neither donor appears to work well for Cas9^{H840A} (Fig. 5.3B). At gTL9, Cas9^{D10A} creates a transcribed strand nick and prefers a cN donor while Cas9^{H840A} creates a non-transcribed strand nick and prefers a cI donor. These data support previously observed tendencies in cI and cN mechanisms. HDR at nicks that use a cN donor relies upon binding of the nicked strand to the donor and creating a 3' end for DNA synthesis. If there is heterology between the donor and the nicked DNA, there will be no 3' end to act as a primer. Nicks undergoing cI repair are more efficiently repaired the shorter the 5' heterology is (Davis and Maizels, under review. 2016). Thus, a gTL1 nick from Cas9^{H840A} serves as a good candidate for cN donors, due to its limited 3' heterology, but a poor candidate for cI, due to its extended 5' heterology, and a ^{D10A} nick at gTL1 is a good candidate for cI but not for cN.

Conclusion

We examined the unique attributes of Cas9 nickases and how they differ from the I-AniI LAGLIDADG homing endonuclease. We found that a nick created by Cas9^{D10A} or Cas9^{H840A} requires XRCC1 activity for efficient HDR while I-AniI created nicks are inhibited by XRCC1 . This may be due to Cas9 retention at the site of the nick which could block the initial ligase activity of the XRCC1/LIG3 complex, an activity which could repair I-AniI created nicks prior to HDR. XRCC1/LIG3 may then be required in the final religation of Cas9 initiated nicks following HDR. While Cas9 and I-AniI nickases differed in their response to XRCC1 depletion, they reacted very similarly to depletion of RAD51 and RECQ5. This suggests that either the nickases may be removed from the site of the nick by the time RAD51 and RECQ5 act; a possibility which further suggests that RAD51 and RECQ5 are not limited to acting at nicks created by targeted nickases. Finally, while Cas9^{D10A} and Cas9^{H840A} nick on opposite strands, they follow the same principles of donor preference. For both nickases, a cI donor was preferred when there was limited 5' heterology while a cN donor was preferred when there was limited 3' heterology.

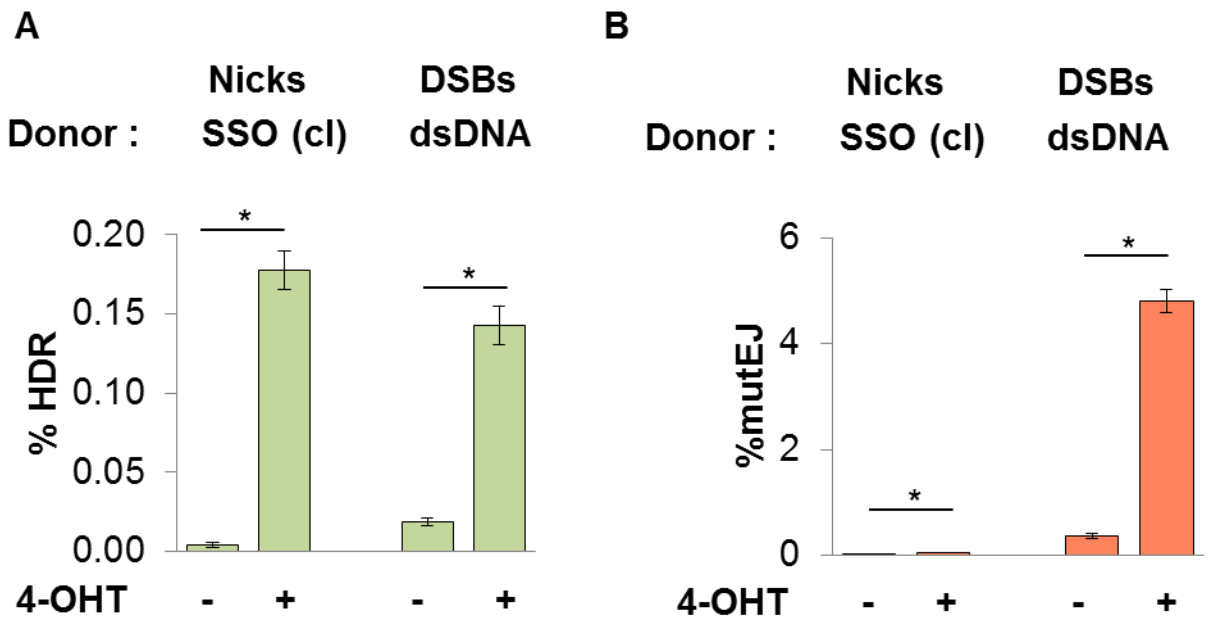

Figure 5.1 Spatiotemporal control of Cas9 and Cas9^{D10A}.

(A) Frequencies of HDR at nicks and DSBs in HEK 293T TL reporter cells treated with Cas9^{D10A}-ERLBD (gTL1) and Cas9-ERLBD (gTL1), and provided a SSO (nicks) or dsDNA (DSBs) donor. Cells were either given 4-OHT (1uM) to induce nuclear entry of ERLBD fused Cas9 constructs or DMSO as a control

(B) mutEJ frequencies of the above described cells.

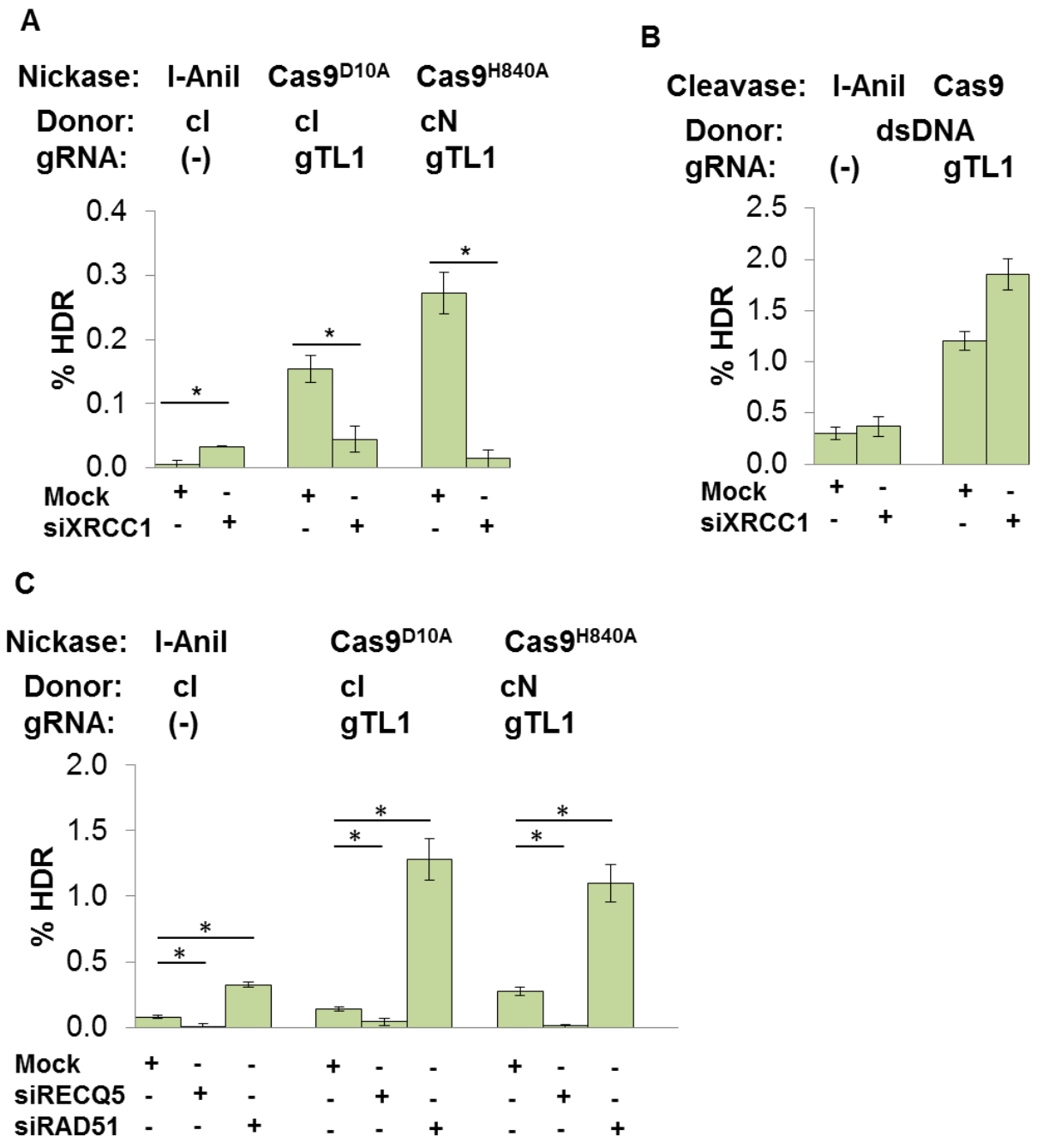

Figure 5.2 Similarities and differences between I-AniI and Cas9 nickases

(A) Frequencies of HDR in HEK 293T TL reporter cells treated with I-AniI , $Cas9^{D10A}$, or $Cas9^{H840A}$ and the indicated donor, gRNA, and siRNA.

B) Frequencies of HDR in HEK 293T TL reporter cells treated with I-AniI (cI) or Cas9 and the indicated donor, gRNA (Cas9 only) and siRNA).

(C) Frequencies of HDR in HEK 293T TL reporter cells treated with I-AniI, $Cas9^{D10A}$, or $Cas9^{H840A}$ and the indicated donor, gRNA, and siRNA.

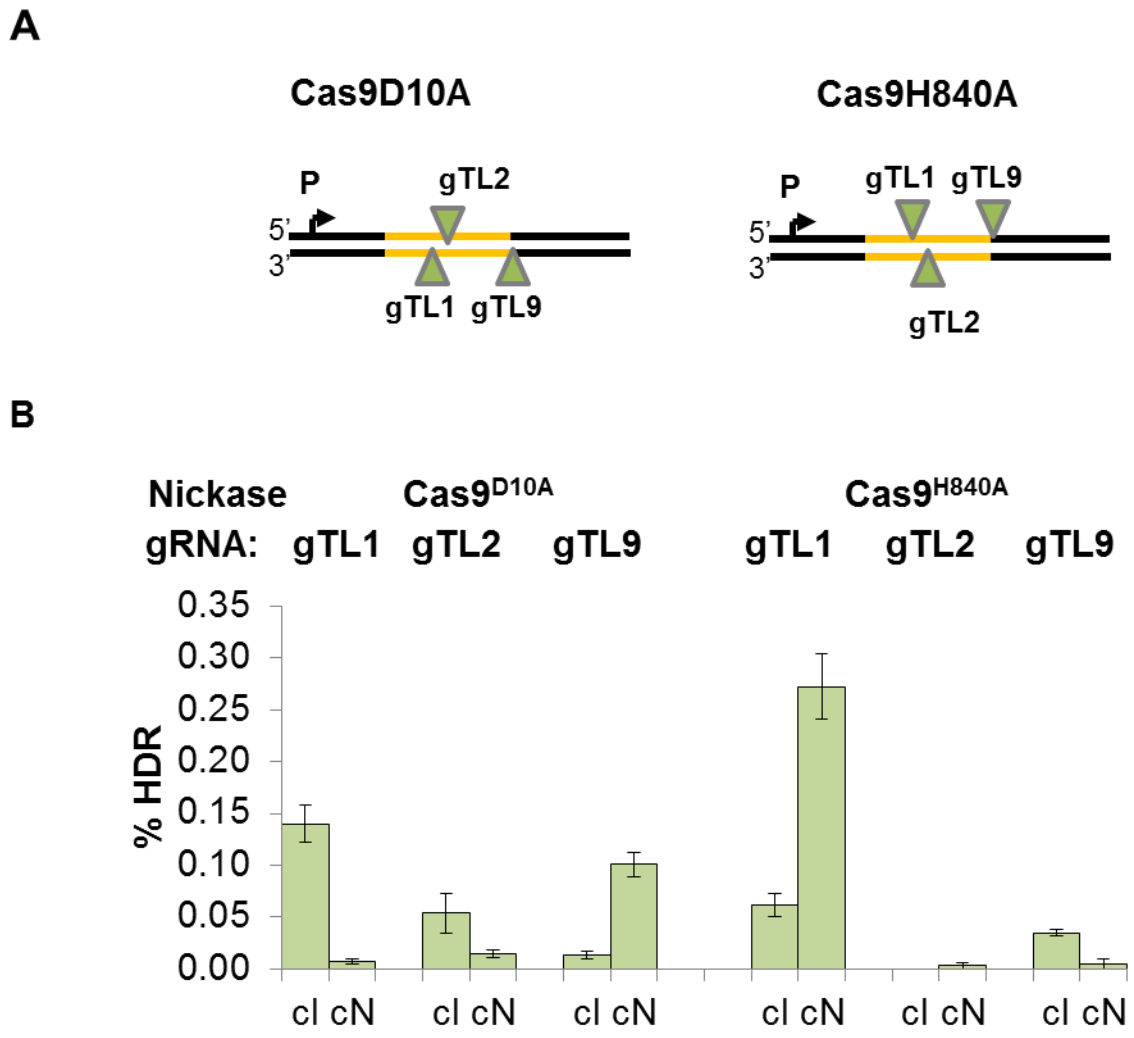

Figure 5.3 I-AniI and Cas9 nickases

(A) Diagram of nick sites with indicated gRNAs for Cas9^{D10A} and Cas9^{H840A}

(B) Frequencies of HDR in HEK 293T TL reporter cells treated with Cas9^{D10A}, or Cas9^{H840A} and the indicated donor and gRNA.

Chapter 6 DISCUSSION

Conclusion

These studies have helped elucidate the mechanism by which a nick in the genome can undergo HDR or mutagenesis. We have shown that RECQ5 is required for HDR at both nicks and DSBs, and that ectopic expression of RECQ5 promotes HDR at nicks with SSO donors but depresses HDR frequency at DSBs. This suggests an intermediate levels of RECQ5 activity is required for HDR at DSBs, but not at nicks.

The effect of RECQ5 on frequency of HDR at nicks is dependent upon an active helicase ATPase and RAD51 interaction domain. Deletion of the SRI RNAPII interaction domain increased the effect of ectopic RECQ5 expression at nicks, suggesting it may act to negatively regulate RECQ5. It is possible that RECQ5 and RNAPII can interact to promote efficient repair of nicks through religation which would be unnoticed by the TL reporter.

The activity of RECQ5 at nicks is also observed only in conditions in which RAD51 has loaded on DNA. When RAD51 or BRCA2 was depleted, subsequent ectopic expression or depletion of RECQ5 had no effect on frequencies of HDR at nicks. In contrast, in cells expressing the $RAD51^{K133R}$ dominant negative mutant, which forms mixed filaments that are resistant to dissociation, depletion of RECQ5 reduced frequencies of HDR at nicks, supporting the view that RECQ5 can use its helicase activity to remove presynaptic RAD51 filaments at nicks.

These results complement earlier analyses of RECQ5 activities at DSBs [183], as we have shown that in some ways RECQ5 functions similarly at DSBs and nicks. This strongly suggests that RAD51 and BRCA2, proteins typically thought to function primarily in the DSB

recombination pathways, are actively inhibiting HDR at nicks by forming RAD51 filaments on ssDNA at nicks. This leads to reannealing of open unwound nicks to the complementary strand. While this prevents HDR with SSO donors, these RAD51-coated ssDNA strands can carry out strand invasion and recombine with dsDNA donors. The ability of RECQ5 to disrupt RAD51 filaments may act to counter excessive RAD51 filament formation at nicks thus preventing recombination with dsDNA donors.

RECQ5 enhances mutEJ at nicks but has no effect on mutEJ at DSBs. RECQ5 has been previously described as lacking any role in NHEJ or alt NHEJ [183]. The lack of impact at DSBs makes our observations at nicks all the more intriguing. At nicks, RECQ5 depletion caused a decrease in mutEJ while ectopic expression of RECQ5 caused an increase in the frequency of mutEJ as reported by the TL reporter. This novel observation was dependent upon the RAD51 interaction domain and an active helicase ATPase. Additionally, no effect on mutEJ was observable when RAD51 or BRCA2 were depleted. Thus, RECQ5 can increase the frequency of frameshift mutations at nicks but only in the presence of RAD51 and BRCA2. This is similar to the ability of RECQ5 to stimulate HDR by SSO donors at nicks. These observations strongly suggest that RECQ5 can promote both the recombinogenic and mutagenic potential of nicks utilizing the same mechanism of RAD51 filament disruption.

Curiously, RECQ5 ectopic expression creates a unique mutagenic signature with deletions present downstream of the cut site. While further experimentation is required to elucidate why this may be, it could be due to eviction of RAD51 from that site, thus creating an unprotected length of DNA which could allow mutEJ. In support of this hypothesis, depletion of BRCA2 also results in a downstream deletion peak. Without BRCA2, RAD51 will not be loaded on the DNA which could result in unprotected and vulnerable DNA.

In tumors, RECQ5 is often amplified though how this affected cells was unknown. We have shown that the exogenous RECQ5 expression leads to increased HDR frequencies and frameshift mutation at nicks, while depletion of RECQ5 leads to a decreased ability to repair DSBs by HDR. Our data suggests endogenous RECQ5 plays a role in suppressing multiple forms of mutagenesis, both by controlling levels of recombination at DSBs and by preventing recombination of nicks with dsDNA donors. This activity of RECQ5 may be especially important in preventing loss of heterozygosity.

We have created a fusion protein (Cas9-ERLBD and Cas9^{D10A}-ERLBD) which grants control over nuclear entry of Cas9. Our evidence that nuclear entry of Cas9 can be controlled through a C terminal linkage to the ERLBD has the potential to synchronize CRISPR/Cas9 targeted DNA damage. While this is of interest and use in the temporal targeting of DSBs, this advancement is particularly useful for the study of targeted nicks. Nicks are transitory and thus present a unique challenge to attempts to document their repair through traditional approaches, such as ChIP or fluorescence microscopy, as they often fall below background noise levels. The generation of a Cas9/Cas9^{D10A}-ERLBD construct, which facilitates coordinated DSBs or nicks will facilitate future study of nicks initiated at a particular time and in a particular place. This potentially opens the door to the study of nicks initiating within unique circumstances (such as heat shock, transcription inhibition, radiation, etc.). Gene therapy requires a coordinated set of actions in order to successfully alter a genome. This coordination is hampered by our limited ability to insert all of the necessary gene therapy components into the cell at the necessary concentrations. As an example, most viral delivery methods would be unable to hold sufficient quantities of the necessary expression vectors and donor DNA required for efficient HDR. We have shown that the fusion of the ERLBD to Cas9 or Cas9^{D10A} grants control over its nuclear

entry. This could allow gene therapy to be used in a multi-step process. In an initial step, Cas9-ERLBD could be added to the cell. Once the construct has had time to express Cas9, donor DNA could be added in addition to 4-OHT to induce nuclear entry of Cas9. This coordination could ensure that the donor DNA is not being degraded while the Cas9 expression vector is undergoing initial rounds of expression. This could also allow for Cas9 targeted nicks or DSBs during treatment with chemical inhibitors which may enhance gene therapy success.

Our comparisons of $Cas9^{D10A}$, Cas9H840A, and I-AniI nickase demonstrate a difference between the nickases. While HDR at nicks is boosted upon XRCC1 depletion for I-AniI nickase, XRCC1 depletion causes a large decrease in Cas9 targeted nick HDR. This may be due to prolonged binding of $Cas9^{D10A}$ and $Cas9^{H840A}$ to the DNA target, blocking religation by the XRCC1/LIG3 complex while still allowing for the progression of the initial stages of HDR. While there is a difference between the nickases in their reaction to XRCC1 depletion, there is no difference in the response of nicks created by I-AniI, $Cas9^{D10A}$, or $Cas9^{H840A}$ to depletion of RECQ5 or RAD51. All nicks exhibit reduced HDR frequencies upon RECQ5 depletion and increased HDR frequencies upon RAD51 depletion. This suggests the role of these proteins occurs after the dissociation of Cas9 or I-AniI nickases. Further analysis of the differences between $Cas9^{D10A}$ and $Cas9^{H840A}$ may illustrate differences in retention time or rate of HDR, two parameters which could have a major impact on any therapeutic strategies developed using Cas9 targeted nicks.

Impact

Our findings on RECQ5 hold promise in both the field of gene correction and diagnosing/treating certain types of tumors. Tumors arise when mutations develop in key genes that control cellular proliferation. In gene therapy, a set of specific mutations are made to an individual's genome that alleviate an undesirable condition. Both processes rely upon or interact with DNA repair pathways to introduce the mutagenic sequence. It is unsurprising then that research into one field can impact the other.

Tumorigenesis occurs when a cell begins to divide in an unregulated fashion. Over the years, key DNA repair proteins have been implicated in the progression of many tumors. BRCA2 has been heavily studied as its disruption or knockout is responsible for higher frequencies of many types of tumors with a particular strong effect on elevating breast cancer frequencies [221]. While BRCA2 is an important factor in DNA repair and genomic stability, it is also an example of the bias of study towards knockout mutation phenotypes. A knockout mutation can be recognized and characterized far more easily than an amplification of a gene. However, even a mild amplification of a repressor gene can be enough to disrupt the function of the gene the repressor acts upon. We have shown that an amplification of RECQ5 can phenocopy a depletion of BRCA2 or RAD51. Overexpression of RECQ5 disrupts the formation of RAD51 presynaptic filaments thus compromising the ability to perform HDR at DSBs and enhancing the frequency of HDR and mutEJ at nicks. BRCA2 knockout mutations are screened for to determine genetic predisposition to many forms of cancer. Our results suggest that screening for the amplification of RECQ5 may be just as useful in diagnosing predispositions to certain cancers and in determining the ideal treatment of tumors as screening for BRCA2 knockouts. Additionally, this work suggests that a main driver of mutagenesis in tumors may be frameshift mutations initiating

from nicks due to heightened levels of RECQ5 or depletions of RAD51 or BRCA2. The role that this mutagenesis plays in tumor development remains understudied and could present opportunities for new targeted treatments aimed at either preventing this form of genomic instability or enhancing it to the point where it is lethal for tumors.

Therapeutic strategies which attempt to alter the DNA sequence, and thus eliminate the cause of a disease, rely upon the targeted correction of a disease-causing mutation. The targeted endonuclease and donor DNA must be introduced into the cells for correction to occur. The nuclease will then initiate repair by creating a nick or DSB at the target site whereupon the donor DNA can act as a template for HDR and pass along the desired sequence to the genome. DSBs are repaired via mutEJ pathways far more than through HDR pathways, with ratios as high as 15:1 observed in the TL reporter. In contrast, $Cas9^{D10A}$ nick initiated HDR gave up to 10-fold more repair than mutEJ at a nick. While nicks are therefore safer than DSBs as a means to initiate HDR, the magnitude of repair is lower than that observed at DSBs. We have shown that transient amplification of RECQ5 levels in the cell can enhance HDR levels at nicks equal to that of DSBs but with far lower levels of mutEJ. Unlike other treatments, such as depletion of RAD51 or BRCA2, the transient amplification of RECQ5 does not impact NHEJ frequencies at DSBs. RECQ5 is thus a potential target for activation to promote higher levels of HDR at nicks for gene therapy.

BIBLIOGRAPHY

1. Aubrey BJ, Strasser A, Kelly GL. Tumor-Suppressor Functions of the TP53 Pathway. Cold Spring Harb Perspect Med. 2016;6(5). doi: 10.1101/cshperspect.a026062. PubMed PMID: 27141080.
2. Lee DS, Yoon SY, Looi LM, Kang P, Kang IN, Sivanandan K, et al. Comparable frequency of BRCA1, BRCA2 and TP53 germline mutations in a multi-ethnic Asian cohort suggests TP53 screening should be offered together with BRCA1/2 screening to early-onset breast cancer patients. Breast Cancer Res. 2012;14(2):R66. doi: 10.1186/bcr3172. PubMed PMID: 22507745; PubMed Central PMCID: PMCPMC3446401.
3. Arcand SL, Maugard CM, Ghadirian P, Robidoux A, Perret C, Zhang P, et al. Germline TP53 mutations in BRCA1 and BRCA2 mutation-negative French Canadian breast cancer families. Breast Cancer Res Treat. 2008;108(3):399-408. doi: 10.1007/s10549-007-9608-6. PubMed PMID: 17541742.
4. Monnerat C, Chompret A, Kannengiesser C, Avril MF, Janin N, Spatz A, et al. BRCA1, BRCA2, TP53, and CDKN2A germline mutations in patients with breast cancer and cutaneous melanoma. Fam Cancer. 2007;6(4):453-61. doi: 10.1007/s10689-007-9143-y. PubMed PMID: 17624602.
5. Blanco A, Graña B, Fachal L, Santamariña M, Cameselle-Teijeiro J, Ruíz-Ponte C, et al. Beyond BRCA1 and BRCA2 wild-type breast and/or ovarian cancer families: germline mutations in TP53 and PTEN. Clin Genet. 2010;77(2):193-6. doi: 10.1111/j.1399-0004.2009.01309.x. PubMed PMID: 19930417.
6. Arnold AG, Otegbeye E, Fleischut MH, Glogowski EA, Siegel B, Boyar SR, et al. Assessment of individuals with BRCA1 and BRCA2 large rearrangements in high-risk breast and ovarian cancer families. Breast Cancer Res Treat. 2014;145(3):625-34. doi: 10.1007/s10549-014-2987-6. PubMed PMID: 24825132.
7. Shibata M, Shen MM. The roots of cancer: stem cells and the basis for tumor heterogeneity. Bioessays. 2013;35(3):253-60. doi: 10.1002/bies.201200101. PubMed PMID: 23027425; PubMed Central PMCID: PMCPMC3687804.
8. Albini A, Bruno A, Gallo C, Pajardi G, Noonan DM, Dallaglio K. Cancer stem cells and the tumor microenvironment: interplay in tumor heterogeneity. Connect Tissue Res. 2015;56(5):414-25. doi: 10.3109/03008207.2015.1066780. PubMed PMID: 26291921; PubMed Central PMCID: PMCPMC4673538.
9. Wang Z, Wang J, Xie R, Liu R, Lu Y. Mitochondria-derived reactive oxygen species play an important role in Doxorubicin-induced platelet apoptosis. Int J Mol Sci. 2015;16(5):11087-100. doi: 10.3390/ijms160511087. PubMed PMID: 25988386; PubMed Central PMCID: PMCPMC4463691.
10. Kienhöfer D, Boeltz S, Hoffmann MH. Reactive oxygen homeostasis - the balance for preventing autoimmunity. Lupus. 2016;25(8):943-54. doi: 10.1177/0961203316640919. PubMed PMID: 27252273.
11. McAdam E, Brem R, Karran P. Oxidative stress-induced protein damage inhibits DNA repair and determines mutation risk and therapeutic efficacy. Mol Cancer Res. 2016. doi: 10.1158/1541-7786.MCR-16-0053. PubMed PMID: 27106867.
12. Guven M, Brem R, Macpherson P, Peacock M, Karran P. Oxidative Damage to RPA Limits the Nucleotide Excision Repair Capacity of Human Cells. J Invest Dermatol. 2015;135(11):2834-41. doi: 10.1038/jid.2015.255. PubMed PMID: 26134950; PubMed Central PMCID: PMCPMC4669849.
13. Evans MD, Dizdaroglu M, Cooke MS. Oxidative DNA damage and disease: induction, repair and significance. Mutat Res. 2004;567(1):1-61. doi: 10.1016/j.mrrev.2003.11.001. PubMed PMID: 15341901.
14. Ito H, Matsui H, Hirayama A, Indo HP, Majima HJ, Hyodo I. Reactive oxygen species induced by non-steroidal anti-inflammatory drugs enhance the effects of photodynamic therapy in gastric cancer cells. J Clin Biochem Nutr. 2016;58(3):180-5. doi: 10.3164/jcbn.15-124. PubMed PMID: 27257342; PubMed Central PMCID: PMCPMC4865595.
15. Lee HM, Kim CW, Hwang KA, Choi DW, Choi KC. Three components of cigarette smoke altered the growth and apoptosis of metastatic colon cancer cells via inducing the synthesis of reactive oxygen

species and endoplasmic reticulum stress. Environ Toxicol Pharmacol. 2016;45:80-9. doi: 10.1016/j.etap.2016.05.016. PubMed PMID: 27262990.
16. Zhang D, Zhou T, He F, Rong Y, Lee SH, Wu S, et al. Reactive oxygen species formation and bystander effects in gradient irradiation on human breast cancer cells. Oncotarget. 2016. doi: 10.18632/oncotarget.9517. PubMed PMID: 27223435.
17. Dan Dunn J, Alvarez LA, Zhang X, Soldati T. Reactive oxygen species and mitochondria: A nexus of cellular homeostasis. Redox Biol. 2015;6:472-85. doi: 10.1016/j.redox.2015.09.005. PubMed PMID: 26432659; PubMed Central PMCID: PMCPMC4596921.
18. Van Raamsdonk JM. Levels and location are crucial in determining the effect of ROS on lifespan. Worm. 2015;4(4):e1094607. doi: 10.1080/21624054.2015.1094607. PubMed PMID: 27123369; PubMed Central PMCID: PMCPMC4826151.
19. Chen YR, Chen CL, Zhang L, Green-Church KB, Zweier JL. Superoxide generation from mitochondrial NADH dehydrogenase induces self-inactivation with specific protein radical formation. J Biol Chem. 2005;280(45):37339-48. doi: 10.1074/jbc.M503936200. PubMed PMID: 16150735.
20. Han D, Williams E, Cadenas E. Mitochondrial respiratory chain-dependent generation of superoxide anion and its release into the intermembrane space. Biochem J. 2001;353(Pt 2):411-6. PubMed PMID: 11139407; PubMed Central PMCID: PMCPMC1221585.
21. Nakamura J, Swenberg JA. Endogenous apurinic/apyrimidinic sites in genomic DNA of mammalian tissues. Cancer Res. 1999;59(11):2522-6. PubMed PMID: 10363965.
22. Carter RJ, Parsons JL. Base Excision Repair, a Pathway Regulated by Posttranslational Modifications. Mol Cell Biol. 2016;36(10):1426-37. doi: 10.1128/MCB.00030-16. PubMed PMID: 26976642.
23. Gupta SC, Hevia D, Patchva S, Park B, Koh W, Aggarwal BB. Upsides and downsides of reactive oxygen species for cancer: the roles of reactive oxygen species in tumorigenesis, prevention, and therapy. Antioxid Redox Signal. 2012;16(11):1295-322. doi: 10.1089/ars.2011.4414. PubMed PMID: 22117137; PubMed Central PMCID: PMCPMC3324815.
24. Struhl K. Is DNA methylation of tumour suppressor genes epigenetic? Elife. 2014;3:e02475. doi: 10.7554/eLife.02475. PubMed PMID: 24623307; PubMed Central PMCID: PMCPMC3949415.
25. Portela A, Liz J, Nogales V, Setién F, Villanueva A, Esteller M. DNA methylation determines nucleosome occupancy in the 5'-CpG islands of tumor suppressor genes. Oncogene. 2013;32(47):5421-8. doi: 10.1038/onc.2013.162. PubMed PMID: 23686312; PubMed Central PMCID: PMCPMC3898323.
26. Kullmann K, Deryal M, Ong MF, Schmidt W, Mahlknecht U. DNMT1 genetic polymorphisms affect breast cancer risk in the central European Caucasian population. Clin Epigenetics. 2013;5(1):7. doi: 10.1186/1868-7083-5-7. PubMed PMID: 23638630; PubMed Central PMCID: PMCPMC3646668.
27. Moelans CB, Verschuur-Maes AH, van Diest PJ. Frequent promoter hypermethylation of BRCA2, CDH13, MSH6, PAX5, PAX6 and WT1 in ductal carcinoma in situ and invasive breast cancer. J Pathol. 2011;225(2):222-31. doi: 10.1002/path.2930. PubMed PMID: 21710692.
28. Cucer N, Taheri S, Ok E, Ozkul Y. Methylation status of CpG islands at sites -59 to +96 in exon 1 of the BRCA2 gene varies in mammary tissue among women with sporadic breast cancer. J Genet. 2008;87(2):155-8. PubMed PMID: 18776644.
29. Bosviel R, Michard E, Lavediaux G, Kwiatkowski F, Bignon YJ, Bernard-Gallon DJ. Peripheral blood DNA methylation detected in the BRCA1 or BRCA2 promoter for sporadic ovarian cancer patients and controls. Clin Chim Acta. 2011;412(15-16):1472-5. doi: 10.1016/j.cca.2011.04.027. PubMed PMID: 21557934.
30. Goodman MF. Better living with hyper-mutation. Environ Mol Mutagen. 2016. doi: 10.1002/em.22023. PubMed PMID: 27273795.

31. Whitmore SE, Potten CS, Chadwick CA, Strickland PT, Morison WL. Effect of photoreactivating light on UV radiation-induced alterations in human skin. Photodermatol Photoimmunol Photomed. 2001;17(5):213-7. PubMed PMID: 11555330.
32. Cordeiro-Stone M, Zaritskaya LS, Price LK, Kaufmann WK. Replication fork bypass of a pyrimidine dimer blocking leading strand DNA synthesis. J Biol Chem. 1997;272(21):13945-54. PubMed PMID: 9153257.
33. Takahashi M, Teranishi M, Ishida H, Kawasaki J, Takeuchi A, Yamaya T, et al. Cyclobutane pyrimidine dimer (CPD) photolyase repairs ultraviolet-B-induced CPDs in rice chloroplast and mitochondrial DNA. Plant J. 2011;66(3):433-42. doi: 10.1111/j.1365-313X.2011.04500.x. PubMed PMID: 21251107.
34. Vilenchik MM, Knudson AG. Endogenous DNA double-strand breaks: production, fidelity of repair, and induction of cancer. Proc Natl Acad Sci U S A. 2003;100(22):12871-6. doi: 10.1073/pnas.2135498100. PubMed PMID: 14566050; PubMed Central PMCID: PMCPMC240711.
35. Tuteja N, Tuteja R. Unraveling DNA repair in human: molecular mechanisms and consequences of repair defect. Crit Rev Biochem Mol Biol. 2001;36(3):261-90. doi: 10.1080/20014091074192. PubMed PMID: 11450971.
36. Osorio A, Milne RL, Kuchenbaecker K, Vaclová T, Pita G, Alonso R, et al. DNA glycosylases involved in base excision repair may be associated with cancer risk in BRCA1 and BRCA2 mutation carriers. PLoS Genet. 2014;10(4):e1004256. doi: 10.1371/journal.pgen.1004256. PubMed PMID: 24698998; PubMed Central PMCID: PMCPMC3974638.
37. Bauer NC, Corbett AH, Doetsch PW. The current state of eukaryotic DNA base damage and repair. Nucleic Acids Res. 2015;43(21):10083-101. doi: 10.1093/nar/gkv1136. PubMed PMID: 26519467; PubMed Central PMCID: PMCPMC4666366.
38. Bellacosa A, Drohat AC. Role of base excision repair in maintaining the genetic and epigenetic integrity of CpG sites. DNA Repair (Amst). 2015;32:33-42. doi: 10.1016/j.dnarep.2015.04.011. PubMed PMID: 26021671; PubMed Central PMCID: PMCPMC4903958.
39. Hashimoto H, Zhang X, Vertino PM, Cheng X. The Mechanisms of Generation, Recognition, and Erasure of DNA 5-Methylcytosine and Thymine Oxidations. J Biol Chem. 2015;290(34):20723-33. doi: 10.1074/jbc.R115.656884. PubMed PMID: 26152719; PubMed Central PMCID: PMCPMC4543634.
40. Pedersen HL, Johnson KA, McVey CE, Leiros I, Moe E. Structure determination of uracil-DNA N-glycosylase from Deinococcus radiodurans in complex with DNA. Acta Crystallogr D Biol Crystallogr. 2015;71(Pt 10):2137-49. doi: 10.1107/S1399004715014157. PubMed PMID: 26457437.
41. Sang PB, Srinath T, Patil AG, Woo EJ, Varshney U. A unique uracil-DNA binding protein of the uracil DNA glycosylase superfamily. Nucleic Acids Res. 2015;43(17):8452-63. doi: 10.1093/nar/gkv854. PubMed PMID: 26304551; PubMed Central PMCID: PMCPMC4787834.
42. Zhou X, Zhuang Z, Wang W, He L, Wu H, Cao Y, et al. OGG1 is essential in oxidative stress induced DNA demethylation. Cell Signal. 2016;28(9):1163-71. doi: 10.1016/j.cellsig.2016.05.021. PubMed PMID: 27251462.
43. Ide H, Kotera M. Human DNA glycosylases involved in the repair of oxidatively damaged DNA. Biol Pharm Bull. 2004;27(4):480-5. PubMed PMID: 15056851.
44. Tsuchimoto D, Sakai Y, Sakumi K, Nishioka K, Sasaki M, Fujiwara T, et al. Human APE2 protein is mostly localized in the nuclei and to some extent in the mitochondria, while nuclear APE2 is partly associated with proliferating cell nuclear antigen. Nucleic Acids Res. 2001;29(11):2349-60. PubMed PMID: 11376153; PubMed Central PMCID: PMCPMC55700.
45. Al-Safi RI, Odde S, Shabaik Y, Neamati N. Small-molecule inhibitors of APE1 DNA repair function: an overview. Curr Mol Pharmacol. 2012;5(1):14-35. PubMed PMID: 22122462.

46. Andres SN, Schellenberg MJ, Wallace BD, Tumbale P, Williams RS. Recognition and repair of chemically heterogeneous structures at DNA ends. Environ Mol Mutagen. 2015;56(1):1-21. doi: 10.1002/em.21892. PubMed PMID: 25111769; PubMed Central PMCID: PMCPMC4303525.
47. Mol CD, Izumi T, Mitra S, Tainer JA. DNA-bound structures and mutants reveal abasic DNA binding by APE1 and DNA repair coordination [corrected]. Nature. 2000;403(6768):451-6. doi: 10.1038/35000249. PubMed PMID: 10667800.
48. Dyrkheeva NS, Khodyreva SN, Lavrik OI. Interaction of APE1 and other repair proteins with DNA duplexes imitating intermediates of DNA repair and replication. Biochemistry (Mosc). 2008;73(3):261-72. PubMed PMID: 18393760.
49. Córdoba-Cañero D, Morales-Ruiz T, Roldán-Arjona T, Ariza RR. Single-nucleotide and long-patch base excision repair of DNA damage in plants. Plant J. 2009;60(4):716-28. doi: 10.1111/j.1365-313X.2009.03994.x. PubMed PMID: 19682284; PubMed Central PMCID: PMCPMC2954439.
50. Robertson AB, Klungland A, Rognes T, Leiros I. DNA repair in mammalian cells: Base excision repair: the long and short of it. Cell Mol Life Sci. 2009;66(6):981-93. doi: 10.1007/s00018-009-8736-z. PubMed PMID: 19153658.
51. Balliano AJ, Hayes JJ. Base excision repair in chromatin: Insights from reconstituted systems. DNA Repair (Amst). 2015;36:77-85. doi: 10.1016/j.dnarep.2015.09.009. PubMed PMID: 26411876; PubMed Central PMCID: PMCPMC4688196.
52. Romanowicz H, Smolarz B, Baszczyński J, Zadrożny M, Kulig A. Genetics polymorphism in DNA repair genes by base excision repair pathway (XRCC1) and homologous recombination (XRCC2 and RAD51) and the risk of breast carcinoma in the Polish population. Pol J Pathol. 2010;61(4):206-12. PubMed PMID: 21290343.
53. Grasso F, Di Meo S, De Luca G, Pasquini L, Rossi S, Boirivant M, et al. The MUTYH base excision repair gene protects against inflammation-associated colorectal carcinogenesis. Oncotarget. 2015;6(23):19671-84. doi: 10.18632/oncotarget.4284. PubMed PMID: 26109431; PubMed Central PMCID: PMCPMC4637313.
54. Jasperson K, Burt RW. The Genetics of Colorectal Cancer. Surg Oncol Clin N Am. 2015;24(4):683-703. doi: 10.1016/j.soc.2015.06.006. PubMed PMID: 26363537.
55. Lukyanchikova NV, Petruseva IO, Evdokimov AN, Silnikov VN, Lavrik OI. DNA with Damage in Both Strands as Affinity Probes and Nucleotide Excision Repair Substrates. Biochemistry (Mosc). 2016;81(3):263-74. doi: 10.1134/S0006297916030093. PubMed PMID: 27262196.
56. Sugasawa K. Molecular mechanisms of DNA damage recognition for mammalian nucleotide excision repair. DNA Repair (Amst). 2016. doi: 10.1016/j.dnarep.2016.05.015. PubMed PMID: 27264556.
57. Fisher LA, Bessho M, Wakasugi M, Matsunaga T, Bessho T. Role of interaction of XPF with RPA in nucleotide excision repair. J Mol Biol. 2011;413(2):337-46. doi: 10.1016/j.jmb.2011.08.034. PubMed PMID: 21875596; PubMed Central PMCID: PMCPMC3200199.
58. Zhang Y, Rohde LH, Wu H. Involvement of nucleotide excision and mismatch repair mechanisms in double strand break repair. Curr Genomics. 2009;10(4):250-8. doi: 10.2174/138920209788488544. PubMed PMID: 19949546; PubMed Central PMCID: PMCPMC2709936.
59. Jensen A, Mullenders LH. Transcription factor IIS impacts UV-inhibited transcription. DNA Repair (Amst). 2010;9(11):1142-50. doi: 10.1016/j.dnarep.2010.08.002. PubMed PMID: 20729154.
60. Sollier J, Stork CT, García-Rubio ML, Paulsen RD, Aguilera A, Cimprich KA. Transcription-coupled nucleotide excision repair factors promote R-loop-induced genome instability. Mol Cell. 2014;56(6):777-85. doi: 10.1016/j.molcel.2014.10.020. PubMed PMID: 25435140; PubMed Central PMCID: PMCPMC4272638.
61. Takedachi A, Saijo M, Tanaka K. DDB2 complex-mediated ubiquitylation around DNA damage is oppositely regulated by XPC and Ku and contributes to the recruitment of XPA. Mol Cell Biol.

2010;30(11):2708-23. doi: 10.1128/MCB.01460-09. PubMed PMID: 20368362; PubMed Central PMCID: PMCPMC2876528.
62. Fuss JO, Tainer JA. XPB and XPD helicases in TFIIH orchestrate DNA duplex opening and damage verification to coordinate repair with transcription and cell cycle via CAK kinase. DNA Repair (Amst). 2011;10(7):697-713. doi: 10.1016/j.dnarep.2011.04.028. PubMed PMID: 21571596; PubMed Central PMCID: PMCPMC3234290.
63. Iovine B, Iannella ML, Bevilacqua MA. Damage-specific DNA binding protein 1 (DDB1): a protein with a wide range of functions. Int J Biochem Cell Biol. 2011;43(12):1664-7. doi: 10.1016/j.biocel.2011.09.001. PubMed PMID: 21959250.
64. Kemp MG, Reardon JT, Lindsey-Boltz LA, Sancar A. Mechanism of release and fate of excised oligonucleotides during nucleotide excision repair. J Biol Chem. 2012;287(27):22889-99. doi: 10.1074/jbc.M112.374447. PubMed PMID: 22573372; PubMed Central PMCID: PMCPMC3391136.
65. Han C, Wani G, Zhao R, Qian J, Sharma N, He J, et al. Cdt2-mediated XPG degradation promotes gap-filling DNA synthesis in nucleotide excision repair. Cell Cycle. 2015;14(7):1103-15. doi: 10.4161/15384101.2014.973740. PubMed PMID: 25483071; PubMed Central PMCID: PMCPMC4614405.
66. Jeon Y, Kim D, Martín-López JV, Lee R, Oh J, Hanne J, et al. Dynamic control of strand excision during human DNA mismatch repair. Proc Natl Acad Sci U S A. 2016;113(12):3281-6. doi: 10.1073/pnas.1523748113. PubMed PMID: 26951673; PubMed Central PMCID: PMCPMC4812718.
67. Modrich P. Mechanisms in E. coli and Human Mismatch Repair (Nobel Lecture). Angew Chem Int Ed Engl. 2016. doi: 10.1002/anie.201601412. PubMed PMID: 27198632.
68. Barwell J, Pangon L, Hodgson S, Georgiou A, Kesterton I, Slade T, et al. Biallelic mutation of MSH2 in primary human cells is associated with sensitivity to irradiation and altered RAD51 foci kinetics. J Med Genet. 2007;44(8):516-20. doi: 10.1136/jmg.2006.048660. PubMed PMID: 17483304; PubMed Central PMCID: PMCPMC2597924.
69. Quiroga D, Lyerly HK, Morse MA. Deficient Mismatch Repair and the Role of Immunotherapy in Metastatic Colorectal Cancer. Curr Treat Options Oncol. 2016;17(8):41. doi: 10.1007/s11864-016-0414-4. PubMed PMID: 27315067.
70. Li SK, Martin A. Mismatch Repair and Colon Cancer: Mechanisms and Therapies Explored. Trends Mol Med. 2016;22(4):274-89. doi: 10.1016/j.molmed.2016.02.003. PubMed PMID: 26970951.
71. Zhang Y, Fox JT, Park YU, Elliott G, Rai G, Cai M, et al. A novel chemotherapeutic agent to treat tumors with DNA mismatch repair deficiencies. Cancer Res. 2016. doi: 10.1158/0008-5472.CAN-15-2974. PubMed PMID: 27262172.
72. Ceccaldi R, Rondinelli B, D'Andrea AD. Repair Pathway Choices and Consequences at the Double-Strand Break. Trends Cell Biol. 2016;26(1):52-64. doi: 10.1016/j.tcb.2015.07.009. PubMed PMID: 26437586; PubMed Central PMCID: PMCPMC4862604.
73. Frankenberg-Schwager M, Gregus A. Chromosomal instability induced by mammography X-rays in primary human fibroblasts from BRCA1 and BRCA2 mutation carriers. Int J Radiat Biol. 2012;88(11):846-57. doi: 10.3109/09553002.2012.711500. PubMed PMID: 22788243.
74. Beucher A, Deckbar D, Schumann E, Krempler A, Frankenberg-Schwager M, Löbrich M. Elevated radiation-induced γH2AX foci in G2 phase heterozygous BRCA2 fibroblasts. Radiother Oncol. 2011;101(1):46-50. doi: 10.1016/j.radonc.2011.05.043. PubMed PMID: 21665305.
75. Ginsburg O, Ghadirian P, Lubinski J, Cybulski C, Lynch H, Neuhausen S, et al. Smoking and the risk of breast cancer in BRCA1 and BRCA2 carriers: an update. Breast Cancer Res Treat. 2009;114(1):127-35. doi: 10.1007/s10549-008-9977-5. PubMed PMID: 18483851; PubMed Central PMCID: PMCPMC3033012.
76. Registry BCF, (Australasia) KCCfRiFBC, (Canada) OCGN. Smoking and risk of breast cancer in carriers of mutations in BRCA1 or BRCA2 aged less than 50 years. Breast Cancer Res Treat. 2008;109(1):67-75. doi: 10.1007/s10549-007-9621-9. PubMed PMID: 17972172.

77. Qing Y, Yamazoe M, Hirota K, Dejsuphong D, Sakai W, Yamamoto KN, et al. The epistatic relationship between BRCA2 and the other RAD51 mediators in homologous recombination. PLoS Genet. 2011;7(7):e1002148. doi: 10.1371/journal.pgen.1002148. PubMed PMID: 21779174; PubMed Central PMCID: PMCPMC3136442.
78. Emerson CH, Bertuch AA. Consider the workhorse: Nonhomologous end-joining in budding yeast. Biochem Cell Biol. 2016:1-11. doi: 10.1139/bcb-2016-0001. PubMed PMID: 27240172.
79. Li J, Xu X. DNA double-strand break repair: a tale of pathway choices. Acta Biochim Biophys Sin (Shanghai). 2016. doi: 10.1093/abbs/gmw045. PubMed PMID: 27217474.
80. Yang K, Guo R, Xu D. Non-homologous end joining: advances and frontiers. Acta Biochim Biophys Sin (Shanghai). 2016. doi: 10.1093/abbs/gmw046. PubMed PMID: 27217473.
81. Baumann P, Benson FE, Hajibagheri N, West SC. Purification of human Rad51 protein by selective spermidine precipitation. Mutat Res. 1997;384(2):65-72. PubMed PMID: 9298115.
82. Gupta RC, Bazemore LR, Golub EI, Radding CM. Activities of human recombination protein Rad51. Proc Natl Acad Sci U S A. 1997;94(2):463-8. PubMed PMID: 9012806; PubMed Central PMCID: PMCPMC19535.
83. Conway AB, Lynch TW, Zhang Y, Fortin GS, Fung CW, Symington LS, et al. Crystal structure of a Rad51 filament. Nat Struct Mol Biol. 2004;11(8):791-6. doi: 10.1038/nsmb795. PubMed PMID: 15235592.
84. Sung P, Krejci L, Van Komen S, Sehorn MG. Rad51 recombinase and recombination mediators. J Biol Chem. 2003;278(44):42729-32. doi: 10.1074/jbc.R300027200. PubMed PMID: 12912992.
85. Chen J, Villanueva N, Rould MA, Morrical SW. Insights into the mechanism of Rad51 recombinase from the structure and properties of a filament interface mutant. Nucleic Acids Res. 2010;38(14):4889-906. doi: 10.1093/nar/gkq209. PubMed PMID: 20371520; PubMed Central PMCID: PMCPMC2919713.
86. Ristic D, Modesti M, van der Heijden T, van Noort J, Dekker C, Kanaar R, et al. Human Rad51 filaments on double- and single-stranded DNA: correlating regular and irregular forms with recombination function. Nucleic Acids Res. 2005;33(10):3292-302. doi: 10.1093/nar/gki640. PubMed PMID: 15944450; PubMed Central PMCID: PMCPMC1145190.
87. Prasad TK, Yeykal CC, Greene EC. Visualizing the assembly of human Rad51 filaments on double-stranded DNA. J Mol Biol. 2006;363(3):713-28. doi: 10.1016/j.jmb.2006.08.046. PubMed PMID: 16979659.
88. Kokabu Y, Ikeguchi M. Molecular modeling and molecular dynamics simulations of recombinase Rad51. Biophys J. 2013;104(7):1556-65. doi: 10.1016/j.bpj.2013.02.014. PubMed PMID: 23561532; PubMed Central PMCID: PMCPMC3617434.
89. Liu J, Ehmsen KT, Heyer WD, Morrical SW. Presynaptic filament dynamics in homologous recombination and DNA repair. Crit Rev Biochem Mol Biol. 2011;46(3):240-70. doi: 10.3109/10409238.2011.576007. PubMed PMID: 21599536; PubMed Central PMCID: PMCPMC4083101.
90. Wright WD, Heyer WD. Rad54 functions as a heteroduplex DNA pump modulated by its DNA substrates and Rad51 during D loop formation. Mol Cell. 2014;53(3):420-32. doi: 10.1016/j.molcel.2013.12.027. PubMed PMID: 24486020; PubMed Central PMCID: PMCPMC4059524.
91. Li X, Heyer WD. RAD54 controls access to the invading 3'-OH end after RAD51-mediated DNA strand invasion in homologous recombination in Saccharomyces cerevisiae. Nucleic Acids Res. 2009;37(2):638-46. doi: 10.1093/nar/gkn980. PubMed PMID: 19074197; PubMed Central PMCID: PMCPMC2632917.
92. Li X, Zhang XP, Solinger JA, Kiianitsa K, Yu X, Egelman EH, et al. Rad51 and Rad54 ATPase activities are both required to modulate Rad51-dsDNA filament dynamics. Nucleic Acids Res. 2007;35(12):4124-40. doi: 10.1093/nar/gkm412. PubMed PMID: 17567608; PubMed Central PMCID: PMCPMC1919488.

93. Sigurdsson S, Van Komen S, Petukhova G, Sung P. Homologous DNA pairing by human recombination factors Rad51 and Rad54. J Biol Chem. 2002;277(45):42790-4. doi: 10.1074/jbc.M208004200. PubMed PMID: 12205100.
94. Bugreev DV, Rossi MJ, Mazin AV. Cooperation of RAD51 and RAD54 in regression of a model replication fork. Nucleic Acids Res. 2011;39(6):2153-64. doi: 10.1093/nar/gkq1139. PubMed PMID: 21097884; PubMed Central PMCID: PMCPMC3064783.
95. Shahid T, Soroka J, Kong EH, Malivert L, McIlwraith MJ, Pape T, et al. Structure and mechanism of action of the BRCA2 breast cancer tumor suppressor. Nat Struct Mol Biol. 2014;21(11):962-8. doi: 10.1038/nsmb.2899. PubMed PMID: 25282148; PubMed Central PMCID: PMCPMC4222816.
96. Jensen RB. BRCA2: one small step for DNA repair, one giant protein purified. Yale J Biol Med. 2013;86(4):479-89. PubMed PMID: 24348212; PubMed Central PMCID: PMCPMC3848102.
97. Reuter M, Zelensky A, Smal I, Meijering E, van Cappellen WA, de Gruiter HM, et al. BRCA2 diffuses as oligomeric clusters with RAD51 and changes mobility after DNA damage in live cells. J Cell Biol. 2015;208(6):857. doi: 10.1083/jcb.20140501402182015c. PubMed PMID: 25778924; PubMed Central PMCID: PMCPMC4362460.
98. Magwood AC, Malysewich MJ, Cealic I, Mundia MM, Knapp J, Baker MD. Endogenous levels of Rad51 and Brca2 are required for homologous recombination and regulated by homeostatic re-balancing. DNA Repair (Amst). 2013;12(12):1122-33. doi: 10.1016/j.dnarep.2013.10.006. PubMed PMID: 24210700.
99. Jensen RB, Carreira A, Kowalczykowski SC. Purified human BRCA2 stimulates RAD51-mediated recombination. Nature. 2010;467(7316):678-83. doi: 10.1038/nature09399. PubMed PMID: 20729832; PubMed Central PMCID: PMCPMC2952063.
100. Liu J, Doty T, Gibson B, Heyer WD. Human BRCA2 protein promotes RAD51 filament formation on RPA-covered single-stranded DNA. Nat Struct Mol Biol. 2010;17(10):1260-2. doi: 10.1038/nsmb.1904. PubMed PMID: 20729859; PubMed Central PMCID: PMCPMC2952495.
101. Carreira A, Kowalczykowski SC. Two classes of BRC repeats in BRCA2 promote RAD51 nucleoprotein filament function by distinct mechanisms. Proc Natl Acad Sci U S A. 2011;108(26):10448-53. doi: 10.1073/pnas.1106971108. PubMed PMID: 21670257; PubMed Central PMCID: PMCPMC3127913.
102. Carreira A, Hilario J, Amitani I, Baskin RJ, Shivji MK, Venkitaraman AR, et al. The BRC repeats of BRCA2 modulate the DNA-binding selectivity of RAD51. Cell. 2009;136(6):1032-43. doi: 10.1016/j.cell.2009.02.019. PubMed PMID: 19303847; PubMed Central PMCID: PMCPMC2669112.
103. Ying S, Hamdy FC, Helleday T. Mre11-dependent degradation of stalled DNA replication forks is prevented by BRCA2 and PARP1. Cancer Res. 2012;72(11):2814-21. doi: 10.1158/0008-5472.CAN-11-3417. PubMed PMID: 22447567.
104. Costanzo V. Brca2, Rad51 and Mre11: performing balancing acts on replication forks. DNA Repair (Amst). 2011;10(10):1060-5. doi: 10.1016/j.dnarep.2011.07.009. PubMed PMID: 21900052.
105. Schlacher K, Christ N, Siaud N, Egashira A, Wu H, Jasin M. Double-strand break repair-independent role for BRCA2 in blocking stalled replication fork degradation by MRE11. Cell. 2011;145(4):529-42. doi: 10.1016/j.cell.2011.03.041. PubMed PMID: 21565612; PubMed Central PMCID: PMCPMC3261725.
106. Costantino L, Sotiriou SK, Rantala JK, Magin S, Mladenov E, Helleday T, et al. Break-induced replication repair of damaged forks induces genomic duplications in human cells. Science. 2014;343(6166):88-91. doi: 10.1126/science.1243211. PubMed PMID: 24310611; PubMed Central PMCID: PMCPMC4047655.
107. Anand RP, Lovett ST, Haber JE. Break-induced DNA replication. Cold Spring Harb Perspect Biol. 2013;5(12):a010397. doi: 10.1101/cshperspect.a010397. PubMed PMID: 23881940; PubMed Central PMCID: PMCPMC3839615.

108. Malkova A, Ira G. Break-induced replication: functions and molecular mechanism. Curr Opin Genet Dev. 2013;23(3):271-9. doi: 10.1016/j.gde.2013.05.007. PubMed PMID: 23790415; PubMed Central PMCID: PMCPMC3915057.
109. Karlin J, Fischhaber PL. Rad51 ATP binding but not hydrolysis is required to recruit Rad10 in synthesis-dependent strand annealing sites in S. cerevisiae. Adv Biol Chem. 2013;3(3):295-303. doi: 10.4236/abc.2013.33033. PubMed PMID: 25346869; PubMed Central PMCID: PMCPMC4205939.
110. McMahill MS, Sham CW, Bishop DK. Synthesis-dependent strand annealing in meiosis. PLoS Biol. 2007;5(11):e299. doi: 10.1371/journal.pbio.0050299. PubMed PMID: 17988174; PubMed Central PMCID: PMCPMC2062477.
111. Aguilera A. Double-strand break repair: are Rad51/RecA--DNA joints barriers to DNA replication? Trends Genet. 2001;17(6):318-21. PubMed PMID: 11377793.
112. Paliwal S, Kanagaraj R, Sturzenegger A, Burdova K, Janscak P. Human RECQ5 helicase promotes repair of DNA double-strand breaks by synthesis-dependent strand annealing. Nucleic Acids Res. 2014;42(4):2380-90. doi: 10.1093/nar/gkt1263. PubMed PMID: 24319145; PubMed Central PMCID: PMCPMC3936725.
113. Lok BH, Carley AC, Tchang B, Powell SN. RAD52 inactivation is synthetically lethal with deficiencies in BRCA1 and PALB2 in addition to BRCA2 through RAD51-mediated homologous recombination. Oncogene. 2013;32(30):3552-8. doi: 10.1038/onc.2012.391. PubMed PMID: 22964643.
114. Liu J, Heyer WD. Who's who in human recombination: BRCA2 and RAD52. Proc Natl Acad Sci U S A. 2011;108(2):441-2. doi: 10.1073/pnas.1016614108. PubMed PMID: 21189297; PubMed Central PMCID: PMCPMC3021045.
115. Cortés-Ledesma F, Malagón F, Aguilera A. A novel yeast mutation, rad52-L89F, causes a specific defect in Rad51-independent recombination that correlates with a reduced ability of Rad52-L89F to interact with Rad59. Genetics. 2004;168(1):553-7. doi: 10.1534/genetics.104.030551. PubMed PMID: 15454565; PubMed Central PMCID: PMCPMC1448092.
116. Davis AP, Symington LS. The Rad52-Rad59 complex interacts with Rad51 and replication protein A. DNA Repair (Amst). 2003;2(10):1127-34. PubMed PMID: 13679150.
117. Serra H, Da Ines O, Degroote F, Gallego ME, White CI. Roles of XRCC2, RAD51B and RAD51D in RAD51-independent SSA recombination. PLoS Genet. 2013;9(11):e1003971. doi: 10.1371/journal.pgen.1003971. PubMed PMID: 24278037; PubMed Central PMCID: PMCPMC3836719.
118. Chen Y, Dui W, Yu Z, Li C, Ma J, Jiao R. Drosophila RecQ5 is required for efficient SSA repair and suppression of LOH in vivo. Protein Cell. 2010;1(5):478-90. doi: 10.1007/s13238-010-0058-2. PubMed PMID: 21203963.
119. Spell RM, Jinks-Robertson S. Role of mismatch repair in the fidelity of RAD51- and RAD59-dependent recombination in Saccharomyces cerevisiae. Genetics. 2003;165(4):1733-44. PubMed PMID: 14704162; PubMed Central PMCID: PMCPMC1462911.
120. Manthey GM, Naik N, Bailis AM. Msh2 blocks an alternative mechanism for non-homologous tail removal during single-strand annealing in Saccharomyces cerevisiae. PLoS One. 2009;4(10):e7488. doi: 10.1371/journal.pone.0007488. PubMed PMID: 19834615; PubMed Central PMCID: PMCPMC2759526.
121. Davis L, Maizels N. Homology-directed repair of DNA nicks via pathways distinct from canonical double-strand break repair. Proc Natl Acad Sci U S A. 2014;111(10):E924-32. doi: 10.1073/pnas.1400236111. PubMed PMID: 24556991; PubMed Central PMCID: PMCPMC3956201.
122. Humbert O, Davis L, Maizels N. Targeted gene therapies: tools, applications, optimization. Crit Rev Biochem Mol Biol. 2012;47(3):264-81. doi: 10.3109/10409238.2012.658112. PubMed PMID: 22530743; PubMed Central PMCID: PMCPMC3338207.
123. Davis L, Maizels N. DNA nicks promote efficient and safe targeted gene correction. PLoS One. 2011;6(9):e23981. doi: 10.1371/journal.pone.0023981. PubMed PMID: 21912657; PubMed Central PMCID: PMCPMC3164693.

124. McConnell Smith A, Takeuchi R, Pellenz S, Davis L, Maizels N, Monnat RJ, et al. Generation of a nicking enzyme that stimulates site-specific gene conversion from the I-AniI LAGLIDADG homing endonuclease. Proc Natl Acad Sci U S A. 2009;106(13):5099-104. doi: 10.1073/pnas.0810588106. PubMed PMID: 19276110; PubMed Central PMCID: PMCPMC2664052.
125. Meers C, Keskin H, Storici F. DNA repair by RNA: Templated, or not templated, that is the question. DNA Repair (Amst). 2016. doi: 10.1016/j.dnarep.2016.05.002. PubMed PMID: 27237587.
126. Keskin H, Shen Y, Huang F, Patel M, Yang T, Ashley K, et al. Transcript-RNA-templated DNA recombination and repair. Nature. 2014;515(7527):436-9. doi: 10.1038/nature13682. PubMed PMID: 25186730.
127. Liu T, Huang J. DNA End Resection: Facts and Mechanisms. Genomics Proteomics Bioinformatics. 2016. doi: 10.1016/j.gpb.2016.05.002. PubMed PMID: 27240470.
128. Liu Y, Zhou K, Zhang H, Shugart YY, Chen L, Xu Z, et al. Polymorphisms of LIG4 and XRCC4 involved in the NHEJ pathway interact to modify risk of glioma. Hum Mutat. 2008;29(3):381-9. doi: 10.1002/humu.20645. PubMed PMID: 18165945.
129. Nick McElhinny SA, Ramsden DA. Sibling rivalry: competition between Pol X family members in V(D)J recombination and general double strand break repair. Immunol Rev. 2004;200:156-64. doi: 10.1111/j.0105-2896.2004.00160.x. PubMed PMID: 15242403.
130. Daley JM, Laan RL, Suresh A, Wilson TE. DNA joint dependence of pol X family polymerase action in nonhomologous end joining. J Biol Chem. 2005;280(32):29030-7. doi: 10.1074/jbc.M505277200. PubMed PMID: 15964833.
131. Sinha S, Villarreal D, Shim EY, Lee SE. Risky business: Microhomology-mediated end joining. Mutat Res. 2016;788:17-24. doi: 10.1016/j.mrfmmm.2015.12.005. PubMed PMID: 26790771; PubMed Central PMCID: PMCPMC4887395.
132. Sfeir A, Symington LS. Microhomology-Mediated End Joining: A Back-up Survival Mechanism or Dedicated Pathway? Trends Biochem Sci. 2015;40(11):701-14. doi: 10.1016/j.tibs.2015.08.006. PubMed PMID: 26439531; PubMed Central PMCID: PMCPMC4638128.
133. Ahrabi S, Sarkar S, Pfister SX, Pirovano G, Higgins GS, Porter AC, et al. A role for human homologous recombination factors in suppressing microhomology-mediated end joining. Nucleic Acids Res. 2016. doi: 10.1093/nar/gkw326. PubMed PMID: 27131361.
134. Truong LN, Li Y, Shi LZ, Hwang PY, He J, Wang H, et al. Microhomology-mediated End Joining and Homologous Recombination share the initial end resection step to repair DNA double-strand breaks in mammalian cells. Proc Natl Acad Sci U S A. 2013;110(19):7720-5. doi: 10.1073/pnas.1213431110. PubMed PMID: 23610439; PubMed Central PMCID: PMCPMC3651503.
135. Ma JL, Kim EM, Haber JE, Lee SE. Yeast Mre11 and Rad1 proteins define a Ku-independent mechanism to repair double-strand breaks lacking overlapping end sequences. Mol Cell Biol. 2003;23(23):8820-8. PubMed PMID: 14612421; PubMed Central PMCID: PMCPMC262689.
136. Tuteja N, Tuteja R. Unraveling DNA helicases. Motif, structure, mechanism and function. Eur J Biochem. 2004;271(10):1849-63. doi: 10.1111/j.1432-1033.2004.04094.x. PubMed PMID: 15128295.
137. Singleton MR, Dillingham MS, Wigley DB. Structure and mechanism of helicases and nucleic acid translocases. Annu Rev Biochem. 2007;76:23-50. doi: 10.1146/annurev.biochem.76.052305.115300. PubMed PMID: 17506634.
138. Rasnik I, Myong S, Ha T. Unraveling helicase mechanisms one molecule at a time. Nucleic Acids Res. 2006;34(15):4225-31. doi: 10.1093/nar/gkl452. PubMed PMID: 16935883; PubMed Central PMCID: PMCPMC1616959.
139. Woodman IL, Brammer K, Bolt EL. Physical interaction between archaeal DNA repair helicase Hel308 and Replication Protein A (RPA). DNA Repair (Amst). 2011;10(3):306-13. doi: 10.1016/j.dnarep.2010.12.001. PubMed PMID: 21195035.

140. Takata K, Reh S, Tomida J, Person MD, Wood RD. Human DNA helicase HELQ participates in DNA interstrand crosslink tolerance with ATR and RAD51 paralogs. Nat Commun. 2013;4:2338. doi: 10.1038/ncomms3338. PubMed PMID: 24005565; PubMed Central PMCID: PMCPMC3778836.
141. Khadka P, Hsu JK, Veith S, Tadokoro T, Shamanna RA, Mangerich A, et al. Differential and Concordant Roles for Poly(ADP-Ribose) Polymerase 1 and Poly(ADP-Ribose) in Regulating WRN and RECQL5 Activities. Mol Cell Biol. 2015;35(23):3974-89. doi: 10.1128/MCB.00427-15. PubMed PMID: 26391948; PubMed Central PMCID: PMCPMC4628069.
142. Larsen NB, Hickson ID. RecQ Helicases: Conserved Guardians of Genomic Integrity. Adv Exp Med Biol. 2013;767:161-84. doi: 10.1007/978-1-4614-5037-5_8. PubMed PMID: 23161011.
143. Rad B, Kowalczykowski SC. Translocation of E. coli RecQ helicase on single-stranded DNA. Biochemistry. 2012;51(13):2921-9. doi: 10.1021/bi3000676. PubMed PMID: 22409300; PubMed Central PMCID: PMCPMC3330151.
144. Harami GM, Nagy NT, Martina M, Neuman KC, Kovács M. The HRDC domain of E. coli RecQ helicase controls single-stranded DNA translocation and double-stranded DNA unwinding rates without affecting mechanoenzymatic coupling. Sci Rep. 2015;5:11091. doi: 10.1038/srep11091. PubMed PMID: 26067769; PubMed Central PMCID: PMCPMC4464074.
145. Watt PM, Louis EJ, Borts RH, Hickson ID. Sgs1: a eukaryotic homolog of E. coli RecQ that interacts with topoisomerase II in vivo and is required for faithful chromosome segregation. Cell. 1995;81(2):253-60. PubMed PMID: 7736577.
146. Klein HL, Symington LS. Sgs1--the maestro of recombination. Cell. 2012;149(2):257-9. doi: 10.1016/j.cell.2012.03.020. PubMed PMID: 22500794.
147. Parvathaneni S, Stortchevoi A, Sommers JA, Brosh RM, Sharma S. Human RECQ1 interacts with Ku70/80 and modulates DNA end-joining of double-strand breaks. PLoS One. 2013;8(5):e62481. doi: 10.1371/journal.pone.0062481. PubMed PMID: 23650516; PubMed Central PMCID: PMCPMC3641083.
148. Lahkim Bennani-Belhaj K, Rouzeau S, Buhagiar-Labarchède G, Chabosseau P, Onclercq-Delic R, Bayart E, et al. The Bloom syndrome protein limits the lethality associated with RAD51 deficiency. Mol Cancer Res. 2010;8(3):385-94. doi: 10.1158/1541-7786.MCR-09-0534. PubMed PMID: 20215422.
149. Bachrati CZ, Hickson ID. Analysis of the DNA unwinding activity of RecQ family helicases. Methods Enzymol. 2006;409:86-100. doi: 10.1016/S0076-6879(05)09005-1. PubMed PMID: 16793396.
150. Bergeron KL, Murphy EL, Brown LW, Almeida KH. Critical interaction domains between bloom syndrome protein and RAD51. Protein J. 2011;30(1):1-8. doi: 10.1007/s10930-010-9295-8. PubMed PMID: 21113733; PubMed Central PMCID: PMCPMC3399514.
151. Rossi ML, Ghosh AK, Bohr VA. Roles of Werner syndrome protein in protection of genome integrity. DNA Repair (Amst). 2010;9(3):331-44. doi: 10.1016/j.dnarep.2009.12.011. PubMed PMID: 20075015; PubMed Central PMCID: PMCPMC2827637.
152. Ghosh A, Rossi ML, Aulds J, Croteau D, Bohr VA. Telomeric D-loops containing 8-oxo-2'-deoxyguanosine are preferred substrates for Werner and Bloom syndrome helicases and are bound by POT1. J Biol Chem. 2009;284(45):31074-84. doi: 10.1074/jbc.M109.027532. PubMed PMID: 19734539; PubMed Central PMCID: PMCPMC2781507.
153. Lu L, Jin W, Wang LL. Aging in Rothmund-Thomson Syndrome and Related RECQL4 Genetic Disorders. Ageing Res Rev. 2016. doi: 10.1016/j.arr.2016.06.002. PubMed PMID: 27287744.
154. Kliszczak M, Sedlackova H, Pitchai GP, Streicher WW, Krejci L, Hickson ID. Interaction of RECQ4 and MCM10 is important for efficient DNA replication origin firing in human cells. Oncotarget. 2015;6(38):40464-79. doi: 10.18632/oncotarget.6342. PubMed PMID: 26588054; PubMed Central PMCID: PMCPMC4747346.
155. Kumari J, Hussain M, De S, Chandra S, Modi P, Tikoo S, et al. Mitochondrial functions of RECQL4 are required for the prevention of aerobic glycolysis-dependent cell invasion. J Cell Sci. 2016;129(7):1312-8. doi: 10.1242/jcs.181297. PubMed PMID: 26906415.

156. Kitao S, Ohsugi I, Ichikawa K, Goto M, Furuichi Y, Shimamoto A. Cloning of two new human helicase genes of the RecQ family: biological significance of multiple species in higher eukaryotes. Genomics. 1998;54(3):443-52. doi: 10.1006/geno.1998.5595. PubMed PMID: 9878247.
157. Sekelsky JJ, Brodsky MH, Rubin GM, Hawley RS. Drosophila and human RecQ5 exist in different isoforms generated by alternative splicing. Nucleic Acids Res. 1999;27(18):3762-9. PubMed PMID: 10471747; PubMed Central PMCID: PMCPMC148633.
158. Sakurai H, Tsutsui A, Higashi T, Azuma R, Ito F, Kawasaki K. RecQ5 protein translocation into the nucleus by a nuclear localization signal. Biol Pharm Bull. 2013;36(7):1159-66. PubMed PMID: 23811565.
159. Hu Y, Raynard S, Sehorn MG, Lu X, Bussen W, Zheng L, et al. RECQL5/Recql5 helicase regulates homologous recombination and suppresses tumor formation via disruption of Rad51 presynaptic filaments. Genes Dev. 2007;21(23):3073-84. doi: 10.1101/gad.1609107. PubMed PMID: 18003859; PubMed Central PMCID: PMCPMC2081974.
160. Liao WQ, Qi YL, Wang L, Dong XM, Xu T, Ding CD, et al. Recql5 protects against lipopolysaccharide/D-galactosamine-induced liver injury in mice. World J Gastroenterol. 2015;21(36):10375-84. doi: 10.3748/wjg.v21.i36.10375. PubMed PMID: 26420964; PubMed Central PMCID: PMCPMC4579884.
161. Dong YZ, Huang YX, Lu T. Single nucleotide polymorphism in the RECQL5 gene increased osteosarcoma susceptibility in a Chinese Han population. Genet Mol Res. 2015;14(1):1899-902. doi: 10.4238/2015.March.13.18. PubMed PMID: 25867335.
162. Wu J, Zhi L, Dai X, Cai Q, Ma W. Decreased RECQL5 correlated with disease progression of osteosarcoma. Biochem Biophys Res Commun. 2015;467(4):617-22. doi: 10.1016/j.bbrc.2015.10.114. PubMed PMID: 26499077.
163. He YJ, Qiao ZY, Gao B, Zhang XH, Wen YY. Association between RECQL5 genetic polymorphisms and susceptibility to breast cancer. Tumour Biol. 2014;35(12):12201-4. doi: 10.1007/s13277-014-2528-2. PubMed PMID: 25394896.
164. Arora A, Abdel-Fatah TM, Agarwal D, Doherty R, Croteau DL, Moseley PM, et al. Clinicopathological and prognostic significance of RECQL5 helicase expression in breast cancers. Carcinogenesis. 2016;37(1):63-71. doi: 10.1093/carcin/bgv163. PubMed PMID: 26586793; PubMed Central PMCID: PMCPMC4715235.
165. Cerami E, Gao J, Dogrusoz U, Gross BE, Sumer SO, Aksoy BA, et al. The cBio cancer genomics portal: an open platform for exploring multidimensional cancer genomics data. Cancer Discov. 2012;2(5):401-4. doi: 10.1158/2159-8290.CD-12-0095. PubMed PMID: 22588877; PubMed Central PMCID: PMCPMC3956037.
166. Gao J, Aksoy BA, Dogrusoz U, Dresdner G, Gross B, Sumer SO, et al. Integrative analysis of complex cancer genomics and clinical profiles using the cBioPortal. Sci Signal. 2013;6(269):pl1. doi: 10.1126/scisignal.2004088. PubMed PMID: 23550210; PubMed Central PMCID: PMCPMC4160307.
167. Ozsoy AZ, Ragonese HM, Matson SW. Analysis of helicase activity and substrate specificity of Drosophila RECQ5. Nucleic Acids Res. 2003;31(5):1554-64. PubMed PMID: 12595564; PubMed Central PMCID: PMCPMC149836.
168. Croteau DL, Popuri V, Opresko PL, Bohr VA. Human RecQ helicases in DNA repair, recombination, and replication. Annu Rev Biochem. 2014;83:519-52. doi: 10.1146/annurev-biochem-060713-035428. PubMed PMID: 24606147; PubMed Central PMCID: PMCPMC4586249.
169. Sakurai H, Okado M, Ito F, Kawasaki K. Anaphase DNA bridges induced by lack of RecQ5 in Drosophila syncytial embryos. FEBS Lett. 2011;585(12):1923-8. doi: 10.1016/j.febslet.2011.04.074. PubMed PMID: 21570978.
170. Blundred R, Myers K, Helleday T, Goldman AS, Bryant HE. Human RECQL5 overcomes thymidine-induced replication stress. DNA Repair (Amst). 2010;9(9):964-75. doi: 10.1016/j.dnarep.2010.06.009. PubMed PMID: 20643585.

171. Islam MN, Fox D, Guo R, Enomoto T, Wang W. RecQL5 promotes genome stabilization through two parallel mechanisms--interacting with RNA polymerase II and acting as a helicase. Mol Cell Biol. 2010;30(10):2460-72. doi: 10.1128/MCB.01583-09. PubMed PMID: 20231364; PubMed Central PMCID: PMCPMC2863711.
172. Popuri V, Tadokoro T, Croteau DL, Bohr VA. Human RECQL5: guarding the crossroads of DNA replication and transcription and providing backup capability. Crit Rev Biochem Mol Biol. 2013;48(3):289-99. doi: 10.3109/10409238.2013.792770. PubMed PMID: 23627586; PubMed Central PMCID: PMCPMC4563991.
173. Aygün O, Svejstrup J, Liu Y. A RECQ5-RNA polymerase II association identified by targeted proteomic analysis of human chromatin. Proc Natl Acad Sci U S A. 2008;105(25):8580-4. doi: 10.1073/pnas.0804424105. PubMed PMID: 18562274; PubMed Central PMCID: PMCPMC2430918.
174. Aygün O, Xu X, Liu Y, Takahashi H, Kong SE, Conaway RC, et al. Direct inhibition of RNA polymerase II transcription by RECQL5. J Biol Chem. 2009;284(35):23197-203. doi: 10.1074/jbc.M109.015750. PubMed PMID: 19570979; PubMed Central PMCID: PMCPMC2749093.
175. Kanagaraj R, Huehn D, MacKellar A, Menigatti M, Zheng L, Urban V, et al. RECQ5 helicase associates with the C-terminal repeat domain of RNA polymerase II during productive elongation phase of transcription. Nucleic Acids Res. 2010;38(22):8131-40. doi: 10.1093/nar/gkq697. PubMed PMID: 20705653; PubMed Central PMCID: PMCPMC3001069.
176. Li M, Xu X, Liu Y. The SET2-RPB1 interaction domain of human RECQ5 is important for transcription-associated genome stability. Mol Cell Biol. 2011;31(10):2090-9. doi: 10.1128/MCB.01137-10. PubMed PMID: 21402780; PubMed Central PMCID: PMCPMC3133350.
177. Kassube SA, Jinek M, Fang J, Tsutakawa S, Nogales E. Structural mimicry in transcription regulation of human RNA polymerase II by the DNA helicase RECQL5. Nat Struct Mol Biol. 2013;20(7):892-9. doi: 10.1038/nsmb.2596. PubMed PMID: 23748380; PubMed Central PMCID: PMCPMC3702667.
178. Li M, Pokharel S, Wang JT, Xu X, Liu Y. RECQ5-dependent SUMOylation of DNA topoisomerase I prevents transcription-associated genome instability. Nat Commun. 2015;6:6720. doi: 10.1038/ncomms7720. PubMed PMID: 25851487.
179. Aguilera A, García-Muse T. R loops: from transcription byproducts to threats to genome stability. Mol Cell. 2012;46(2):115-24. doi: 10.1016/j.molcel.2012.04.009. PubMed PMID: 22541554.
180. Hu Y, Lu X, Zhou G, Barnes EL, Luo G. Recql5 plays an important role in DNA replication and cell survival after camptothecin treatment. Mol Biol Cell. 2009;20(1):114-23. doi: 10.1091/mbc.E08-06-0565. PubMed PMID: 18987339; PubMed Central PMCID: PMCPMC2613109.
181. Zheng L, Kanagaraj R, Mihaljevic B, Schwendener S, Sartori AA, Gerrits B, et al. MRE11 complex links RECQ5 helicase to sites of DNA damage. Nucleic Acids Res. 2009;37(8):2645-57. doi: 10.1093/nar/gkp147. PubMed PMID: 19270065; PubMed Central PMCID: PMCPMC2677886.
182. Schwendener S, Raynard S, Paliwal S, Cheng A, Kanagaraj R, Shevelev I, et al. Physical interaction of RECQ5 helicase with RAD51 facilitates its anti-recombinase activity. J Biol Chem. 2010;285(21):15739-45. doi: 10.1074/jbc.M110.110478. PubMed PMID: 20348101; PubMed Central PMCID: PMCPMC2871440.
183. Keijzers G, Maynard S, Shamanna RA, Rasmussen LJ, Croteau DL, Bohr VA. The role of RecQ helicases in non-homologous end-joining. Crit Rev Biochem Mol Biol. 2014;49(6):463-72. doi: 10.3109/10409238.2014.942450. PubMed PMID: 25048400; PubMed Central PMCID: PMCPMC4244233.
184. Graham FL, Smiley J, Russell WC, Nairn R. Characteristics of a human cell line transformed by DNA from human adenovirus type 5. J Gen Virol. 1977;36(1):59-74. doi: 10.1099/0022-1317-36-1-59. PubMed PMID: 886304.

185. Shaw G, Morse S, Ararat M, Graham FL. Preferential transformation of human neuronal cells by human adenoviruses and the origin of HEK 293 cells. FASEB J. 2002;16(8):869-71. doi: 10.1096/fj.01-0995fje. PubMed PMID: 11967234.
186. Lin YC, Boone M, Meuris L, Lemmens I, Van Roy N, Soete A, et al. Genome dynamics of the human embryonic kidney 293 lineage in response to cell biology manipulations. Nat Commun. 2014;5:4767. doi: 10.1038/ncomms5767. PubMed PMID: 25182477; PubMed Central PMCID: PMCPMC4166678.
187. Rasheed S, Nelson-Rees WA, Toth EM, Arnstein P, Gardner MB. Characterization of a newly derived human sarcoma cell line (HT-1080). Cancer. 1974;33(4):1027-33. PubMed PMID: 4132053.
188. Certo MT, Ryu BY, Annis JE, Garibov M, Jarjour J, Rawlings DJ, et al. Tracking genome engineering outcome at individual DNA breakpoints. Nat Methods. 2011;8(8):671-6. doi: 10.1038/nmeth.1648. PubMed PMID: 21743461; PubMed Central PMCID: PMCPMC3415300.
189. Lucas P, Otis C, Mercier JP, Turmel M, Lemieux C. Rapid evolution of the DNA-binding site in LAGLIDADG homing endonucleases. Nucleic Acids Res. 2001;29(4):960-9. PubMed PMID: 11160929; PubMed Central PMCID: PMCPMC29605.
190. Horvath P, Barrangou R. CRISPR/Cas, the immune system of bacteria and archaea. Science. 2010;327(5962):167-70. doi: 10.1126/science.1179555. PubMed PMID: 20056882.
191. Barrangou R, Fremaux C, Deveau H, Richards M, Boyaval P, Moineau S, et al. CRISPR provides acquired resistance against viruses in prokaryotes. Science. 2007;315(5819):1709-12. doi: 10.1126/science.1138140. PubMed PMID: 17379808.
192. Kunin V, Sorek R, Hugenholtz P. Evolutionary conservation of sequence and secondary structures in CRISPR repeats. Genome Biol. 2007;8(4):R61. doi: 10.1186/gb-2007-8-4-r61. PubMed PMID: 17442114; PubMed Central PMCID: PMCPMC1896005.
193. Gasiunas G, Barrangou R, Horvath P, Siksnys V. Cas9-crRNA ribonucleoprotein complex mediates specific DNA cleavage for adaptive immunity in bacteria. Proc Natl Acad Sci U S A. 2012;109(39):E2579-86. doi: 10.1073/pnas.1208507109. PubMed PMID: 22949671; PubMed Central PMCID: PMCPMC3465414.
194. Ran FA, Hsu PD, Lin CY, Gootenberg JS, Konermann S, Trevino AE, et al. Double nicking by RNA-guided CRISPR Cas9 for enhanced genome editing specificity. Cell. 2013;154(6):1380-9. doi: 10.1016/j.cell.2013.08.021. PubMed PMID: 23992846; PubMed Central PMCID: PMCPMC3856256.
195. Cho SW, Kim S, Kim Y, Kweon J, Kim HS, Bae S, et al. Analysis of off-target effects of CRISPR/Cas-derived RNA-guided endonucleases and nickases. Genome Res. 2014;24(1):132-41. doi: 10.1101/gr.162339.113. PubMed PMID: 24253446; PubMed Central PMCID: PMCPMC3875854.
196. Slaymaker IM, Gao L, Zetsche B, Scott DA, Yan WX, Zhang F. Rationally engineered Cas9 nucleases with improved specificity. Science. 2016;351(6268):84-8. doi: 10.1126/science.aad5227. PubMed PMID: 26628643; PubMed Central PMCID: PMCPMC4714946.
197. Caldecott KW. Single-strand break repair and genetic disease. Nat Rev Genet. 2008;9(8):619-31. doi: 10.1038/nrg2380. PubMed PMID: 18626472.
198. Martin LJ. DNA damage and repair: relevance to mechanisms of neurodegeneration. J Neuropathol Exp Neurol. 2008;67(5):377-87. doi: 10.1097/NEN.0b013e31816ff780. PubMed PMID: 18431258; PubMed Central PMCID: PMCPMC2474726.
199. Saponaro M, Kantidakis T, Mitter R, Kelly GP, Heron M, Williams H, et al. RECQL5 controls transcript elongation and suppresses genome instability associated with transcription stress. Cell. 2014;157(5):1037-49. doi: 10.1016/j.cell.2014.03.048. PubMed PMID: 24836610; PubMed Central PMCID: PMCPMC4032574.
200. Maruyama S, Ohkita N, Nakayama M, Akaboshi E, Shibata T, Funakoshi E, et al. RecQ5 interacts with Rad51 and is involved in resistance of Drosophila to cisplatin treatment. Biol Pharm Bull. 2012;35(11):2017-22. PubMed PMID: 23123473.

201. Colavito S, Prakash R, Sung P. Promotion and regulation of homologous recombination by DNA helicases. Methods. 2010;51(3):329-35. doi: 10.1016/j.ymeth.2010.02.009. PubMed PMID: 20156560; PubMed Central PMCID: PMCPMC2948243.
202. Stark JM, Hu P, Pierce AJ, Moynahan ME, Ellis N, Jasin M. ATP hydrolysis by mammalian RAD51 has a key role during homology-directed DNA repair. J Biol Chem. 2002;277(23):20185-94. doi: 10.1074/jbc.M112132200. PubMed PMID: 11923292.
203. Forget AL, Loftus MS, McGrew DA, Bennett BT, Knight KL. The human Rad51 K133A mutant is functional for DNA double-strand break repair in human cells. Biochemistry. 2007;46(11):3566-75. doi: 10.1021/bi062128k. PubMed PMID: 17302439; PubMed Central PMCID: PMCPMC2952636.
204. Rukść A, Birmingham EC, Baker MD. Altered DNA repair and recombination responses in mouse cells expressing wildtype or mutant forms of RAD51. DNA Repair (Amst). 2007;6(12):1876-89. doi: 10.1016/j.dnarep.2007.07.006. PubMed PMID: 17719855.
205. Kim TM, Ko JH, Hu L, Kim SA, Bishop AJ, Vijg J, et al. RAD51 mutants cause replication defects and chromosomal instability. Mol Cell Biol. 2012;32(18):3663-80. doi: 10.1128/MCB.00406-12. PubMed PMID: 22778135; PubMed Central PMCID: PMCPMC3430192.
206. Baumann P, Benson FE, West SC. Human Rad51 protein promotes ATP-dependent homologous pairing and strand transfer reactions in vitro. Cell. 1996;87(4):757-66. PubMed PMID: 8929543.
207. Chi P, Van Komen S, Sehorn MG, Sigurdsson S, Sung P. Roles of ATP binding and ATP hydrolysis in human Rad51 recombinase function. DNA Repair (Amst). 2006;5(3):381-91. doi: 10.1016/j.dnarep.2005.11.005. PubMed PMID: 16388992.
208. Khadka P, Croteau DL, Bohr VA. RECQL5 has unique strand annealing properties relative to the other human RecQ helicase proteins. DNA Repair (Amst). 2016;37:53-66. doi: 10.1016/j.dnarep.2015.11.005. PubMed PMID: 26717024.
209. Epshtein V, Kamarthapu V, McGary K, Svetlov V, Ueberheide B, Proshkin S, et al. UvrD facilitates DNA repair by pulling RNA polymerase backwards. Nature. 2014;505(7483):372-7. doi: 10.1038/nature12928. PubMed PMID: 24402227; PubMed Central PMCID: PMCPMC4471481.
210. Epshtein V. UvrD helicase: an old dog with a new trick: how one step backward leads to many steps forward. Bioessays. 2015;37(1):12-9. doi: 10.1002/bies.201400106. PubMed PMID: 25345862; PubMed Central PMCID: PMCPMC4418501.
211. Petrova V, Chen SH, Molzberger ET, Tomko E, Chitteni-Pattu S, Jia H, et al. Active displacement of RecA filaments by UvrD translocase activity. Nucleic Acids Res. 2015;43(8):4133-49. doi: 10.1093/nar/gkv186. PubMed PMID: 25824953; PubMed Central PMCID: PMCPMC4417151.
212. Park J, Myong S, Niedziela-Majka A, Lee KS, Yu J, Lohman TM, et al. PcrA helicase dismantles RecA filaments by reeling in DNA in uniform steps. Cell. 2010;142(4):544-55. doi: 10.1016/j.cell.2010.07.016. PubMed PMID: 20723756; PubMed Central PMCID: PMCPMC2943210.
213. Fagerburg MV, Schauer GD, Thickman KR, Bianco PR, Khan SA, Leuba SH, et al. PcrA-mediated disruption of RecA nucleoprotein filaments--essential role of the ATPase activity of RecA. Nucleic Acids Res. 2012;40(17):8416-24. doi: 10.1093/nar/gks641. PubMed PMID: 22743269; PubMed Central PMCID: PMCPMC3458574.
214. Gwynn EJ, Smith AJ, Guy CP, Savery NJ, McGlynn P, Dillingham MS. The conserved C-terminus of the PcrA/UvrD helicase interacts directly with RNA polymerase. PLoS One. 2013;8(10):e78141. doi: 10.1371/journal.pone.0078141. PubMed PMID: 24147116; PubMed Central PMCID: PMCPMC3797733.
215. Brosh RM. UvrD helicase: the little engine that could. Cell Cycle. 2014;13(8):1213-5. doi: 10.4161/cc.28382. PubMed PMID: 24621500; PubMed Central PMCID: PMCPMC4049952.
216. Tuteja R, Tuteja N. Analysis of DNA repair helicase UvrD from Arabidopsis thaliana and Oryza sativa. Plant Physiol Biochem. 2013;71:254-60. doi: 10.1016/j.plaphy.2013.07.022. PubMed PMID: 23974358.

217. Pinello L. CRISPResso: sequencing analysis toolbox for CRISPR-cas9 genome editing. In: **Canver MC**, editor. bioRxiv2015. p. pages 031203+.
218. Lieber MR. The mechanism of double-strand DNA break repair by the nonhomologous DNA end-joining pathway. Annu Rev Biochem. 2010;79:181-211. doi: 10.1146/annurev.biochem.052308.093131. PubMed PMID: 20192759; PubMed Central PMCID: PMCPMC3079308.
219. Ishibashi T, Nakabeppu Y, Sekiguchi M. Artificial control of nuclear translocation of DNA repair methyltransferase. J Biol Chem. 1994;269(10):7645-50. PubMed PMID: 8125990.
220. Richardson CD, Ray GJ, DeWitt MA, Curie GL, Corn JE. Enhancing homology-directed genome editing by catalytically active and inactive CRISPR-Cas9 using asymmetric donor DNA. Nat Biotechnol. 2016;34(3):339-44. doi: 10.1038/nbt.3481. PubMed PMID: 26789497.
221. Foulkes WD. BRCA1 and BRCA2: chemosensitivity, treatment outcomes and prognosis. Fam Cancer. 2006;5(2):135-42. doi: 10.1007/s10689-005-2832-5. PubMed PMID: 16736282.

Henry Olson Ph.D., h5c5o5@gmail.com , 206-495-8085, Apt. 106M – 14330 12th Ave NE Seattle

Innovator Communicator Leader

Experience

Research Associate– Maizels Lab, Biochemistry Department, U. of Washington (2011- Aug 2016)

- Designed experiment to differentiate between direct and indirect inhibition at the site of damage of DNA repair pathways.
- Performed statistical analysis of data on canonical repair factors to prove DNA repair pathways were being directly inhibited.
- Won funding for my research and salary through competitive training grants: Molecular Medicine Training grant (1 year), Howard Hughes Medical Institute Training Grant (1 year), Cellular and Molecular Biology Training Grant (3 years).
- Author of two Record of Innovations filed with the UW Center for Commercialization. Titles – "Enhanced Gene Correction by Overexpression of RECQ5 Helicase and its Derivatives" and "Induction of Targeted DNA Cleavage with Cas9/CRISP".
- Owned Lab safety training for over 20 people. This included training in personal protective equipment, blood based pathogens biohazards, work place accidents, and chemical spills. Training was refreshed yearly.

Publications, Presentations, and Posters

- RECQ5 promotes alternative homology directed repair through disruption of RAD51 filaments (in preparation for submission to PLoS Genetics)
- Speaker at the international RECQ2016 helicase conference hosted in Seattle (May -2016)
- Speaker at the Cellular and Molecular Biology Retreat (2015 - UW)

- Speaker at the Molecular Medicine Capstone (2014 - UW)
- Poster at the Biochemistry Department retreat (2011-2016 - UW)
- Poster at Immunology Department Retreat (2013 -UW)
- Speaker/Poster at Undergraduate Research Symposium (2011 – University of British Columbia)

Teaching Assistant – Biochemistry 440, 406, 426 (2013)

- Lab and classroom teaching experience (class size ~30)
- Aided in writing, editing, grading lectures and exams

Senator for Biochemistry, GPSS; Chair of GPSS Finance and Budget Committee (2014-2016)

- Recruited and led the 20 member F&B committee in allocation of $30,000 budget to departments and student organizations. Aided applicants through the process and interviewed finalists.

Education

University of Washington – PhD in Biochemistry, GPA 3.9

Bachelor of Science – Honors Biochemistry University of British Columbia, GPA 3.4

Scholarships and Awards

University of British Columbia

- President's Entrance Scholarship
- Outstanding International Student Award

University of Washington

- Graduate School Top Scholar Award
- Urdal Fellowship – Awarded to one member of the department to allow for advanced technical training